Influence of Lead Impurity and Manganese Addition on Main Operating Parameters of Zinc Electrowinning

Mémoire

Chaoran Su

Maîtrise en génie des matériaux et de la métallurgie
Maître ès sciences (M. Sc.)

Québec, Canada

Influence of Lead Impurity and Manganese Addition on Main Operating Parameters of Zinc Electrowinning

Mémoire

Chaoran Su

Sous la direction de :

Edward Ghali, directeur de recherche

RÉSUMÉ

L'influence des ions Pb^{2+} sur le dépôt de zinc a été étudiée dans l'électrolyte acide de sulfate de zinc avec et sans Mn^{2+}. La polarisation galvanostatique, la polarisation potentiodynamique, la voltammétrie cyclique (VC), les mesures de bruit électrochimique (MBE) et la spectroscopie d'impédance électrochimique (SIE) en conjonction avec la microscopie électronique à balayage (MEB) et la diffraction des rayons-X (XRD) ont été considérés. L'effet de différents paramètres de fonctionnement tels que la concentration de Zn^{2+}, la concentration d'acide sulfurique, la densité de courant, l'agitation de l'électrolyte et la température a été étudié en présence de Mn^{2+} et Pb^{2+}.

Les résultats galvanostatiques utilisant un électrolyte standard de zinc contenant 12 g/L de Mn^{2+} (ES) ont montré que les ions de plomb ajoutés à l'ES conduisaient à une augmentation du potentiel cathodique et de l'efficacité de courant (EC) du dépôt de zinc. L'augmentation de la concentration de Mn^{2+} dans l'électrolyte a entraîné une diminution du potentiel cathodique et d'EC du dépôt de zinc à cause de l'effet de dépolarisation du MnO_4^- formé. En outre, l'augmentation de la densité de courant de 45 à 60 mA/cm^2 et de l'agitation de 60 à 412 tr/min ont donné lieu à une augmentation du potentiel et à une diminution d'EC. L'augmentation de la température de 35 à 45°C a conduit à une diminution du potentiel cathodique. Pour l'électrolyse de longue durée (72 h), la teneur de Pb dans le dépôt de zinc en utilisant l'anode Pb-0,7%Ag était de 1,90-1,98 ppm, presque équivalente à celle employant l'anode de Pt avec l'addition de 0,15-0,2 mg/L de Pb^{2+}.

L'électrolyse à 40°C et 52,5 mA/cm^2 en présence de plomb jusqu'à 0,1-0,2 mg/L dans un électrolyte contenant 12 g/L Mn^{2+} pourrait être considérée comme des meilleurs paramètres opérationnels pour le procédé d'extraction électrolytique. Les études SIE ont montré que le dépôt de zinc sur le zinc est plus facile que celui du zinc sur l'aluminium. L'analyse des MBE a révélé que l'augmentation des concentrations de Pb^{2+} (0,05-0,8 mg/L) dans l'électrolyte de zinc sans Mn^{2+} s'accompagne d'une diminution de l'inclinaison et d'une augmentation des valeurs du kurtosis qui puissent être corrélées à la morphologie du dépôt de zinc.

ABSTRACT

The influence of Pb^{2+} ions on zinc deposition was investigated in acidic zinc sulfate electrolyte with and without Mn^{2+} ions. Galvanostatic polarization, potentiodynamic polarization, cyclic voltammetry (CV), electrochemical noise measurements (ENM) and electrochemical impedance spectroscopy (EIS) in conjunction with scanning electron microscopy (SEM) and X-ray diffraction (XRD) have been considered. Effects of different operating parameters such as Zn^{2+} ions concentration, sulfuric acid concentration, current density, electrolyte agitation and temperature were investigated in presence of Mn^{2+} and Pb^{2+} ions.

The galvanostatic results using standard zinc electrolyte containing 12 g/L Mn^{2+} (SE) showed that lead ions added to the SE led to an increase in the cathodic potential and current efficiency (CE) of zinc deposit. Increasing Mn^{2+} concentration in the electrolyte resulted in decrease of cathodic potential and CE of zinc deposit due to the depolarization effect of formed MnO_4^-. In addition, increases of current density from 45 to 60 mA/cm^2 and agitation from 60 to 412 rpm resulted in an increase of overpotential and decrease of CE. Increase of temperature from 35 to 45°C led to a decrease of cathodic potential. For long time electrolysis (72 h), the Pb content in zinc deposit using Pb-0.7%Ag anode was 1.90-1.98 ppm, almost equivalent to that employing Pt anode with addition of 0.15-0.2 mg/L of Pb^{2+}.

Electrolysis at 40°C and 52.5 mA/cm^2 in presence of lead up to 0.1-0.2 mg/L in an electrolyte containing 12 g/L of Mn^{2+} could be considered as best conducted operating parameters for electrowinning process. EIS studies showed that zinc deposition on zinc is easier than that of zinc on aluminum. ENM revealed that increase of Pb^{2+} concentration (0.05-0.8 mg/L) in zinc electrolyte without Mn^{2+} is accompanied with a decrease of skew and increase of kurtosis values that could be correlated to the morphology of zinc deposit.

Table of Contents

List of Tables

List of Figures

"To my great country, beloved parents and my precious 24"

Acknowledgments

My deepest gratitude goes first and foremost to Professor Edward Ghali, my supervisor, for his constant encouragement and guidance. He has walked me through all the stages of my two years master project. Without his consistent and illuminating instructions, this thesis could not have reached its present form.

Second, I would like to express my appreciation to Dr. Wei Zhang, Dr. Georges Gabra, Dr. Fariba Safizadeh and Mr. Georges Houlachi who have offered me valuable suggestions in the academic studies and whose useful suggestions, incisive comments and constructive criticism have contributed greatly to the completion of my study. I wish also to acknowledge my dear colleagues: Dr. Ahmet Deniz Bas and Mr. Nabil Naguib Mowafy Sorour, who have instructed and helped me a lot in the past two years. I would like also to thank Mr. André Ferland, Mrs. Vicky Dodier, Mr. Jean Frenette, and Mr Alain Brousseau for their professional technical participation.

At the end, I am also greatly indebted to my dear friends; the best Bolbol, lovely Olivia, powerful Ramzi and beautiful Sarah, beloved family and friends in China, great Mr. Kururugi Suzaku, and the memory of Xixi who supported me to pass the endless winter in Québec city.

Foreword

This dissertation is consisting of seven chapters and presented as articles insertion form. The first chapter introduces the zinc electrowinning process, challenges in this process, and the objectives of this research project. Second chapter introduces full literature review based on previous works and electrochemical techniques which have been used during evaluation. The experimental procedures and conditions are explained in chapter three. Chapters four, five and six explain the obtained results in the form of three research papers as follows:

Chapter four

Electrochemical Investigation of Electrolyte Composition and Electrolysis Parameters during Zinc Electrowinning

C. Su[1,*], W. Zhang[1], E. Ghali[1], and G. Houlachi[2]

[1]Department of Mining, Metallurgical and Materials Engineering, Laval University, QC, Canada

[2]Hydro-Québec research centre (LTE) Shawinigan, QC, Canada

This paper was submitted to the Journal of Applied Electrochemistry on 5 January 2017.

In this paper, a full understanding based on experimental results and observations has been highlighted with concluding the optimum working parameters in zinc electrowinning. The experiments, measurements and analysis, also writing the paper were done by the first author. The scientific analysis and revision were done by Dr. W. Zhang and Prof. E. Ghali. The process was supervised by Prof. E. Ghali and Mr. G. Houlachi.

Chapter five

The Effect of Lead Impurity in Presence of Manganese Addition on Zinc Electrowinning

C. Su[1, *], N. Sorour[1], W. Zhang[1], E. Ghali[1], and G. Houlachi[2]

[1]*Department of Mining, Metallurgical and Materials Engineering Laval University, Québec, Canada*

[2]*Hydro-Québec research centre (LTE) Shawinigan, QC, Canada*

This paper was presented in the XXVIII International Mineral Processing Congress (IMPC 2016), Québec City, Canada (September 11-15) and published in the Proceeding, paper #952, ISBN: 978-1-926872-29-2.

In this work, the effect of manganese and lead addition to the zinc sulfate electrolyte has been examined employing different electrochemical techniques. The experiments, measurements, analysis and presentation were done by the first author. The scientific analysis and writing were done by first author and Mr. N. Sorour. Revision was done by Dr. W. Zhang and Prof. E. Ghali. The project was supervised by Prof. E. Ghali and Mr. G. Houlachi.

Chapter six

Investigation of the Zinc Deposit Contamination by Lead during Electrowinning Employing Electrochemical Noise Measurements

*F. Safizadeh[1], **C. Su[1]**, E. Ghali[1], and G. Houlachi[2]

[1]*Department of Mining, Metallurgical and Materials Engineering Laval University, Québec, Canada*

[2]*Hydro-Québec research centre (LTE) Shawinigan, QC, Canada*

This paper was presented in the XXVIII International Mineral Processing Congress (IMPC 2016), Québec city, Canada (September 11-15) and published in the Proceeding, paper #953, ISBN: 978-1-926872-29-2.

The effect of lead contamination on zinc deposition has been examined employing electrochemical noise measurements. The experiments, measurements and analysis were done by the second author. The scientific analysis, writing and presentation were done by Dr. F. Safizadeh. Revision was done Prof. E. Ghali. The project was supervised by Prof. E. Ghali and Mr. G. Houlachi.

Chapter seven

At the end, chapter seven offers conclusions for this thesis and recommends future work plan. This is followed by Bibliography for all chapters according to Chicago Manual of Style's 16th edition 2010 (Last updated Winter 2016).

CHAPTER 1

INTRODUCTION

1.1 Background

More than 85% of the high grade zinc metal is produced by the electrolytic method. During this production method there are many metallurgical processes taking place. The zinc sulfide (ZnS) ore is roasted at high temperature (700-1000°C) in presence of oxygen to form zinc oxide (ZnO). The roasted concentrate sent from a roasting furnace is dissolved in dilute sulfuric acid in the leaching tank to form zinc sulfate ($ZnSO_4$) (Equation. 1.1) (Sinclair 2005; Porter 1991).

$$ZnO + H_2SO_4 \rightarrow ZnSO_4 + H_2O \quad (1.1)$$

The $ZnSO_4$ electrolyte is then circulated to the tank house for the electrowinning process. Before electrolysis some iron and other metallic impurities contained in the calcine are dissolved then. These impurities are removed by precipitation with added manganese, lime, zinc dust or other additives such as glues and gelatines (Fig. 1.1) (Yokogawa 2016).

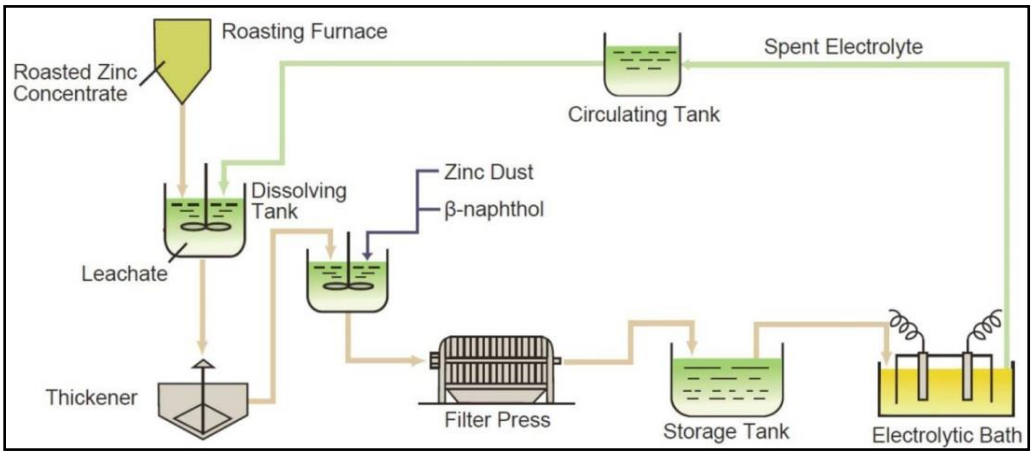

Fig. 1.1 Metallurgical processing of zinc (Yokogawa 2016)

1.2 Zinc Electrowinning Process

The industrial electrolytic production of zinc requires electrodeposition of zinc metal from generally aqueous acidic zinc sulfate electrolytes. The electrowinning process is always carried out in a cell house consisting of hundreds of electrolytic cells (Mahon et al. 2014). Typically, zinc electrodeposition takes place on aluminum cathodes according to the following reaction:

$$Zn^{2+} + 2e^{-} \rightarrow Zn_{(s)} \qquad E^{o} = -0.763V \qquad (1.2)$$

The evolution of H_2 gas is often included in the reaction mechanism of zinc deposition in acidic zinc sulfate medium (Equation. 1.3). The theoretical reduction potential of hydrogen in standard conditions is equal to zero. However, the high overpotential of cathodic hydrogen evolution reaction on zinc cannot be neglected in this process, hydrogen evolution shifts to a potential behind that for zinc deposition (Scott et al. 1987; Zhang 2010).

$$2H^{+} + 2e^{-} \rightarrow H_{2(g)} \qquad E^{o} = 0.00V \qquad (1.3)$$

The aluminum cathodes proved their high performance during the electrolysis due to their low overpotentials and also the deposit is adherent to the aluminum cathodes, and it is separated easily by mechanical methods during the stripping process after the electrodeposition (Han and O'Keefe 1992). The lead-based alloys have been used as anodes in the zinc electrowinning industry since the first industrial electrolytic production of zinc in 1909 (Newnham 1992). The cell zinc house is responsible for approximately 80% of the total consumed energy by a zinc refinery.

1.3 Lead-based Anodes in Zinc Electrowinning

Presently, most of zinc plants use lead-silver alloys as anodes due to their high conductivity, certain stability, and low overpotential during oxygen evolution (Eq. 1.4) (Yu and O'Keefe 1999).

$$H_2O \rightarrow 2H^{+} + 2e^{-} + \frac{1}{2}O_{2(g)} \qquad E^{o} = -1.229V \qquad (1.4)$$

Pure lead is a weak material and it tends to creep and warp during use. Therefore, lead must be alloyed in order to improve its mechanical properties. Lead has a relatively low melting point, which facilitates its casting, and it is also a very ductile material and can be machined easily (Umetsu et al. 1985). Small amounts of Ag (0.4-1.0wt.%) alloyed with lead could decrease the oxygen overvoltage, and increase the corrosion resistance of the material during electrolysis. A well established custom in the most electrolytic zinc plants is to use Pb-Ag alloys containing 0.7-1.0%Ag as anode material. The resulting benefits are to have

long lifetime and a high resistance towards the formation of PbO_2 (Tikkanen and Hyvarinen 1972). However, the contamination of deposited zinc by lead is still one of the challenges in any electrowinning industry.

1.4 Operating Parameters in Zinc Electrowinning

The goal of any zinc plant is to achieve very pure zinc with high current efficiency and low power consumption. The electrowinning process is so sensitive to the change of any working parameter as well as the metallic impurities presented in the electrolyte (Alfantazi and Dreisinger 2001). Many working parameters such as electrolyte composition, current density, temperature, and electrolyte agitation control the electrowinning process and the change of any of them could affect negatively or positively the process.

Most zinc plants operate over 90% of current efficiency. The presence of certain impurities such as Pb^{2+} and Mn^{2+} in the zinc electrolyte could affect this percentage, so adjusting the concentration of these impurities by controlling the operational parameters could yield optimum current efficiency and pure zinc deposit with acceptable surface morphology of zinc deposit (Tripathy et al. 2003).

1.5 Objectives

The aim of this project can be divided into the following objectives:

1. Study the effect of electrolyte contamination by different concentrations of $Pb^{2+}$and Mn^{2+} on the cathodic current efficiency, overpotential, morphology and lead contamination of the deposited zinc.

2. Determine the contamination of zinc deposit by employing Pb-0.7wt.%Ag anode and Pt anode added lead to the electrolyte separately.

3. Evaluate the influence of different operating parameters such as electrolyte Zn^{2+} concentration, acid content, current density, temperature, and electrolyte agitation

on current efficiency, cathodic polarization, deposit morphology, and lead contamination of zinc deposit.

Electrochemical techniques such as: galvanostatic polarization, potentiodynamic polarization, cyclic voltammetry, electrochemical noise measurements, and electrochemical impedance spectroscopy are then considered. There are accompanied by physical and chemical characterization techniques, such as X-ray diffraction (XRD), Scanning Electron Microscope (SEM) and Inductively Coupled Plasma (ICP), in order to evaluate the effect of each parameter on the electrowinning process and produced zinc quality.

CHAPTER 2

LITERATURE REVIEW

2.1 Zinc Electrowinning Process

Electrowinning is an old electrolytic extraction process, which was initially introduced in 1807 by English chemist Humphry Davy when it was succeeded to obtain sodium from the electrolysis of NaOH as molten salt. Today electrowinning became a largely modern technology in metal recovery, mining, refining and wastewater treatment applications (Soofastaei and Mirenayat 2015).

Electrolytic extraction process of zinc is almost exclusively depending on sulfate solutions, so that the leaching operation involving the dissolution of zinc from calcine using sulfuric acid in the form of spent electrolyte requirement. As described in chapter 1, this leaching process generally uses calcine as the primary feed and is simply based on the acid-base reaction shown in Equation 2.1.

$$ZnO + H_2SO_4 = ZnSO_4 + H_20 \quad (2.1)$$

Sulfuric acid is usually supplied in the form of spent electrolyte after electrowinning and commonly containing around 150-180 g/L sulfuric acid and 50-70 g/L Zn^{2+}. These concentrations vary from one plant to another depending on the operating conditions (Sinclair 2005).

In the electrowinning plant, the zinc sulfate electrolyte is circulated in big tanks, aluminum cathodes and lead-base anodes are immersed in parallel. A current density of ~500 A/m^2 is supplied to the electrodes and zinc starts to electrodeposit on the cathodes (Fig. 2.1). For electrolysis alone, the electric power requirement is approximately 3300 kWh/ton of zinc produced out of 4000 kWh/ton of total electrical requirements of the smelter, and the electrowinning process consumes ~80% of the total electrical consumption by the smelter (Cole, E.R. 1970).

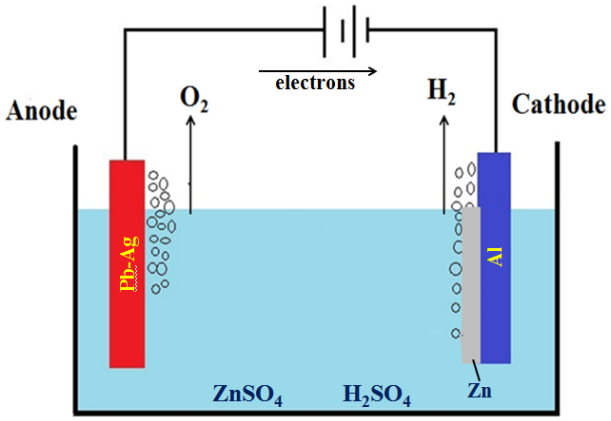

Fig. 2.1 Simple electrolysis cell of zinc electrowinning

2.1.1 Cathodic Process

In zinc electrodeposition, aluminum cathodes are usually used as they proved their high performance. During the electrolysis the deposit is adherent to the aluminum cathodes while, it is removed easily by mechanical methods after the electrodeposition (Han and O'Keefe 1992). Approximately, 90% of the cathodic current is consumed in producing zinc metal (Eq. 2.2), the electrodeposition of zinc in acidic electrolyte is accompanied frequently by hydrogen reduction and generally described as Equation (2.3) (Scott 1987). Due to the high overpotential of hydrogen on zinc, hydrogen evolution shifts to a potential behind that for zinc deposition. This is a favorable required overpotential in order to undergo the electrodeposition of zinc.

$$Zn^{2+} + 2e^- \rightarrow Zn_{(s)} \qquad E^o = -0.763V \qquad (2.2)$$

$$2H^+ + 2e^- \rightarrow H_{2(g)} \qquad E^o = 0.00V \qquad (2.3)$$

However, the kinetic of cathodic reactions are complicated due to the interactions of both zinc reduction and hydrogen evolution. Lee and Jorné (1992) introduced a reaction mechanism as follows:

$$H^+ + e^- \overset{K_1}{\rightarrow} H_{ads} \qquad (2.4)$$

$$H^+ + H_{ads} + e^- \overset{K_2}{\rightarrow} H_2 \qquad (2.5)$$

$$Zn^{2+} + Zn^{+}_{ads} + e^{-} \overset{K_3/K_3'}{\longleftrightarrow} 2Zn^{+}_{ads} \quad (2.6)$$

$$Zn^{+}_{ads} + H_{ads} \overset{K_4}{\rightarrow} H^{+} + Zn \quad (2.7)$$

$$Zn^{+}_{ads} + e^{-} \overset{K_5}{\rightarrow} Zn \quad (2.8)$$

$$Zn^{2+} + H_{ads} \overset{K_6}{\rightarrow} Zn^{+}_{ads} + H^{+} \quad (2.9)$$

H^+ reacts directly with the active sites as Equation (2.4), while Equation (2.5) corresponds to the evolution of hydrogen in the form of gas, Equation (2.6) is an intermediate process of adsorption of Zn^{2+} ions on the cathode surface, and finally the formation of zinc deposit is presented by Equations (2.7&2.8) (Lee and Jorné 1992). Variations in operating parameters such as current density, pH, temperature, and electrolyte circulation speed can have a significant effect on the thermodynamics of this process.

2.1.2 Anodic Process

About 99% of the anodic current is consumed to produce oxygen gas by Equation (2.10). This reaction represents ~60% of the energy consumed during electrowinning (2000 kWh/ton) (Barton and Scott 1992).

$$H_2O \rightarrow 2H^{+} + 2e^{-} + \tfrac{1}{2}O_{2(g)} \qquad E° = -1.229\ V \quad (2.10)$$

The thermodynamic potential for the total reaction is given by:

$E°_{cell} = E°_{anode} + E°_{cathode}$ = -1.23 + (-0.763) = -1.993 V, so the theoretical cell potential for the overall zinc electrowinning reaction is $E°_{cell}$ = -1.993 V. During electrolysis, a considerably larger amount of energy is required to overcome factors such as electrical resistance in the circuit, ionic resistance as well as polarization at the anode and cathode. These added voltage requirements are called overpotentials (Zhang 2010).

In the electrowinning process, lead and its alloys have been the recommended anode material for a long time. Ivanov et al. (2000) suggested that a useful anode material should have high electrical conductivity, an electrocatalyst, and show high stability (certain resistance to the formation of PbO_2). In industry, long-term stability during electrolysis is

an important factor as electrode wear and corrosion may cause zinc deposit contamination, increase in power consumption, material and labor costs due to the regular maintenance. In addition, the anode should have fine and uniform granular texture with minimum segregation of alloying elements at the grain boundary (Prengaman 1984). Pure lead is a weak metal with extremely low strength, aggravated by its creep and fatigue behaviors which are unsuitable for applications that require moderate strength. Therefore, lead can be alloyed in order to improve its mechanical properties. In zinc electrowinning plants, lead-silver alloy has been widely used as an insoluble anode material. The lead-silver alloy anode in acidic sulfate bath has favorable features (Umetsu et al. 1985). Small amounts of Ag (0.7-1.0wt.%) alloyed with lead decrease the oxygen overpotential and increase the corrosion resistance of material during electrolysis. The resulting benefits are a longer anode life and a lower Pb content in the cathodic zinc deposit (Tikkanen and Hyvarinen1972).

2.1.3 Lead Anode Corrosion

Many research works have been done on different lead-base anodes in order to optimize the anodic process with low overpotential of oxygen evolution reaction (OER) and high corrosion resistance (Stelter et al. 2006; Yu and O'Keefe 2002). Zhang (2010) studied different concentrations of silver (0.25, 0.58, 0.60, and 0.69wt.%) alloyed with lead (Table 2.1).

Table 2.1 Chemical composition (wt.%) of four lead alloy anodes (Zhang 2010)

Anode	Ag	Zr	Ca	Al	Au	Fe	Cu	Ba	Ni	W	S	Pb
#1	0.25	0.22	0.10	<0.05	<0.01	<0.05	<0.05	<0.05	<0.05	0.10	0.12	bal.
#2	0.60	0.23	0.05	<0.05	<0.01	<0.05	<0.05	<0.05	<0.05	0.10	0.09	bal.
#3	0.58	0.24	0.06	<0.05	<0.01	<0.05	<0.05	<0.05	<0.05	<0.05	<0.05	bal.
#4	0.69	0.22	0.22	<0.05	<0.01	<0.05	<0.05	<0.05	<0.05	<0.05	<0.05	bal.

At a current density of 50 mA/cm^2 and 38°C, the anode Pb-0.69%Ag alloy had the lowest overpotential followed closely by that of anodes Pb-0.6%Ag and Pb-0.58%Ag alloys and then anode Pb-0.25%Ag alloy. The overpotentials of the anodes #4, #2, #3 and #1 were 712, 725, 733 and 753 mV, respectively. The corrosion rates of the four anodes decreased with

the potential decay time. The higher decay potential leads to the higher corrosion rate for all anodes (Table 2.2).

Table 2.2 Corrosion potentials, corrosion currents of the four lead-base anode after 1 h and 2 h potential decay following 5 h gavanostatic polarization at 50 mA/cm^2 in acid zinc sulfate electrolyte without $MnSO_4$ addition at 38°C (Zhang 2010)

Anodes	E_{corr} (mV vs SHE)		i_{corr} (μA/cm^2)	
	First hour decay	Second hour decay	First hour decay	Second hour decay
#3	1257	1128	18.02	9.37
#1	989	612	7.43	3.59
#2	872	558	5.84	2.96
#4	764	476	5.07	1.81

Petrova et al. (1999) studied another four different anodes as follows: Pb-1% Ag (#1), Pb-0.18% Ag-0.012% Co (#2), Pb-0.2% Ag-0.06% Sn-0.03% Co (#3) and Pb–0.2% Ag-0.12% Sn-0.06% Co (#4). The ternary alloy (#2) showed a higher anodic potential and lower corrosion resistance than the industrially used binary alloy (#1). The quaternary alloys (#3) and (#4) displayed lower anodic polarization than the industrial Pb-1%Ag (alloy #1) anode. This could be due to the favorable effect of cobalt inclusions. Thus, the energy cost of the zinc electrowinning process using sulfate electrolytes could be reduced by improving the anodic material composition (Fig. 2.2).

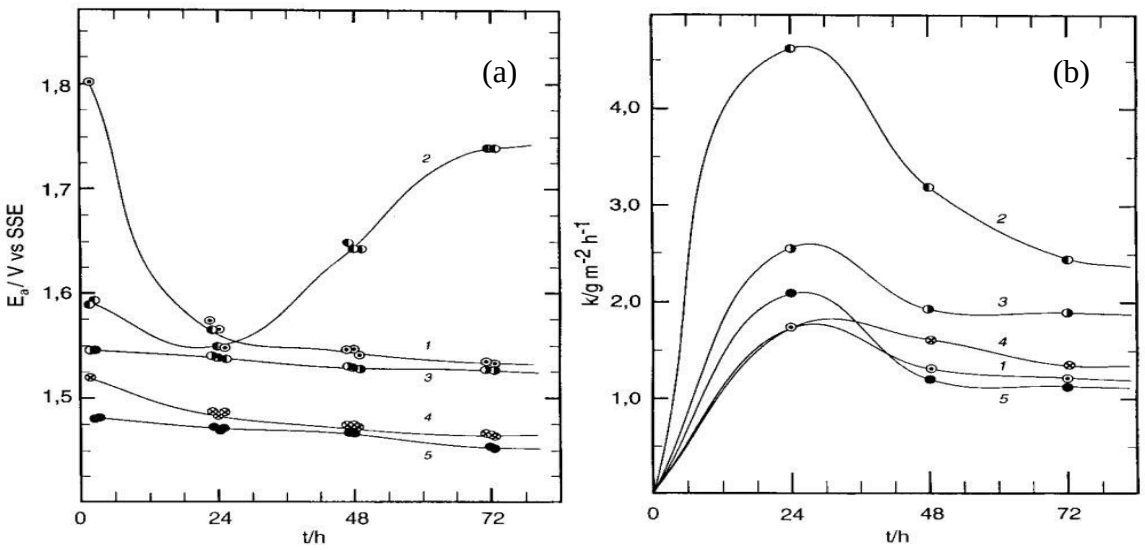

Fig. 2.2 (a) anodic potential vs. time, (b) corrosion resistance vs. time of lead alloy electrodes in zinc electrowinning electrolyte 1) Pb-1%Ag; 2) Pb-0.18%Ag-0.012%Co; 3) Pb-0.18%Ag-0.012%Co; 4) Pb-0.2%Ag-0.06%Sn-0.03%Co; 5) Pb-0.2%Ag-0.12%Sn-0.06%Co (Petrova et al. 1999)

2.2 Impurities in Zinc Electrowinning

During the hydrometallurgical processing of zinc, some metallic impurities which were present in the zinc concentrated ores can pass through various steps of the plant (blend roasting, zinc oxide leaching, and electrolyte purification) and contaminate the electrolysis baths. Some of these impurities such as arsenic, cadmium, and selenium are already removed to a considerable extent during blend roasting through controlling the temperature and duration of the process. In the successive zinc oxide leaching, with sulfuric acid solution coming from the electrolysis cells, most of the impurities are eliminated. Actually, during the leaching process, ferric hydroxide precipitates and adsorbs impurities such as antimony, arsenic, and germanium, dragging them into the mud. The electrolyte coming from the leaching is further purified with zinc dust or zinc plates to precipitate copper, cadmium, and thallium and by addition of organic compounds like nitrosonaphthol and dimethylglyoxime to eliminate cobalt and nickel. The efficiency of the purification during the leaching can decrease if the characteristics of the concentrated ores abruptly vary and the amount of ferric hydroxide is insufficient to adsorb the impurities or if some zinc sulfide remains in the roasted material. In the last case zinc sulfide exerts a reducing action

on the ferric hydroxide causing its local dissolution and consequent desorption of the impurities (Maja et al. 1982).

The electrolyte, newly enriched in zinc, passes again through the cell and more zinc is deposited. The electricity requirements for an industrial electrolytic zinc process are of prime concern economically, and are best indicated by two factors: current efficiency and cell voltage (Alfantazi and Dreisinger 2001). Even though the current efficiency may be near maximum (100%), it does not necessarily follow that the corresponding power efficiency is also a maximum. The reason for this lies in the cell voltage factor of the power efficiency. The cell voltage contains important contributions from activation, resistance, concentration overpotentials at the zinc cathode & anode, within the electrolyte, ohmic-potential differences in the conductors and connectors external to the cell (Mackinnon et al. 1979). In most cases, the current efficiency can be used to adequately describe the behavior of the process. Impurity concentration in the electrolyte is one of the challenges faced by the electrolytic zinc industry (Muresan et al. 1996).

The presence of metallic impurities in zinc sulfate electrolyte has a detrimental effect on zinc electrowinning industry. Low concentrations of metallic impurities have negative influence on the zinc deposited on the cathode, leading to a decrease in current efficiency, deposit morphology, and cell voltage (Ault and Frazer 1988; Muresan et al. 1996). In fact, the reduction of hydrogen ions in solution is affected in the presence of the impurities. Certain impurities, such as: Ge and Sb may facilitate the hydrogen evolution reaction (HER), other impurities such as: Ni and Co cause re-dissolution of the zinc deposit, but this occurs only after an incubation period that is dependent on the impurity concentration and on zinc-acid ratio (Mackinnon et al. 1987; Bozhkov et al. 1990a; Jianming et al. 2013). Cd is found to promote zinc deposition by diminishing the nucleation overpotential and it is co-deposited with zinc on an aluminum cathode, the grain size of the deposit is larger than in the absence of cadmium. In addition, Cu is found to have a harmful effect on zinc electrowinning. The cathodic deposit is non-adherent, consisting of porous microspheres, a parallel discharge of Cu ions takes place and hydrogen evolution and zinc deposition are enhanced (Mursean et al. 1996).

2.2.1 Effect of Manganese on Electrowinning Process

After many purification steps, manganese is found in the concentrates as an impurity in divalent form. The amount of manganese contained in zinc concentrates can vary considerably and some manganese is advantageous for leaching and electrolysis. About 1.5-3 g/L of Mn^{2+} is required in the electrolyte to minimize lead anode corrosion and to reduce the contamination of the cathodic zinc with lead (Ivanov and Stefanov 2002). Sorour et al. (2015) studied the effect of certain additives in a zinc electrolyte containing 8 g/L Mn^{2+} similar to that used in the Canadian zinc electrowinning industry. Stender and Pecherskaya (1950) studied the effect of Mn^{2+} ions on the zinc electrodeposition and found that Mn^{2+} ions, oxidized anodically to form MnO_4^- ions, cause depolarization of the H^+ ion discharge during the electroreduction of Zn^{2+} and thus reduce the current efficiency for zinc deposition. The formed MnO_4^- reacts immediately with Mn^{2+} ions and produces Mn^{3+} ions then MnO_2, which can absorb deleterious ions. It was also found that the amount of MnO_2 formed depends on the anode material (Tswuoka 1960). Kiryakov et al. (1958) have found that the presence of manganese in the electrolyte improved the structure of the zinc deposit at low concentration but decreased the current efficiency by a few percent when the concentration exceeded 10 g/L.

Lower concentrations of $MnSO_4$ did not influence significantly the cathodic process in zinc electrowinning, whereas they played a significant role in the anodic process, where it was intimately involved in the formation of oxide layers on the Pb-Ag anodes and thus helped to minimize anode corrosion and thus the Pb content of the zinc deposit. With high concentrations of Mn^{2+} >10 g/L, a slight decrease in current efficiency may occur because of the reduction of higher valence of manganese species at the cathode. Similar results are also observed by (MacKinnon 1994; MacKinnon and Brannen 1991; Vakhidov and Kiryakov 1959). MnO_2 demonstrated good catalytic activity for the oxygen evolution reaction (OER) in both acidic and alkaline solutions. Since manganese usually exists in the zinc electrowinning electrolyte, its dissolution in the electrolyte does not affect the electrowinning process (Mohammadi and Alfantazi 2015).

2.2.1.1 Effect of Manganese Ions on the Cathode

Zhang and Hua (2009) investigated the effect of Mn^{2+} ion on the reduction of Zn^{2+} ion on aluminum cathode from the synthetic acid zinc sulfate electrolyte using cyclic voltammetry. As shown in Fig. 2.3. The point 'B' is referred to as the nucleation potential (E_{nu}), corresponding to the reduction of Zn^{2+} ion. The point 'D' is referred to as the cross overpotential where the current reaches zero.

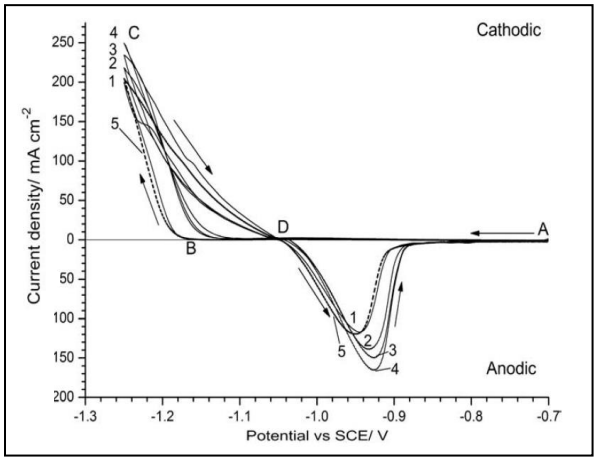

Fig. 2.3 (a) Cyclic voltammograms on aluminum of acidic zinc sulfate solutions in the presence of Mn^{2+}: (1) Blank, (2) 1 g/L, (3) 5 g/L, (4) 10 g/L, (5) 10 g/L with a membrane separation of the electrode compartments (Cathodic and anodic values are introduced by C. Su) (Zhang et al. 2009)

The values of nucleation overpotential potential (NOP) can be determined from the cyclic voltammograms (Mohanty et al. 2001), which are regarded as an indicator of the extent of polarization of a cathode. It is found that the NOP is very sensitive to the presence of Mn^{2+} in the electrolyte without separation of the cathodic and anodic compartments (curves 2-4). This addition depolarizes the cathode (decreases the NOP) and promotes a progressive shift of the deposition potential to more positive values compared to the manganese-free electrolyte. It is observed that the NOP is essentially unchanged in the presence of 10 g/L of Mn^{2+} ions when the electrode compartments are separated (curve 5). Comparing this with the result obtained with the same Mn^{2+} concentration but without separation of the compartments (curve 4) it is apparent that this depolarization of the cathode is caused by the diffusion of MnO_4^- ions and oxidized products to the cathode. These products build up

after repetitive scans and are prevented by a membrane when the electrode compartments are separated (Ivanov and Stefanov 2002). The decrease in the NOP value is likely to increase the rate of zinc deposition as well as hydrogen evolution and this effect enhances with an increase in manganese addition concentration (Zhang et al. 2009).

The cathodic potentiodynamic polarization curves for zinc electrodeposition of aluminum electrode from acidic zinc sulfate solutions in the absence and in presence of Mn^{2+} are presented in Fig. 2.4. It can be seen that the electro-reduction potential of Zn^{2+} ion practically did not change in the presence of Mn^{2+} with separation of the compartments using a membrane in comparison to the manganese-free solution (curves 1 and 5). Whereas an increase in the Mn^{2+} concentration in the electrolyte without separation of the compartments causes a progressive decrease in the electroreduction potential of Zn^{2+} ion (curves 2-4). This depolarizing effect could be due to the increase in the rate of electron transfer for both Zn^{2+} and H^{+} reduction by the oxidation products of manganese rather than dissolved Mn^{2+} ions and this result is consistent with the results obtained from cyclic voltammetry (Zhang et al. 2009).

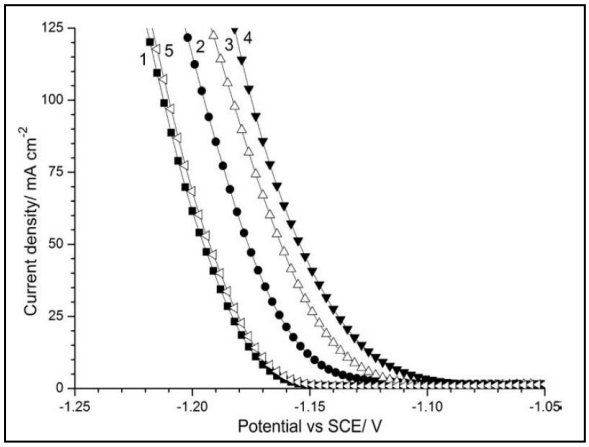

Fig. 2.4 Cathodic polarization on aluminum of acidic zinc sulfate solutions in the presence of Mn^{2+}: (1) Blank, (2) 1 g/L, (3) 5 g/L, (4) 10 g/L, (5) 10 g/L with a membrane separation of the electrode compartments (Zhang et al. 2009)

At lower Mn^{2+} concentration in the range of 1-10 g/L, the current efficiency (CE) does not change significantly. For example, the CE is 90.8% in the Mn-free solution and it is practically unaffected by the presence of Mn^{2+} at ≤ 5 g/L. Increasing the concentration up to 10 g/L decreases the CE by 1.7% in comparison to Mn-free solution. MacKinnon and Brannen (1991) reported a ~2% decrease in the CE for zinc electrodeposition from acidic zinc sulfate solutions in the presence of 10 g/L Mn^{2+}. However, a decrease in CE of ~8% is observed when Mn^{2+} concentration increases up to 20 g/L; and CE drops rapidly to 55.6% with 50 g/L Mn^{2+}. It is shown that there is a progressive decrease in the fraction of Mn^{2+} ions remaining after 2h electrolysis as the initial concentration increases, which can be attributed to the partial oxidation of Mn^{2+} ions at the anode, either to permanganate and other manganates (Wark 1979).

2.2.1.2 Effect of Manganese Ions on the Anode

The formation of a MnO_2 layer on the lead-base anode surface changes the anodic polarization behavior and probably the corrosion rate and life of the anodes. This could affect the transfer of lead impurities to the deposited zinc on the cathode (Yu and O'Keefe 2002). In the numerous studies reported on manganese oxidation, it is generally agreed that when the potential is scanned in a positive direction, Mn^{2+} may be oxidized to Mn^{4+} (Zhang et al. 2013):

$$Mn^{2+} + 2H_2O \rightarrow MnO_2 + 4H^+ + 2e^- \qquad E^0 = 1.223\ V \qquad (2.11)$$

While this reaction is favored at higher pH values, Mn^{3+} formation would be preferred in more acidic solutions (it should be noted that the E^0 values are for the reduction reaction)

$$Mn^{2+} \rightarrow Mn^{3+} + e^- \qquad E^0 = 1.509\ V \qquad (2.12)$$

The E^0 values reported for Mn^{2+} / Mn^{3+} may actually be much lower than those listed above according to some studies. Also, Mn^{3+} is readily hydrolyzed and complexation with sulfate may occur:

$$Mn^{3+} + H_2O \rightarrow MnOH^{2+} + H^+ \qquad \log K = 0.4 \qquad (2.13)$$

$$Mn^{3+} + HSO_4^- \rightarrow MnSO_4^+ + H^+ \qquad (2.14)$$

this lowers the potential of the Mn^{3+} / Mn^{2+} couple. At higher potentials, the formation of MnO_4^- dominates, which could also form from Mn^{2+}

$$Mn^{2+} + 4H_2O \rightarrow MnO_4^- + 8H^+ + 5e^- \qquad E^0 = 1.512 \text{ V} \qquad (2.15)$$

or possibly from MnO_2 (Zhang and Park 1994)

$$MnO_2 + 2H_2O \rightarrow MnO_4^- + 4H^+ + 3e^- \qquad E^0 = 1.705 \text{ V} \qquad (2.16)$$

Increasing the Mn^{2+} concentration favored the formation of Mn^{3+}, demonstrating that stable Mn^{3+} solutions could be formed in 4.6-7.2 M sulfuric acid. When PbO_2 anodes were polarized in different concentrations of sulphuric acid, the electrolytic oxidation of Mn^{2+} to Mn^{3+} was also confirmed (Welsh 1967).

The MnO_2 formation mechanisms have been discussed extensively (Bai et al. 1993). The primary hypothesis includes formation through various adsorbed species such as MnOOH and disproportionation of Mn^{3+}. For the MnOOH mechanism, the reaction is

$$Mn^{3+} + 2H_2O \rightarrow MnOOH + 3H^+ \qquad K = 1.8 \qquad (2.17)$$

and the subsequent oxidation of MnOOH is believed to be responsible for the nucleation of MnO_2

$$MnOOH \rightarrow MnO_2 + H^+ + e^- \qquad E^0 = 0.952 \text{ V} \qquad (2.18)$$

While different mechanisms may be possible, the results observed in this study tend to show that disproportionation should definitely be considered. MnO_2 appears not only on the PbO_2 surface, but extensive deposition is present on the insulating epoxy surrounding the anode in areas where no direct Faradic reactions such as Equations 2.11 and 2.18 should occur. The MnO_2 precipitate also seemed to follow the natural convection direction, rising upward and forming away from the anode surface. It is possible that MnO_2 nucleated on the anode surface and was then carried away and redeposited on surrounding areas. However, the disproportionation reaction proposed by Welsh (1967) is written as follows:

$$2Mn^{3+} + 2H_2O \rightarrow MnO_2 + Mn^{2+} + 4H^+ \qquad \log K = 9.67 \qquad (2.19)$$

or, in the hydrolyzed form as

$$2MnOH^{2+} \rightarrow Mn^{2+} + MnO_2 + 2H^+ \qquad \log K = 8.06 \qquad (2.20)$$

which should be considered as another alternative. It was also reported that the MnO_2 formed could further catalyze the disproportionation of Mn^{3+} (Ciavatta et al. 1969). The source of the Mn^{3+} could be either from Mn^{2+} oxidation or the reaction between Mn^{2+} and MnO_4^- as

$$4Mn^{2+} + MnO_4^- + 8H^+ \rightarrow 5Mn^{3+} + 4H_2O \qquad \log K = 0.268 \qquad (2.21)$$

$$4Mn^{2+} + MnO_4^- + H_2O + 3H^+ \rightarrow 5MnOH^{2+} \qquad \log K = 43.1 \qquad (2.22)$$

and/or the oxidation of Mn^{2+} by PbO_2 (Randle and Kuhn 1989) as

$$2Mn^{2+} + PbO_2 + HSO_4^- + 3H^+ \rightarrow 2Mn^{3+} + PbSO_4 + 2H_2O \qquad \log K = 4.02 \qquad (2.23)$$

$$2Mn^{2+} + PbO_2 + HSO_4^- + H^+ \rightarrow 2MnOH^{2+} + PbSO_4 \qquad \log K = 4.82 \qquad (2.24)$$

The higher acid concentration generated at the anode interface by water oxidation also favors Equations 2.22 through 2.24. Equations 2.23 and 2.24 are most feasible at higher Mn^{2+} concentrations and when the electrode potential is in a medium range where transitions between Pb^{2+} and Pb^{4+} are active.

In recent studies carried out for electrolytes containing 180 g/L H_2SO_4 and Mn^{2+} without Zn^{2+} ions, XRD studies for the anode confirmed the presence of α-MnO_2. In Mn^{2+}-free Zn electrolyte, lead sulfates and oxides are formed and the generated corrosion layer has a uniform appearance, whereas the anodic potential was by approximately 50 mV higher with respect to the Mn^{2+}-containing system (Jaimes et al. 2015).

2.2.2 Effect of Lead Ions

As long as Pb-base anodes continue to be used in zinc electrowinning, the possibility of varying degrees of Pb contamination of the zinc deposits exists, either as a result of improperly conditioned anodes or because the anodes were deteriorated over a period of time. Pb is deposited at the cathode, decreasing the purity of the zinc (Sorour et al. 2015; MacKinnon and Brannen 1979).

The addition of lead as a lead acetate solution to acid zinc electrolyte containing 55 g/L Zn^{2+}, 150 g/L H_2SO_4 produced significant changes in the morphology and crystallographic orientation of zinc deposits obtained from addition-free zinc electrolyte at all different

current densities (Table 2.3). The lead acetate addition had a significant effect on the morphology but not on the orientation of zinc deposits obtained at high current density (807 A/m^2). However, at low current densities (215 A/m^2) lead acetate addition to the electrolyte affected both the morphology and orientation of the zinc deposits (MacKinnon and Brannen 1979).

Table 2.3 Effect of lead contamination as a function of current density on zinc deposition, crystallographic orientation and lead content of zinc deposits obtained from addition-free electrolyte (electrolysis conditions: 150 g/L H_2S0_4, 55 g/L Zn^{2+}, 215 A/m^2, and Pt anodes) (MacKinnon and Brannen 1979)

Current density (A/m^2)	Impurities Pb (mg/L)	Crystallographic orientation	Cathode lead (wt.%)
807	0	(112)(102)	0.0040
807	1	(101)	0.0047
807	3	(101)(100)	0.0164
807	9	(100)(101)	0.0465
430	0	(112)(102)	0.0024
430	3	(100)(101)	0.0399
430	9	(100)(101)	0.1535
215	1	(101)	0.0285
215	9	(101)(100)	0.0680

Lead added to the addition-free electrolyte as slurry of $PbSO_4$ or PbO had only a slight effect on the zinc deposit morphology as indicated by the SEM photomicrographs shown in Fig. 2.5. For example, the addition of 9 mg/L $PbSO_4$ or PbO at 870 A/m^2, Fig. 2.5b and 2.5e, resulted in a zinc deposit morphology very similar to that obtained for the addition of 1 mg/L Pb (as lead acetate) (Fig. 2.5b) under similar experimental conditions. All three zinc deposits contained similar concentrations of lead (Table 2.3). At 430 A/m^2 the effect of $PbSO_4$ and PbO (Fig. 2.5c and 2.5f) was similar to that produced at 870 A/m^2. The crystallographic orientation was predominantly (101), i.e. the platelets were intermediate but tending towards a perpendicular alignment to the A1 cathode. Lead contamination of the zinc deposits was less than when lead acetate was added under similar conditions (Table 2.3). The poor solubility of $PbSO_4$ or PbO added to the zinc electrolyte as compared to lead

acetate probably accounts for the difference. Contamination of the deposits by particulate $PbSO_4$ or PbO does not appear to be important under the conditions employed in these tests.

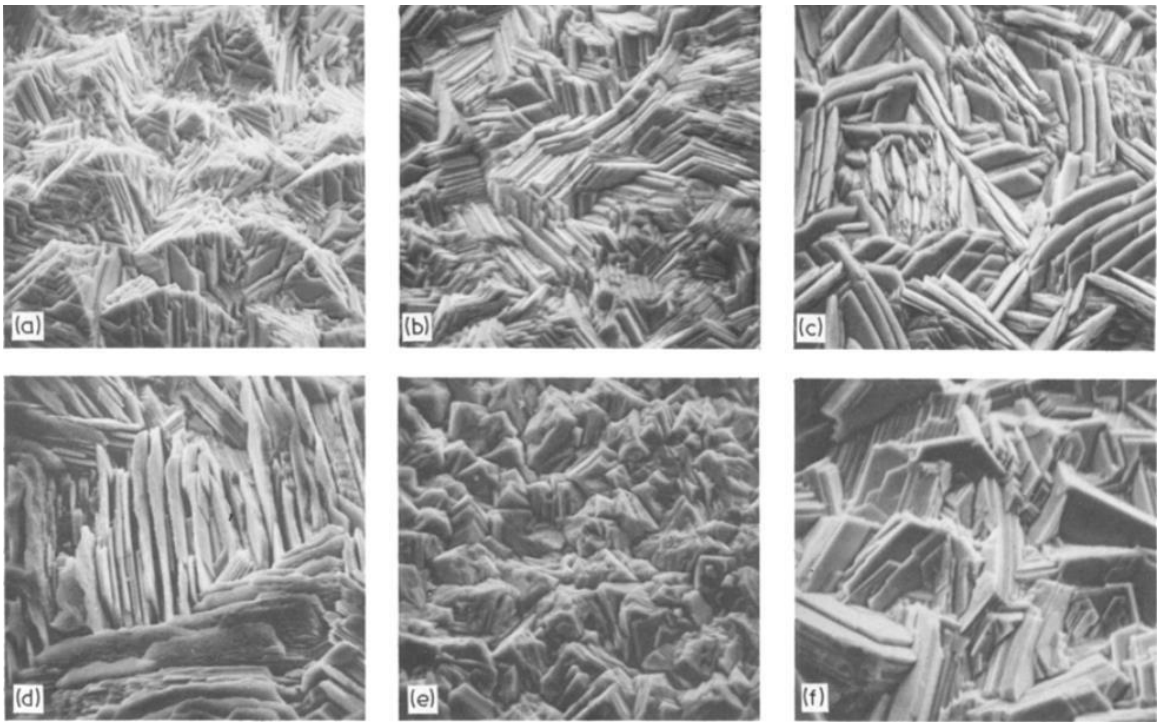

Fig. 2.5 SEM photomicrographs at 770X of zinc deposits obtained from addition-free electrolyte at (a), (b), (d), (e) 807 A/m^2 and (c), (f) 430 A/m^2: (a) 3 mg/L $PbSO_4$; (b) 9 mg/L $PbSO_4$; (c) 9 mg/L $PbSO_4$; (d) 3 mg/L PbO; (e) 9 mg/L PbO, (f) 9 mg/L PbO (electrolysis conditions: 150 g/L H_2SO_4 and 55 g/L Zn^{2+}at 35°C) (MacKinnon and Brannen 1979)

Sorour et al. (2015) examined the effect of different organic additives on the contamination of zinc deposits by lead. The zinc deposits were analyzed using inductively coupled plasma (ICP) to determine the lead concentration. It was found that additives [EMIM]MSO_3 and [BMIM]Br have the same effect on reducing lead concentration, as adding 3 mg/L to the zinc electrolyte reduced lead concentration from 26.5 ppm to 5.1-5.6 ppm in the absence of antimony and to 4.0-5.1 ppm in the presence of antimony (Table 2.4).

Table 2.4 Lead concentration of zinc deposits obtained by adding 3 mg of gelatin, [EMIM]MSO_3 and [BMIM]Br in the absence and presence of Sb(III) during zinc electrodeposition for 2 h at 50 mA/cm^2 and 38°C with agitation at 60 rpm (electrolysis conditions: 180 g/L H_2SO_4, 60 g/L Zn^{2+} and 8 g/L Mn^{2+}) (Sorour et al. 2015)

	Additive (mg/L)	Sb (III) (mg/L)	Lead conc. (ppm)
SE	0	0	26.5
	0	0.0055	3.6
Gelatin	3	0	17.4
	3	0.0055	4.1
[EMIM]MSO_3	3	0	5.1
	3	0.0055	5.1
[BMIM]Br	3	0	5.6
	3	0.0055	4.0

2.2.3 Other Metallic Impurities

Antimony has long time been recognized as one of the most detrimental impurities with respect to zinc deposition CE, and its effects have been studied by many researchers. The antimony impurity co-deposited with zinc and behaves as a cathode with respect to the zinc deposit and catalyzes the hydrogen discharge. In spite of its detrimental effect on CE due to the hydrogen evolution reaction, a small concentration of antimony is usually added to the zinc electrolyte because it is thought to reduce zinc deposit adherence to the aluminum cathode and because of its beneficial interaction with glue (Mackinnon et al. 1990 a).

For Sb > 0.02 mg/L to the electrolyte, there is a significant decrease in CE; for Sb > 0.06 mg/L, the decrease in CE becomes disastrous and at 0.08 mg/L Sb, the CE is only 29.0%. The addition of 0.005 mg/L Sb to the electrolyte changed the deposit orientation from (002), (103) to (114), (112), (103), (102), (101) which persisted for Sb concentrations up to 0.02 mg/L. This is reflected in the deposit morphology, which shows sharply defined hexagonal zinc platelets aligned at intermediate angles to the A1 cathode. However, at 0.02 mg/L Sb, the deposit surface consists of numerous circular depressions. At 0.04 mg/L Sb, the circular depressions are more developed and appear as large circular holes in the surface, suggesting resolution of the deposit (Fig. 2.6).

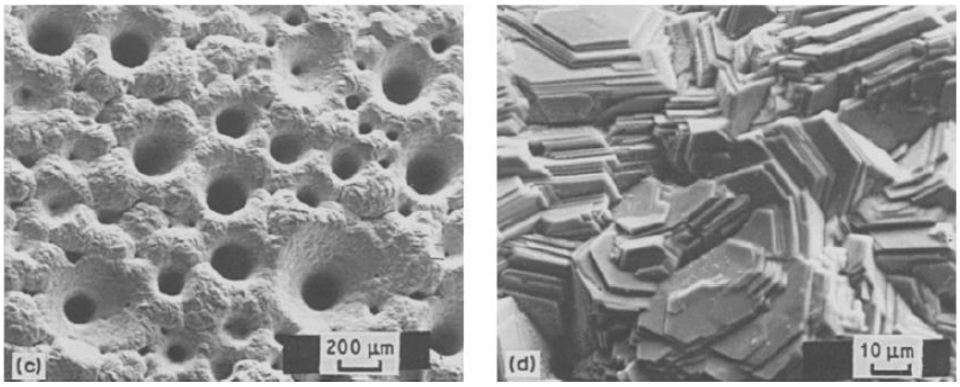

Fig. 2.6 SEM micrographs of 6 h zinc deposits electrowinning at 500A/m^2 and 38°C from electrolytes containing 0.04 mg/L Sb, 200 g/L H_2SO_4 and 55 g/L Zn^{2+} (Mackinnon et al. 1990 a).

During zinc electrowinning from sulfate electrolytes containing nickel, a process of re-dissolution of deposited metal takes place (Mackinnon and Morrison 1986). During this induction period, which is linked with the beginning of zinc electrodeposition, the zinc deposits are uniform and adhere firmly to the cathode. The typical current efficiency is about 95%. Following this induction time, zinc re-dissolution occurs with hydrogen evolution. After the zinc is completely dissolved, deposition restarts. The induction time depends on several factors such as temperature, cathodic current density, concentrations of sulphuric acid and zinc ions and finally the impurities. The nickel impurities co-deposited with zinc behave as a cathode with respect to the zinc deposit and catalyzes the hydrogen discharge. However, the induction time is only observed in the presence of iron-group metal impurities. The overpotential of hydrogen evolution on nickel is about 0.6 V lower than that on zinc (Bozhkov et al. 1990). Nickel can dramatically depolarize the discharge of hydrogen ions acting as Sb. The induction time is related to the hydrogen bubble formation stage on the active regions of the cathode surface, containing co-deposited nickel (Wiart et al. 1990).

Morrison et al. (1992) determined the individual effect of cobalt on the CE, the polarization behavior for zinc deposition, the morphology/orientation, and the impurity content of 24 h zinc deposits in electrolyte containing of 60 g/L Zn^{2+}, 200 g/L H_2SO_4 at 500 A/m^2 and 38°C. The CE begins to decrease significantly when the Co concentration in the electrolyte

becomes > 0.5 mg/L. The decrease in CE with increasing Co when concentrations are > 1 mg/L as the deposit orientation remains intermediate and the deposit electrowon from the electrolyte containing 5 mg/L has yielded a basal orientation. At low concentrations of Co (i.e., < l mg/L), the deposit morphology remains similar to that obtained in the absence of added impurity. When concentration of Co is > 1 mg/L, the surface of the zinc deposit is characterized by numerous circular holes and depressions. At 5 mg/L Co, the deposit morphology still consists of hexagonal zinc platelets aligned at intermediate angles to the Al cathode (Morrison et al. 1992).

2.3 Operating Parameters

In zinc electrowinning, one of the major goals is minimizing the energy requirements. Optimum performance of a cell room occurs when the energy per ton of zinc produced is minimized. The cathodic current efficiency and cell voltage are the most important factors, which determine the energy consumption. Several studies reported that zinc and sulfuric acid concentrations, current density, temperature, impurities, additives levels and cathode as well as anode materials are the variables which can affect these two factors. The time of deposition can also be important if impurities are present in the electrolyte solution (Scott 1988; Alfantazi and Dreisinger 2001).

2.3.1 Electrolyte Composition

Alfantazi and Dreisinger (2001) reported change in current efficiency as a function of simultaneously varying the zinc and acid concentration in the cell electrolyte at plating cycles of 24 and 30 h (Fig. 2.7). Increasing the zinc concentration (decreasing acid concentrations) increased the current efficiency in a non-linear mode and the highest rate of increase occurred when the zinc concentration was increased from 42 to 50 g/L. The current efficiency decreases as the acid concentration increases. This is mainly due to the increase in the zinc deposition reaction rate as the number of H^+ ions in solution decreases and the rate of hydrogen evolution reaction is reduced. These results are also reported by Scott (1988) and Tozawa et al. (1993).

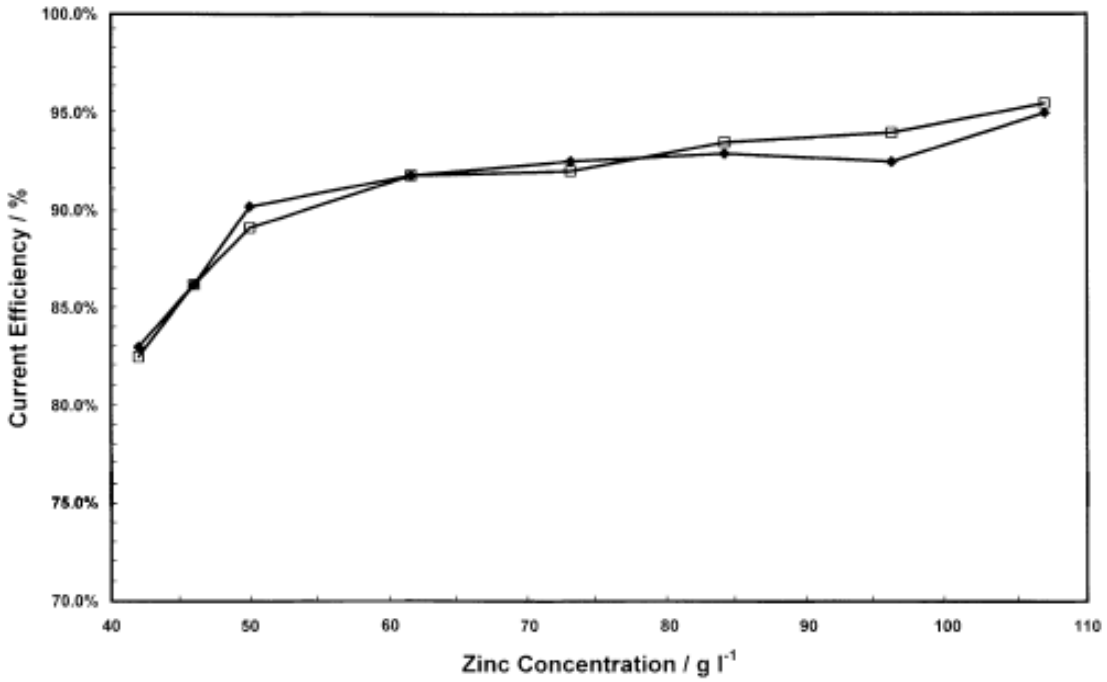

Fig. 2.7 Effects of zinc concentration in the electrolyte on current efficiency for 24 and 30 h plating cycles (◆) 24 h and (□) 30 h at 500A/m^2 and 38°C (electrolysis conditions: 189.2 g/L H_2SO_4) (Alfantazi and Dreisinger 2001)

The cell voltage drops as the zinc concentration decreases (Fig. 2.8). This behavior can be attributed mainly to the rise in the electrolyte electrical conductivity resulting from the higher acid levels (Fig. 2.9).

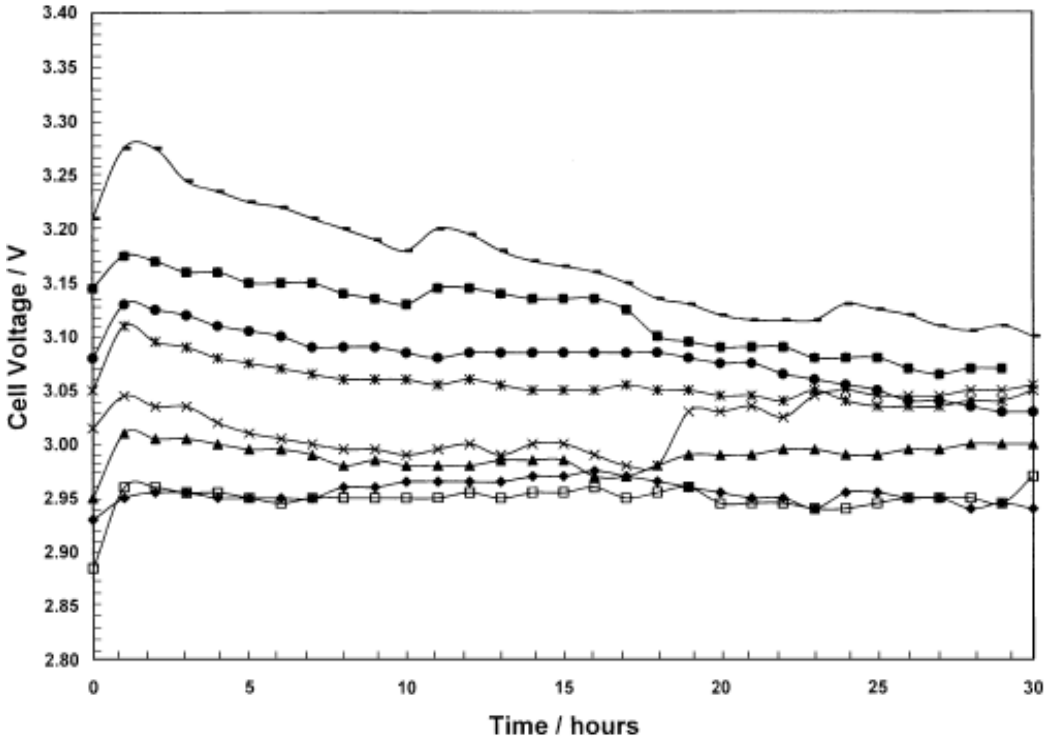

Fig. 2.8 Change of cell voltage as a function of time at various zinc concentration: (◆) 42.0, (□) 46.0, (▲) 50.0, (×) 61.5, (✱) 73.0, (●) 83.5, (■) 96.0 and (—) 107.5 g/L Zn at 500A/m^2 and 38°C (electrolysis conditions: 189.2 g/L H_2SO_4) (Alfantazi and Dreisinger 2001)

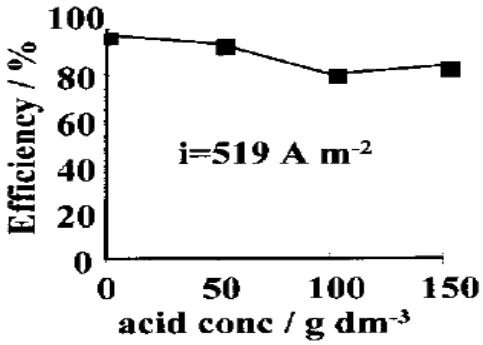

Fig. 2.9 Current efficiency against initial acid concentration at 27, 37, 47 and 57°C, 519 A/m^2 (electrolysis conditions: 35 g/L H_2SO_4, 78 g/L Zn^{2+}) (McColm and Evans 2001)

There is a decrease in current efficiency with increasing acid concentration, particularly at lower current density. Efficiencies were slightly reduced at lower current densities, the

trend with acid concentration remaining almost constant. At current densities close to 519 A/m^2, current efficiencies remain in the region of 90% for acid concentrations up to the maximum examined 150 g/L (McColm and Evans 2001).

2.3.2 Current Density

Few research works have been done on the effect of current density on zinc electrowinning process. Most of these works use high range of different densities of current. According to our knowledge, no one examined the tight range around the industrial conditions. Scott et al. (1988) had investigated the effect over a large range of current densities (100-650 A/m^2). As shown in Fig. 2.10, the mass transfer resistance is negligible over this range of current densities and zinc concentrations used industrially. The cell voltage was increased from 2.86 V at 100 A/m^2 to 3.47 V at 650 A/m^2. This could be due to the increase in the IR drop (voltage drop that appears at the resistive components) across the solution. Accordingly, there was an increase in the energy consumption from 2440 kWh/t to 2990 kWh/t by increasing current density from 100 A/m^2 to at 650 A/m^2, respectively. This was confirmed previously by Wark (1979) when similar results over the range of 95-920 A/m^2 were obtained using similar electrolyte.

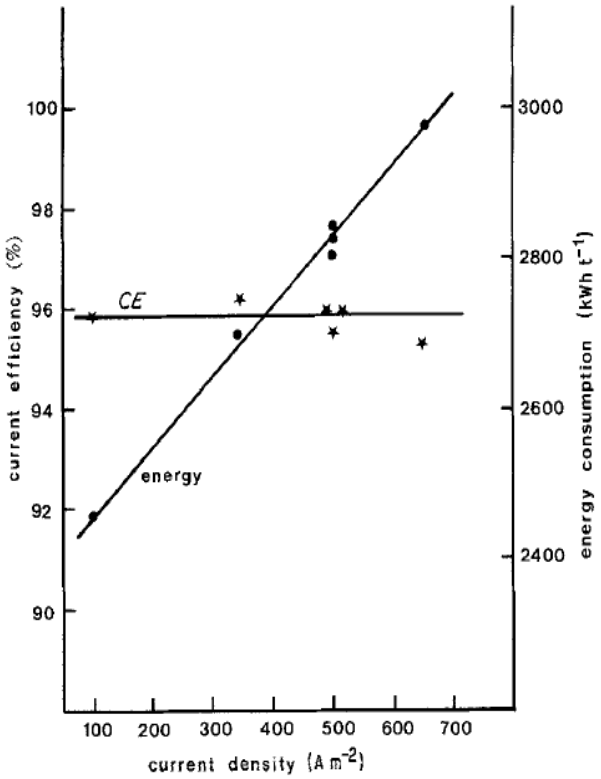

Fig. 2.10 Effect of current density on electrowinning performance (110 g/L acidity, 55 g/L Zn^{2+} at 35°C) (Scott et al. 1988)

2.3.3 Electrolyte Agitation

Normally, electrolyte agitation is intended to improve the transport and enhanc the deposit rate of metallic ions. However, bath agitation was found to reduce the current efficiency at increasing agitation rate within a certain range. Tuaweri et al. (2013) found that cathodic current efficiency was better without or at lower rates of solution agitation at a constant current density of 5 A/dm^2 (Fig. 2.11). Since the main cathodic reactions are a competition between zinc reduction and hydrogen evolution, as the limiting current density is approached during zinc deposition, the zinc ion concentration near the cathode is quickly reduced and the cathode reaction shifts from zinc deposition to hydrogen evolution.

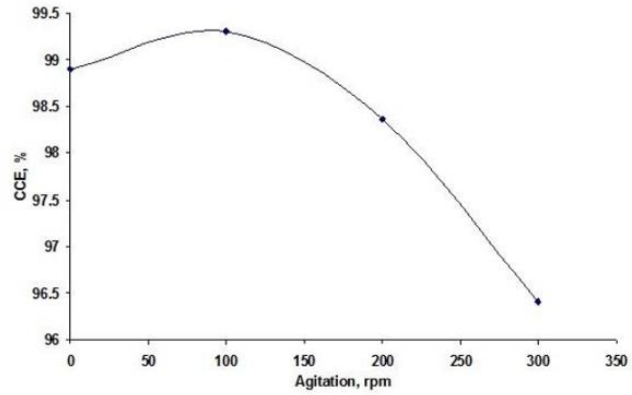

Fig. 2.11 Effect of bath agitation on the cathode current efficiency of the bath at a current density of 5 A/dm^2, and pH 2.8 at 22°C (electrolyte: 250 g/L $ZnSO_4 \cdot 7H_2O$, 80 g/L Na_2SO_4) (Tuaweri et al. 2013)

Another study has been done by Safizadeh et al. (2016) to examine the effect of agitation speed on the nucleation overpotential of zinc reduction. The relationship of E-I obtained from CV test at different agitation rates of 0, 60, 100, 412 rpm has been plotted in Fig. 2.12, also and the corresponding nucleation overpotential (NOP) values are listed in Table 2.5. It was found that agitation rate does not affect the NOP of zinc reduction as the obtained values are 91, 89, 93, 91 mV for agitation of 0, 60, 100, 412 rpm, respectively.

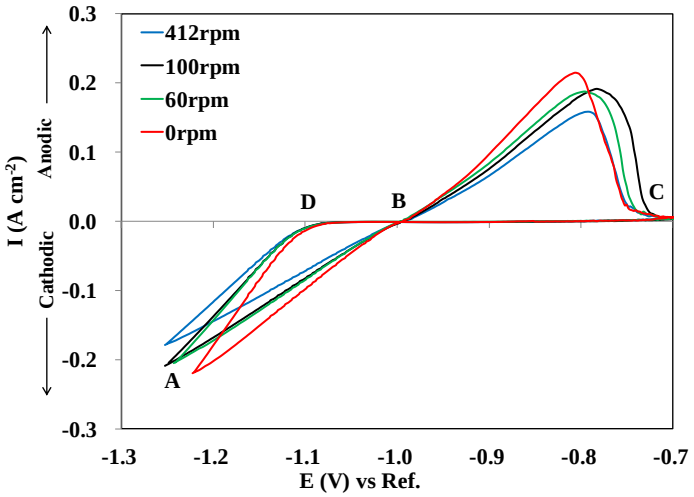

Fig. 2.12 Cyclic voltammogram curves of the Pt anode and Al cathode in zinc electrolyte containing 170 g/L H_2SO_4, 60 g/L Zn^{2+} and 0.15 mg/L of Pb^{2+} at 40°C, at different agitation rates 0, 60, 100, and 412 rpm (Safizadeh et al. 2016)

Table 2.5 Effect of different agitation rates on NOP in zinc electrolyte containing 170 g/L H_2SO_4, 60 g/L Zn^{2+} and 0.15 mg/L of Pb^{2+} at 40°C under atmospheric conditions (Safizadeh et al. 2016)

Agitation Rate	0 rpm	60 rpm	100 rpm	412 rpm
NOP (mV)	91	89	93	91

Mohammadi et al. (2013) investigated the effect of different agitation rates 0, 600, and 1000 rpm on the anodic polarization of lead-calcium anode. They found that, the oxygen evolution overpotential (OER) is increased by increasing the agitation rate of the electrolyte. Oxygen evolution potential was increased from 1.998 to 2.033 V/SCE and 2.067 V/SCE after 24 h with agitation rate of 600 and 1000 rpm in solution, respectively (Fig. 2.13)

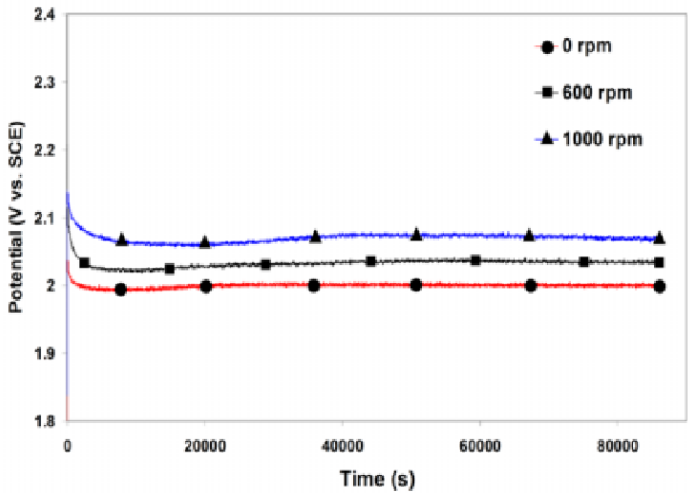

Fig. 2.13 Potential variation of the Pb-Ca anode during anodic polarization in the electrowinning solution 180 g/L H_2SO_4 and 60 g/L Zn^{2+} at 50 mA/cm^2 and 37°C (Mohammadi et al. 2013)

2.3.4 Electrolyte Temperature

Mccolm and Evans (2001) had conducted four experiments using Hull cell at different temperatures of 27, 37, 47 and 57°C. The lowest temperature was set at 27°C (room temperature) while, higher temperatures were set by the constant temperature water bath controlled by a thermostatic bath (Fig. 2.14). The electrolyte employed was synthesized

from reagent grade zinc sulfate and sulfuric acid. After a deposition time of 30 min, it was found that the optimal operating temperature was in the region of 40°C across the whole range of current densities.

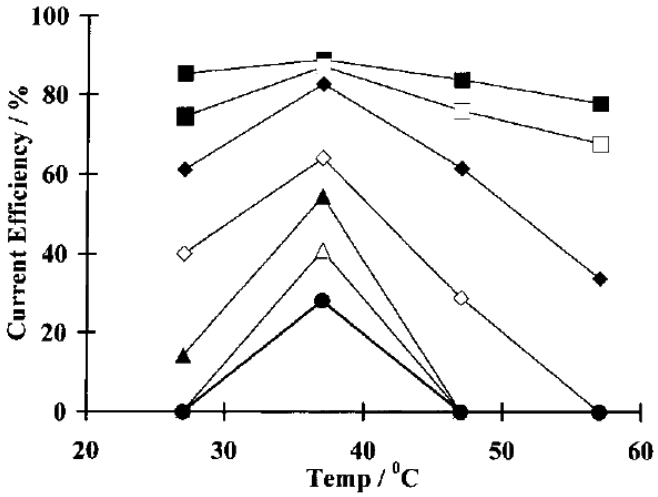

Fig. 2.14 Current efficiency against temperature at different current densities: (■) 732, (□) 563, (◆) 297, (◇) 149, (▲) 98, (△) 94 and (●) 91 A/m^2 at 27, 37, 47 and 57°C, 519 A/m^2 (electrolysis conditions: 35 g/L H_2SO_4, 78 g/L Zn^{2+}) (Mccolm and Evans 2001)

Zhang et al. (2009) studied the effect of different temperatures at certain current densities on the current efficiency, cell voltage and power consumption. It was found that current efficiency was increased with increasing temperature for the examined zone, whereas specific energy consumption decreased with increasing temperature. For example, at 500 A/m^2 the electrodeposition at standard temperature of 303K (30°C) the current efficiency was 90.4 % and cell voltage was 3.07 V, the value of CE was increased gradually up to 92.3 %, while the cell voltage was decreased to 2.95 V (Table 2.6). It is clear that increasing the temperature results in an increase in deposit current efficiency and a drop in the cell voltage (power consumption), this is associated with a reduction in the average crystallite size of the zinc deposits.

Table 2.6 Effect of temperature and current density on current efficiency and specific energy consumption during zinc electrodeposition (electrolysis conditions: 150 g/L H_2SO_4, 55 g/L Zn^{2+}) (Zhang et al. 2009)

Current Density (A/m^2)	Temperature (K)	Current Efficiency (%)	Cell Voltage (V)	Specific Energy Consumption (kWh/t)
300	303	90.2	2.95	2683
	308	90.3	2.92	2653
	313	90.6	2.90	2627
	318	91.3	2.84	2552
400	303	89.8	3.11	2841
	308	90.5	2.96	2683
	313	90.8	2.89	2611
	318	91.7	2.88	2576
500	303	90.4	3.15	2858
	308	90.9	3.07	2770
	313	91.5	3.00	2690
	318	92.3	2.95	2622
600	303	89.7	3.21	2936
	308	90.7	3.12	2822
	313	91.8	3.02	2699
	318	92.6	2.98	2640

2.4 Electrochemical Test Methods

Electrochemical testing techniques are some of the powerful tools to understand and control electrolysis and corrosion processes (Thompson and Payer 1998). Electrochemical test methods offer several benefits for studying corrosion and electrochemical activities during electrolysis: (i) electrochemical tests are relatively rapid giving results in a matter of minutes or hours preferably; (ii) real time corrosion rate measurements can be designed to provide continuous monitoring of process changes on the order of few minutes; (iii) corrosion behavior can be measured over a wide range of oxidizing conditions; and (iv) many of these methods can be applied in the laboratory or in process plants (Beavers et al. 1993).

Current electrochemical techniques applied in the mentioned studies of this thesis are:

1. Galvanostatic polarization;
2. Potentiodynamic polarization technique;

3. Cyclic voltametry (CV);
4. Electrochemical impedance spectroscopy (EIS); and
5. Electrochemical noise measurements (ENM).

2.4.1 Galvanostatic Polarization Technique

Galvanostatic refers to an experimental technique whereby an electrode is maintained at a constant current in an electrolyte. Galvanostatic is a polarization technique that allows for the controlled polarization of metal surfaces in electrolytes, in order to directly observe cathodic and anodic behaviors. In galvanostatic tests, the change in potential is plotted versus time at constant current. A constant DC current is applied to the metal of interest while it is immersed in the electrolyte. This technique is also important in determination of the kinetics and mechanism of electrode reactions based on the control of the current flowing through the system. The control apparatus used is called a galvanostat (Plonski 1969; Kopistko and Batyrbekova 1992; Corrosion 2016).

In the galvanostatic approach to measure linear polarization resistance a low current is applied.

1. The electrode potential changes;
2. The potential changes are measured;
3. Overvoltage vs. current is plotted and the slope calculated.

2.4.2 Potentiodynamic Polarization Technique

Potentiodynamic polarization technique monitors the measurement of polarization behavior by scanning the potential continuously while monitoring the current response. This experimental method permits the easy automation of curves and real time plots of the experimental data. The ability to automate data taking, potentiodynamic polarization techniques has become much more popular than the potentiostatic technique for producing polarization curves. Potentiodynamic polarization provides better potential resolution when compared to the potentiostatic technique where potential steps of 25 to 50 mV are typically used. Potentiodynamic polarization tests have become fully automated with computer-based, menu-selectable programs for establishing test parameters and performing the tests.

However, it is more instructive to discuss the individual components of the required instrumentation to permit a complete understanding of the test methods (Beavers et al. 1993).

Potentiodynamic polarization is the characterization of a metal specimen by its current-potential relationship. The specimen potential is scanned slowly normally with scanning rate of 0.166 V/s according to ASTM G5 and sometimes even lower than 0.1 V/s (Thompson and Payer. 1998) in the positive going direction and therefore acts as an anode such that it corrodes or forms an oxide coating. These measurements are used to determine corrosion characteristics of metal specimens in aqueous environments. A complete current-potential plot of a specimen can be measured in a few hours or, in some cases, a few minutes depending on the scan rate.

Investigations such as passivation phenomena and effects of inhibitors or oxidizers on specimens are easily detected with this technique. With this knowledge, the corrosion characteristics of different metals and alloys can be compared on a rational basis and compatible specimen-environment combinations secured for further long term testing. When the investigated metal specimen is immersed in a corrosive medium, both reduction and oxidation processes occur on its surface. Typically, the specimen oxidizes (corrodes $M \rightarrow M^{z+} + ze^-$) and the medium (solvent) is reduced. In acidic media in absence of dissolved oxygen, hydrogen ions are reduced ($H^{2+} + 2e^- \rightarrow H_2$). The specimen must function as both anode and cathode and both anodic and cathodic currents occur on the specimen surface. Any corrosion processes that occur are usually a result of anodic currents.

Fig. 2.15 shows the diagrams of this process. The vertical axis is potential and the horizontal axis is the logarithm of absolute current. The theoretical current for the anodic and cathodic reactions are shown as straight lines. The curved line is the total current, the sum of the anodic and cathodic currents. This is the current measured when you sweep the potential of the metal with the potentiostat. The sharp point is due to the use of logarithmic axis. The use of a log axis is necessary because of the wide range of current values that must be displayed during a corrosion experiment. Due to the phenomenon of passivity, it is not uncommon for the current to change by six orders of magnitude during corrosion (West 1970; Jones 1996).

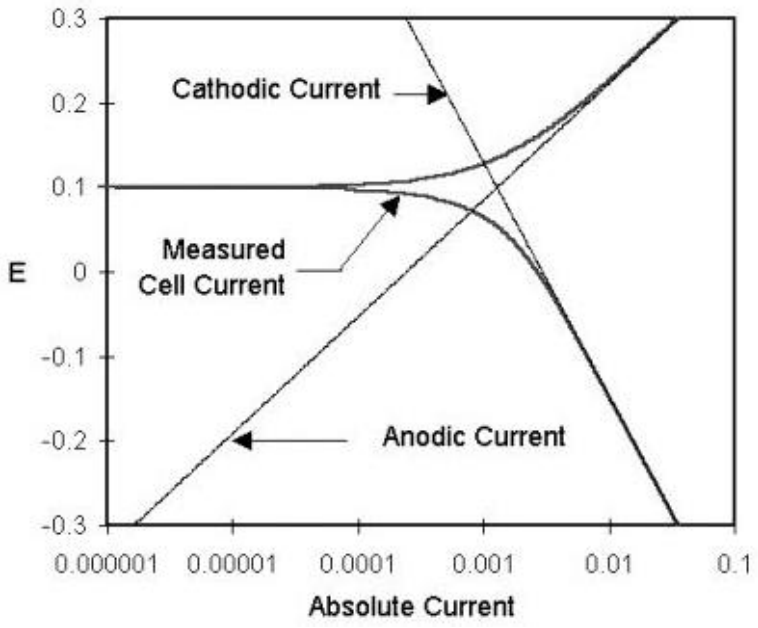

Fig. 2.15 Typical corrosion process showing anodic and cathodic current components (Jones 1996).

To determine both the anodic and cathodic curves with a single sweep, the starting potential usually is a very negative potential (e.g. 200 to 400 mV more negative than the corrosion potential), and the potential is swept in the positive direction to produce both the cathodic and anodic curves. The starting potential for a polarization curve depends on the purpose of the test. If only an anode curve is to be determined, a starting potential approximately 50 mV more negative than the corrosion potential should be used. The initial current will be cathodic, and current will switch to anodic at potentials more positive than the corrosion potential. If a cathodic polarization curve is to be determined, a starting potential should be selected that is approximately 50 mV more positive than the corrosion potential. In this case, the initial current will be anodic, and the current will switch to cathodic as the potential passes through the corrosion potential. One of the most important electrochemical rules is that the net applied current must be zero at the corrosion potential; if it is not, there are typically some problems with the experimental setup (Krauses et al. 1984; Thompson and Payer 1998; Pourbaix 1973).

2.4.3 Cyclic Voltammetry Technique

Cyclic voltammetry (CV) is used to study electrochemical reaction mechanisms that give rise to electro-analytical current signals. The method involves linearly varying an electrode potential between two limits at a specific rate while monitoring the current that develops in an electrochemical cell under conditions where voltage is in excess of that predicted by Nernst equation. Although CV is best at providing qualitative information about electrode reaction mechanisms, several quantitative properties of the charge transfer reaction can also be determined (Bard et al. 1980).

Cyclic voltammetry involves applying a voltage to an electrode immersed in an electrolyte solution, and seeing how the system responds. In CV, a linear sweeping voltage is applied to an aqueous solution containing the compound of interest. The voltage is initially given by Equation (2.25). After the voltage reaches a certain maximum value, the potential is reversed and the sign of v_t reversed and E_i becomes the maximum voltage, E_λ. The process can then be repeated in a periodic or cyclic manner. As an important tool for studying mechanisms and rate of oxidation and reduction process, CV provides the capability for generating a species during the forward scan and then probing its rate with the reverse scan or subsequent cycles, all within seconds. The unique aspect of cyclic voltammetry is the three electrodes used, which consist of a working electrode, a reference electrode and a counter electrode. The working electrode can be seen as a medium which is reductive or oxidative power can be extremely adjusted by the magnitude of the applied potential, as the potential is increased or decreased linearly versus time, it becomes a stronger oxidant or reductant, respectively. Therefore, the working electrode, which typically consists of a chemically noble conductive material such as platinum, acts as a donor or acceptor of electrons participating in the general electrode reaction as Equation (2.26), as following:

$$A + ne^- \rightarrow B^- \qquad (2.25)$$

$$O + ne^- \rightarrow R \qquad (2.26)$$

The reference electrode, typically AgCl or calomel, keeps the potential between itself and the working electrode constant. The potential is measured between the reference and working electrodes, and the current is measured between the working and counter

electrodes. A counter electrode is employed to allow accurate measurements to be made between the working and reference electrodes (Heineman and Kissinger 1983; Yang and Bard 1992; Compton and Banks 2011).

After the direction of the potential sweep is reversed, a second current peak is observed corresponding to oxidation of the product B. When Equation (2.25) is reversible, implying that B is stable, the height of the peak is equal to that observed on reduction, but with the current flowing in the opposite direction. The method of estimating peak currents is illustrated in Fig. 2.16, where Epc is the peak potential in the cathodic sweep.

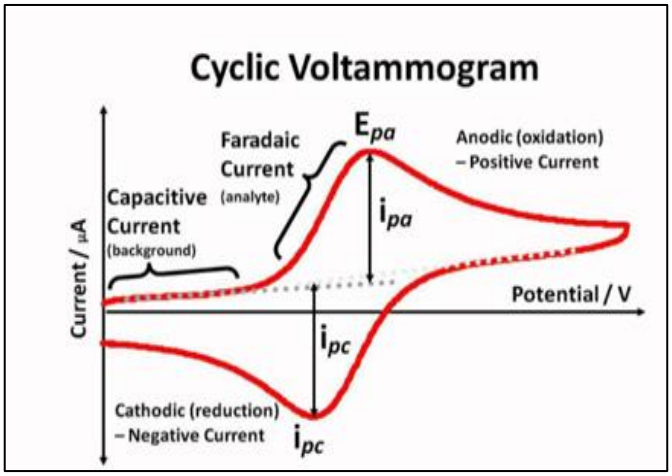

Fig. 2.16 Typical cyclic voltammogram (Compton and Banks 2011)

The cyclic voltammogram for the process A + ne^- ↔ B (Fig. 2.16) assumes that only A is initially present in the solution. ΔEp is then defined as Equation (2.27):

$$\Delta Ep = \left| Epc - Epa \right| \tag{2.27}$$

When the electrode process is reversible, ΔEp = 0.059/n and it is independent of sweep speed. As potential is increased to the stage at which Nernst equilibrium for Equation (2.25) cannot be maintained, ΔEp increases with increasing sweep rate, and the shape and position of peaks depend on both cathodic – anodic potentials and the kinetic parameters of the electrode reaction (Compton and Banks 2011).

2.4.4 Electrochemical Impedance Spectroscopy

An electrochemical reaction at the electrode/electrolyte interface cannot be fully understood by using traditional electrochemical measurements. A complete description requires impedance measurements made over a broad frequency range at various potentials and determination of all the electrical characteristics on the interface which can be thought of as a thin capacitor that forms between the charged electrode and the counter ions lined up parallel to it (Park and Yoo 2003). Electrochemical Impedance Spectroscopy (EIS) or AC impedance methods have seen tremendous increase in popularity in recent years. Initially applied to the determination of the double-layer capacitance and in AC polarography, they are now applied to the characterization of electrode processes and complex interfaces. EIS studies the system response to the application of a periodic small amplitude AC signal. These measurements are carried out at different AC frequencies and, thus, the name impedance spectroscopy was later adopted. Analysis of the system response contains information about the interface, its structure and reactions taking place there. EIS is now described in the general books on electrochemistry, and there are also numerous articles and reviews (Lasia 2002; Scully and Silverman 1993).

Electrochemical impedance spectroscopy (EIS) has been applied for over a decade for studying corrosion processes on aluminum and aluminum alloys. The technique is widely used and because of the similarities of impedance magnitude Bode plots with Electrochemical noise spectral plots, EIS can assume an important role in the analysis and comprehension of data from EN (Gouveia-Caridade et al. 2004).

2.4.5 Electrochemical Noise Measurements

The foundation of electrochemical noise (EN) technology for corrosion studies lies in the original work undertaken by Iverson et al. (1985). Initial work studies the fluctuations of electrochemical potential. Subsequently the combination of electrochemical potential and current noise arising from the coupling current between two nominally identical electrodes was investigated in detail. In 1986, Eden et al. introduced the concept of electrochemical

noise resistance and described statistical methods for analysis of electrochemical noise (Revie and Uhlig 2011).

Electrochemical noise measurements have been widely used for the characterisation and monitoring of corrosion processes during the last 20 years (Aballe et al. 1999). Types of systems which have been analyzed are many, such as iron and aluminum and its alloys (Isaac et al. 1999), coatings on metal substrates (Greisiger and Schauer 2000), erosion-corrosion (Wood et al. 2002) and microbiologically influenced corrosion (Tan et al. 2002). The increased interest in the analysis of electrochemical noise is due to the low cost of the equipment, to the possibility of measurements in situ and to the lack of intrusiveness (Aballe et al. 2002 a).

The current noise is associated with discrete dissolution events on the corroding metal surface, while the potential noise is associated with the action of current noise on interfacial impedance. The potential and current noise signals can be measured simultaneously or at different times. During the EN measurements, no external potential or current signals are applied. As a result, the EN measurements are passive monitoring of the corrosion system at freely corroding potential. Electrochemical noise resistance and corrosion mechanisms can be derived from the analysis of the electrochemical noise (Dawson et al. 1983; Smulko and Darowicki 2003).

The analysis of electrochemical noise data can be performed in both time and frequency domains. In the time domain the most interesting parameter is the noise resistance (Rn), defined as the ratio of the standard deviations of potential and current noises (Smulko et al. 2002) which can be associated with the polarization resistance (R_p), although there is controversy concerning this (Bertocci et al. 1997). In the frequency domain, the spectral noise resistance (R_{sn}), defined as the square-root of the ratio of power spectral densities (PSD) of potential and current fluctuations, can be compared with the magnitude of the electrochemical impedance at the same frequency (Mansfeld and Lee 1997). Nevertheless, these parameters can only be obtained if potential and current noises are measured simultaneously (Xiao and Mansfeld 1994). In recent years, the theory of electrochemical noise has been further developed to consider factors such as methods for trend removal (Mansfeld et al. 2001), different transient shapes and electrode asymmetry (Lowe et al.

2003), detection of localized and pitting corrosion (Smulko et al. 2003), and partition of current fluctuations between different electrodes (Aballe et al. 2002b).

2.5 Summary

The zinc electrowinning process consumes ~80% of the total power consumption by any smelter. This power consumption is controlled by the cathodic current efficiency and the cell voltage. Many factors affect these two parameters such as: metallic impurities present in the electrolyte, lead impurity due to the corrosion of lead-based anode, and operating parameters in industry (such electrolyte composition, current density, temperature, and agitation).

As highlighted in this literature review, there are several research works that have been done to study some of these parameters individually in specific conditions. However, there is no full laboratory scale study which has been done to our knowledge for the electrolytic extraction of zinc, on the influence of impurities such as lead in considering conditions close to the operating parameters in the Canadian industry. Also, the optimum operating parameters around an acceptable range by this industry for high electrochemical efficiency during the electrowinning process should be considered. This study could lead or underline then the optimum operating parameters during electrowinning process. This work has been also conducted in cooperation with Canadian Electrolytic Zinc plant in Valleyfield (Quebec, Canada) to better understand the factors affecting the power consumption.

CHAPTER 3

EXPERIMENTAL

3.1 Preparation of Standard Electrolyte

The standard electrolyte (SE) was prepared in laboratory as close as possible in composition to that of the zinc electrolytic industry (CEZinc) in Quebec, Canada. It was composed of 60 g/L of Zn^{2+} ($ZnSO_4 \cdot 7H_2O$) and 170 g/L of H_2SO_4 (98%). This electrolyte was used to evaluate the current efficiency of zinc deposition during electrolysis. Chemicals were dissolved in double distilled water in 1000 ml double-glazed beaker. The solution was heated by a flow of thermostatically controlled circulating water in order to maintain a constant working temperature.

During the evaluation of the effect of lead, Pb^{2+} ions were added to the SE with different concentrations of 0.05, 0.1, 0.15, 0.2, 0.4, 0.8, 2, 2.5 mg/L in the form of Pb $(C_2H_3O_2)_2$. In some experiments, Mn^{2+} was added in the form of $MnSO_4.2H_2O$ to the electrolyte in variable concentrations of 4, 8, 12, and 16 g/L to evaluate the influence of manganese on zinc deposition. All chemicals used in this project were supplied from Laboratories Mat, Sigma-Aldrich and VWR Canada, and meet the purity standards set by American Chemical Society (ACS).

3.2 Fabrication of Electrodes

Copper wire using two components silver adhesive was welded to 1 cm^2 area of pure aluminum (99%) plate (Fig. 3.1a). The welded piece was dried at 80°C in oven for 2 h, and then casted in acrylic resin in order to have 1 cm^2 of exposed area electrode.

The newly developed laminated Pb-0.7wt.%Ag alloy (Fig. 3.1b) and Pt (Fig. 3.1c) were selected as anodes in this study. The chemical composition of Pb-0.7%Ag anode is given in Table 3.1. These anodes were prepared by the same method as aluminum cathodes (described previously). A saturated silver chloride electrode Ag-AgCl/$KCl_{sat.}$ (0.202 V versus SHE) was used as the reference electrode.

Both aluminum and lead-silver electrodes were supplied from Canadian Electrolytic Canada (CEZinc), while reference electrode was supplied from Sensorex–USA.

Table 3.1 Chemical composition (wt %) of the Pb-0.7%Ag anode

Anode (wt. %)	Ag	Fe	Ca	Al	Mn	S	Si	Ti	Zr	Pb
0.7%Ag	0.672	0.009	< 0.001	< 0.05	< 0.05	0.07	0.07	0.25	0.19	bal.

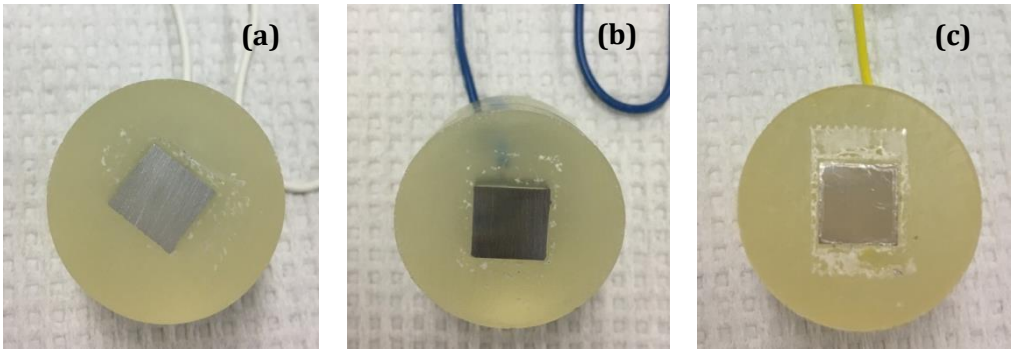

Fig. 3.1 Electrodes used for electrolysis after polishing (a) pure aluminum cathode (99%), (b) Pb-0.7%Ag alloy anode, and (c) Pt anode

3.3 Operating Parameters during Electrolysis

The variation in the studied parameters was considered to be close to the current industrial practice of refining plants to evaluate the relevance and impact of each parameter on energy efficiency, deposit morphology and contamination of zinc deposition by lead.

3.3.1 Current Density

Different values of current density (45, 50, 52.5 and 60 mA/cm^2) were applied during polarization studies in order to examine the effect of changing current density on the electrolysis process. These values were controlled using a Galvanostat / Potentiostat model PC4/750 Gamry-USA.

3.3.2 Operating Temperature

Operating temperature values of 35, 38, 40, and 45°C were used and controlled by a thermostatic bath model Fisher Isotemp 3013D–Ficher, Canada, which was inter-connected to a double-glazed beaker (Fig. 3.2).

Fig. 3.2 Fisher thermostatic bath model 3013D

3.3.3 Electrolyte Agitation

Different agitation rates of 60, 100, and 412 rpm were applied during polarization studies to examine the effect of different electrolyte agitation on the electrodeposition parameters and their corresponding zinc deposits. Magnetic bar (L=38 mm and D=10 mm) was immersed into the electrolyte and agitation rate was controlled using a magnetic agitator device model 131325SP - Thermo Scientific, Canada (Fig. 3.3).

Fig. 3.3 Thermo Scientific Agitator model 131325SP.

3.4 Electrolysis and Electrochemical Measurements

3.4.1 Electrolysis

Electrodes were mounted in a three electrode cell with an inter distance of 2 cm. Before electrolysis, both cathode and anode were manually polished by several grits (80, 320, 800, 1000 and 3000) of SiC papers then washed with distilled water, ethanol and dried before immersing them in the electrolyte. The three electrode cell was connected to a Galvanostat Gamry PC4/270–USA. Electrodeposition was conducted for 2 hours generally, and up to 72 hours in case of long-term electrodeposition studies. The cathodic potential was monitored versus time every 5 seconds and results were plotted using the analysis software installed in the computer connected to the Galvanostat. All results are carried out in duplicates (±5%) and triplicate tests were also conducted when required.

After electrolysis, the cathode was dried and current efficiency (CE) was calculated by weight of zinc deposit using Faraday's law: $CE(\%) = (W.F.n /I.t.M)\times 100\%$, where W is the weight of deposit (g), F the Faraday's constant (96 500 coulombs), n the number of electrons, I the total cell current (A), t the time of electrodeposition period (s), and M the atomic weight of Zn (Barton and Scott 1992).

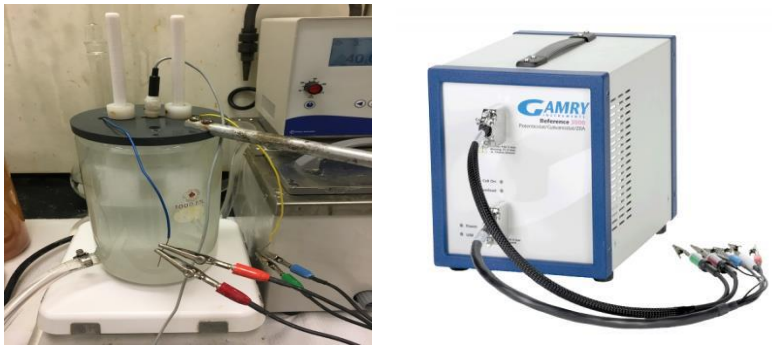

Fig. 3.4 Electrolysis cell set-up

3.4.2 Cyclic Voltammetry

Polarization for zinc deposit was carried out from initial potential of -1.30 V to reversible potential of -0.70 V in presence of atmospheric air. This is considered mainly in this work to determine the formal reduction and nucleation overpotential (NOP). This is the

difference between the crossover potential "the start of the dissolution" and the point at which the Zn begins to deposit. This could be a useful technique to identify the best operating parameter during electrowinning (Heinze 1984).

3.4.3 Potentiodynamic Polarization

Potentiodynamic polarization in the zinc electrolyte has been measured over a scan range from -1.35 V to -1.05 V at scan rate of 5 mV/s. An 1 cm^2 each of Al working electrode, platinum auxiliary electrode, and Ag, $AgCl/KCl_{(sat)}$ reference electrode were used. The three-cell electrode cell was connected to the potentiostat Gamry Reference 3000 – Gamry USA. The cathodic Tafel slope (b_c) and the cathodic overpotential (η_c) can be determined from this technique. The Tafel slope (b_c) can be obtained by selecting two points on the cathodic curve, first point is far by ~20-40 mV from the corrosion potential and the other point is far by one decade of current density (Fig. 3.5) (Kelly et al. 2003). The cathodic overpotential (η_c) can be calculated by the potential difference between a half-reaction's thermodynamically determined reduction potential and the potential at which the redox even is experimentally observed in the same conditions of electrolysis. Precisely, the later can be determined from the following equations at 25°C and atmospheric pressure:

$$E_{e,Zn} = -0.763 + (RT/2F)\, ln[\, a_{Zn^{2+}} / a_{Zn}] \quad (3.1)$$

$$E_{e,H_2} = 0.0 + (RT/F)\, ln[\, a_{H^+} / (a_{H_2})^{0.5}\,] \quad (3.2)$$

$$\eta_{Zn} = E_m - (E_{e,Zn} + E_{e,H_2}) \quad (3.3)$$

$$\eta_{H_2} = E_m - E_{e,H_2} \quad (3.4)$$

where, E_e is the equilibrium potential, R the gas constant (equal to 8.314 J/mol K), F the Faraday's constant and E_m the measured potential at working current density (Baboian and Dean 1991; Brad and Faulkner 2000; McDonald 2012).

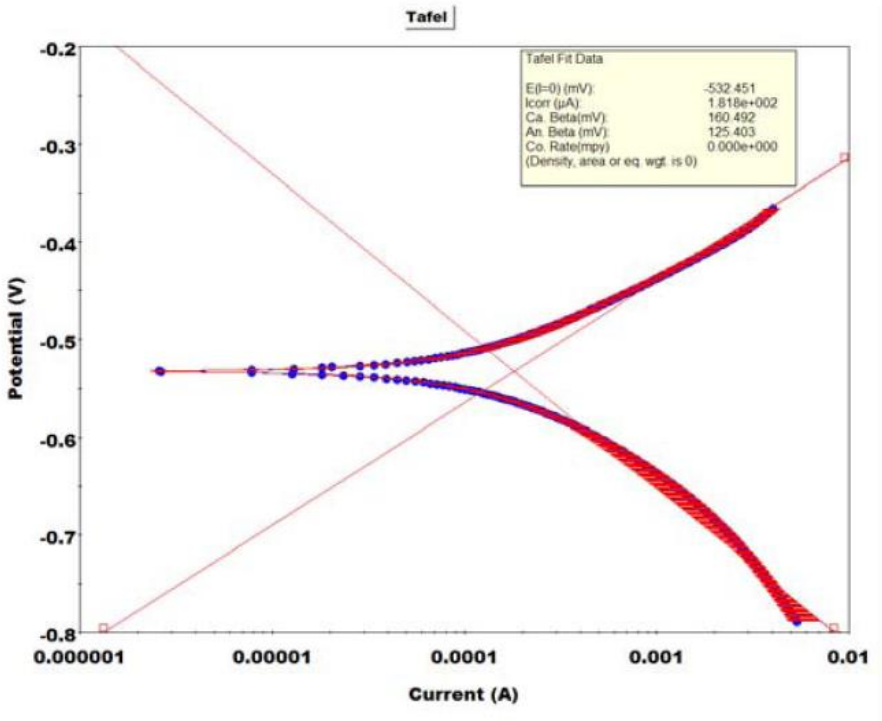

Fig. 3.5 Typical combined anodic and cathodic Tafel plots (Greene 1962)

3.4.4 Electrochemical Noise Measurements

Electrochemical noise measurements (ENM) was used to evaluate the effect of Pb^{2+} on potential skew and kurtosis of statistical parameters of ENM. ENM records containing 1024 data points were collected at a scan rate of f_s=10 Hz and analysed in time domain using two statistical parameters of skewness (S) and kurtosis (K). Skew and kurtosis are dimensionless measures indicating the shape and symmetry of data distribution around the mean value of the data, respectively (Iverson et al. 1985; Bertocci et al. 1997; Revie 2011).

3.4.5 Electrochemical Impedance Measurements

Electrochemical impedance measurements were used to evaluate the effect of Pb^{2+} on charge transfer resistance and double capacitance of zinc deposit on Zn and Al substrates. The electrochemical impedance measurements were carried out using a Solartron 1255 HF frequency response analyzer and a Solartron 1286 electrochemical interface over the

frequency range from 100 kHz to 0.5 Hz. The amplitude of the sinusoidal signal was kept at 10 mV. The following equivalent circuit was applied to the obtained Nyquist curves (Fig. 3.6) (Walter 1986; Park and Yoo 2003; Gouveia-Caridade et al. 2004).

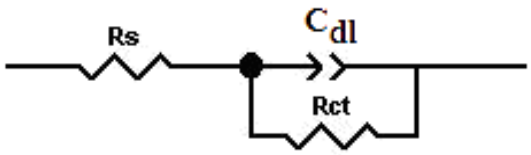

Fig. 3.6 Equivalent circuit proposed for fitting the experimental data of electrochemical impedance measurements of zinc deposit reaction on aluminum substrate

3.4.6 Deposit Examination

The surface morphology and crystallographic orientation were determined using Scanning Electron Microscope (SEM, JEOL JSM-840a) and X-ray Diffractometer (XRD, Siemens - D5000). Lead content in the deposit has been measured using Inductively Coupled Plasma (ICP, Optima 8300 ICP-OES).

CHAPTER 4

ELECTROCHEMICAL INVESTIGATION OF ELECTROLYTE COMPOSITION AND ELECTROLYSIS PARAMETERS DURING ZINC ELECTROWINNING

Electrochemical Investigation of Electrolyte Composition and Electrolysis Parameters during Zinc Electrowinning

C. Su[1,*], W. Zhang[1], E. Ghali[1], and G. Houlachi[2]

[1]*Department of Mining, Metallurgical and Materials Engineering, Laval University, QC, Canada, G1V0A6*

[2]*Hydro-Québec research centre (LTE) Shawinigan, QC, Canada, G9N 7N5*

* Corresponding author. Tel.: +1 418-656 8657 Fax: +1 418-656 5343.
E-mail address: chaoran.su.1@ulaval.ca (C. Su)

This paper was submitted to the Journal of Applied Electrochemistry on January 5th 2017.

Résumé

L'effet de différentes concentrations de Mn^{2+} et de Pb^{2+} ajoutées à l'électrolyte acide de sulfate de zinc pendant le processus d'extraction électrolytique du zinc a été étudié. Des paramètres d'opération tels que la concentration des ions de zinc, la concentration d'acide, la densité de courant, l'agitation magnétique et la température ont été étudiés en présence de Mn^{2+} et Pb^{2+}. Des études de polarisation galvanostatique, de polarisation potentio-dynamique, de voltammétrie cyclique et d'impédance électrochimique ont été considérées afin d'examiner le comportement cathodique. La microscopie électronique à balayage (MEB) et la diffraction des rayons-X (DRX) ont été utilisées pour caractériser la surface de dépôt. On a trouvé que des ions de plomb ajoutés à l'électrolyte de zinc ont conduit à une augmentation du potentiel cathodique et des rendements de courant du dépôt de zinc. L'addition de Mn^{2+} à l'électrolyte de zinc a entraîné une diminution du potentiel cathodique et du rendement de courant de dépôt de zinc en raison de l'effet catalytique du MnO_4^- sur l'évolution de l'hydrogène. En outre, l'augmentation de la densité de courant de 45 à 60 mA/cm^2 et l'agitation de 60 à 412 tour/min ont entraîné une augmentation du potentiel cathodique et une diminution des rendements de courant. De plus, l'augmentation de température de 35 à 45°C a conduit à une diminution du potentiel cathodique. La comparaison de la teneur en Pb dans le dépôt de zinc à la fin de 2 et 72 h d'électrodéposition en utilisant des anodes en Pb-0,7%Ag et en Pt a été examinée dans cette étude. La teneur en Pb dans le dépôt de zinc en utilisant comme anode Pb-0,7%Ag était plus élevée pendant les 2 à 4 premières heures que l'anode de Pt utilisée en raison de la présence des ions de plomb solubles (supérieurs à 0,15 mg Pb^{2+} avec des anodes Pb-Ag). Après 72 h, la teneur en Pb dans le dépôt de zinc en utilisant Pb-0,7%Ag comme anode était pratiquement la même que celle mesurée en utilisant l'anode Pt ajouté de quantités de 0,15 à 0,2 mg/L de Pb^{2+} dans la solution.

Abstract

The effect of different Mn^{2+} and Pb^{2+} concentrations added to the zinc sulfate acid electrolyte during zinc electrowinning process has been investigated. Operating parameters such as zinc ions concentration, acid concentration, current density, electrolyte agitation and temperature were investigated in presence of Mn^{2+} and Pb^{2+}. Galvanostatic polarization, potentiodynamic polarization, cyclic voltammetry and electrochemical impedance spectroscopy studies have been considered to examine the cathodic behavior. Scanning electron microscopy (SEM) and X-ray diffraction (XRD) have been employed to characterize the surface of zinc deposit. It was found that lead ions added to the zinc electrolyte led to an increase in the cathodic potential and current efficiencies of zinc deposit. Addition of Mn^{2+} into the zinc electrolyte resulted in decrease of cathodic potential and current efficiency of zinc deposition. Increase of current density from 45 to 60 mA/cm^2 and electrolyte agitation from 60 to 412 rpm resulted in an increase of cathodic potential and decrease of current efficiencies. Temperature increase from 35 to 45°C led to a decrease of cathodic potential. After short initial part of electrodeposition (2-4 h), using Pb-0.7%Ag anode, lead content was higher than that with Pt anode (0.15 mg/L Pb^{2+}). Long deposition period over 72 h has been considered also and Pb was almost the same in the deposit for Pb^{2+} quantities (0.15 or 0.2 mg/L).

Keywords

Zinc electrowinning, Impurities, Cyclic voltammetry, Electrochemical impedance, Current efficiency, Morphology

4.1. Introduction

The production of zinc from sulfides is predominantly conducted through roast-leach-electrowinning process (Sinclair 2005). More than 80% of the power requirements of a zinc electrolytic refinery originate from the electrowinning process. It is important to operate the electrolysis as close as possible to the optimal operating conditions. Optimum performance of the electrolysis occurs when the energy per ton of the produced zinc is minimized. The two parameters which control directly the energy consumption are current efficiency (CE) and total cell voltage (Alfantazi and Dreisinger 2001). The major variables affecting these two parameters are: zinc and sulfuric acid concentrations, current density, temperature, metallic impurities, and additives (Sorour et al. 2015). Also, the influence of electrolysis time on deposition in presence of impurities and additives is a significant parameter to consider.

For zinc electrowinning, the overpotential of hydrogen evolution of zinc is very high in comparison with some metals. The effect of impurities is an important matter in the electrolysis process. Impurities in the electrolyte affect greatly the electrowinning process. Impurities which cause low hydrogen overpotential such as antimony and nickel result to a decrease in current efficiency (Ivanov 2004; Stefanov and Ivanov 2002). The negative role of lead as impurity in reducing the purity and quality of deposited zinc cannot be neglected as long as lead-based anodes are still used in the zinc electrowinning process (Sorour et al. 2015; MacKinnon and Brannen 1977).

In practice, the anodic potential corresponding to the applied current density could enable the formation of H_2O_2 which diffuses towards the cathode and causes detrimental effect (Bozhkov et al. 1990). The dissolution of lead from the anode introduces the formation of Pb^{2+} ions in solution, which are co-deposited at the cathode. Mansfeld and Gilman (1970) showed that traces of lead on the cathode were beneficial, inhibiting dendritic growth of the zinc deposit. Mackinnon et al. (1979) reported that the lead co-deposited with zinc causes an orientation change of the zinc crystals and increases cathodic polarization. As the original electrolyte contains manganese, there are also other species anodically formed which could influence the cathodic process (Zhang and Hua 2009).

A strong correlation between polarization behavior, current efficiency and morphology of zinc deposits was shown by many research groups (Sorour et al. 2015; Hosny 1993; Zhang et al. 2009; Tripathy et al. 1998). It was found that various impurities and additives can affect the polarization behavior of zinc deposition in a characteristic manner. It is possible to associate a given deposit morphology with a particular polarization (overpotential) condition (Tripathy et al. 1999). A combination of polarization and morphology observations, or possibly either individually, may be used to obtain valuable information on zinc electrodeposition process for possible applications to industrial plant practice and control.

Scott et al. (1987) found that higher cell temperatures reduced the energy consumption but only in presence of additives capable of controlling deposit morphology. Bratt (1977) gave a qualitative description of the most major variables such as impurities and additives and considered them just for modeling. Fosnacht and O'Keefe (1980) reported that increasing acid concentration enhanced the hydrogen reduction on the cathode surface and increased the zinc re-dissolution leading to low current efficiency. Hosny et al. (1991) provided limited industrial data on the effect of current density, however it can be stated that very little information was supplied for other variables.

It was observed that the zinc deposit morphology and crystallographic orientation are extremely sensitive to lead levels as low as 1 mg/L in the electrolyte (Mackinnon et al. 1979). It is desirable to correlate the Pb content and the morphology of zinc deposits under chosen overpotentials and defined conditions of electrolysis. Manganese can decrease the negative effect of the other impurities. It was found that, Mn^{2+} is anodically oxidized to MnO_4^-. The latter immediately reacts with Mn^{2+} and produces Mn^{3+} then MnO_2 which can absorb deleterious ions and affect the current efficiency of zinc deposition (Zhang and Hua 2009). Hence, it can be stated not only the impurity in the electrolyte, but also the oxidized species produced at the anode, could characterize the behavior of zinc deposition.

The aim of this work is divided into two main objectives. The first is to study the effect of chemical composition of the electrolyte such as the Mn^{2+}, Pb^{2+}, Zn^{2+} and acid concentrations on zinc electrodeposition process and zinc deposit quality (Pb content and morphology). The second objective involved is studying the effect of operating parameters

such as current density, temperature, and magnetic agitation on current efficiency, deposit morphology, cathodic polarization, and lead contamination.

4.2. Experimental

4.2.1 Reagents and Electrolysis

The standard acidic zinc electrolyte was prepared from 60 g/L of Zn^{2+} in the form of $ZnSO_4.7H_2O$, added to 170 g/L of H_2SO_4. The Mn^{2+} and Pb^{2+} cations were added as $MnSO_4.2H_2O$, and Pb $(C_2H_3O_2)_2$, respectively. All reagents were supplied from Laboratories MAT and VWR Canada.

Laboratory scale of galvanostatic electrolysis was considered in 1000 ml solution in a double-wall beaker, thermostated at the desired working temperature. One plate of pure Al as cathode and one plate of Pb-0.7wt.%Ag alloy or Pt as anode were used. During the evaluation of the Pb^{2+} ions effect in the electrolyte, a plate of Pt was also used as anode. All electrode plates were casted in polyester resin in order to obtain an exposed surface area of 1 cm^2. The reference electrode was a $Ag/AgCl/KCl_{(sat)}$ (0.199 V/SHE). Electrodes were mounted in a three-cell electrode with an inter distance of 2 cm. Before electrolysis, both cathode and anode were manually polished using several grits SiC papers then washed with distilled water, ethanol and dried before immersing them in the electrolyte. The three-cell electrode was connected to a potentiostat Gamry PC4/270–USA. All the results are carried out in duplicates ($\pm$5%), triplicate tests were also conducted when required.

4.2.2 Electrochemical Measurements

Electrochemical studies were conducted employing cyclic voltammetry, potentiodynamic polarization, and electrochemical impedance techniques. Cyclic voltammetry (CV) experiments were carried out scanning from initial potential of -1.3 V to a potential of -0.7 V at a scan rate of 10 mV/s. The potential was scanned from -1.05 to -1.25 V for the cathodic potentiodynamic polarization with a constant scan rate of 5 mV/s. The CV and potentiodynamic tests were performed using the potentiostat Gamry 3000–USA. The

electrochemical impedance measurements were carried out using a Solartron 1255 HF frequency response analyzer and a Solartron 1286 electrochemical interface over the frequency range from 10 kHz to 0.5 Hz. The amplitude of the sinusoidal signal was kept at 10 mV.

4.2.3 Deposit Examination

The surface morphology and crystallographic orientation were determined using scanning electron microscope (SEM, JEOL JSM-840a) and X-ray diffractometer (XRD, Siemens-D5000). The lead content in the deposit was measured using inductively coupled plasma (ICP, Optima 8300 ICP-OES).

4.3. Results and Discussion

Initial galvanostatic duration studies for a period of 2 hours were considered for parts electrolysis (4.3.1) and zinc deposit characterization (4.3.2), while for long duration of galvanostatic polarization stimulating industrial operating conditions is examined in section 4.3.3.

4.3.1 Galvanostatic Measurements

In the galvanostatic tests, a constant current was applied between the auxiliary and working electrodes. The potential of working electrode was recorded versus time with respect to the reference electrode. The used counter electrode was Pb-0.7%Ag or Pt anode. After electrolysis, the deposit was rinsed, dried and weighted for current efficiency calculations using Faraday's law. Values of cathodic potentials and current efficiencies are given in Table 4.1.

Table 4.1 The cathodic potential and current efficiency values after 2 h of electrodeposition for Mn^{2+} and Pb^{2+}ion concentrations employing Pb-Ag or Pt anodes at various operating conditions for the standard ones (170 g/L H_2SO_4, 60 g/L Zn^{2+}, 12 g/L Mn^{2+} at current density of 52.5 mA/cm^2, 40°C and agitation of 60 rpm)

Parameters		Pb-Ag anode		Pt anode	
		CE (%)	Cathodic Potential (V/Ref)	CE (%)	Cathodic Potential (V/Ref)
Mn^{2+} (g/L)	0 (blank)	96.3	-1.128	Experiments made with Pt anode had no added manganese	
	4	95.6	-1.118		
	8	95.5	-1.102		
	12	95.3	-1.083		
	16	94.3	-1.072		
Pb^{2+} (mg/L)	0 (blank)	Experiments made with Pb-Ag anode had no added lead		94.2	-1.076
	0.1			94.4	-1.079
	0.15			94.4	-1.081
	0.2			94.7	-1.083
	2			95.0	-1.116
	2.5			95.6	-1.134
Zn^{2+} (g/L)	56	94.6	-1.092	93.7	-1.088
	60	95.3	-1.083	94.4	-1.081
	65	95.5	-1.076	94.5	-1.075
H_2SO_4 (g/L)	158	95.7	-1.096	95.5	-1.093
	165	95.5	-1.090	95.0	-1.086
	170	95.3	-1.083	94.4	-1.081
CD (mA/cm^2)	45	94.6	-1.072	93.8	-1.071
	50	95.3	-1.081	94.1	-1.078
	52.5	95.3	-1.083	94.4	-1.081
	60	95.9	-1.089	95.5	-1.088
Agitation (rpm)	60	95.3	-1.083	94.4	-1.081
	100	95.1	-1.090	93.8	-1.088
	412	94.7	-1.093	93.6	-1.090
Temperature (°C)	35	95.1	-1.096	94.1	-1.093
	38	95.2	-1.081	94.2	-1.0825
	40	95.3	-1.083	94.4	-1.081
	45	95.9	-1.074	95.1	-1.073

4.3.1.1 Effect of Mn^{2+} Concentration

The profile of cathodic potential was monitored for 2 h of electrodeposition in standard zinc electrolyte containing 170 g/L H_2SO_4 , 60 g/L Zn^{2+} at a current density of 52.5 mA/cm^2, 40°C, and electrolyte agitation of 60 rpm. In this work, Pb-0.7%Ag was used as anode. The influence of Mn^{2+} ion concentration (0, 4, 8, 12 and 16 g/L) is given in Fig. 4.1. It was found that increasing of Mn^{2+} ion in the zinc electrolyte decreased the overpotential of zinc deposit. The measured cathodic potential without Mn^{2+} addition was -1.128 V, and was decreased gradually by the addition of Mn^{2+} up to -1.072 V at 16 g/L (Table 4.1). This depolarization up to 56 mV could be due to the effect of MnO_4^- formation at high concentrations of Mn^{2+}, which catalyzes the hydrogen evolution reaction (HER) and reduces its overpotential (Zhang and Hua 2009).

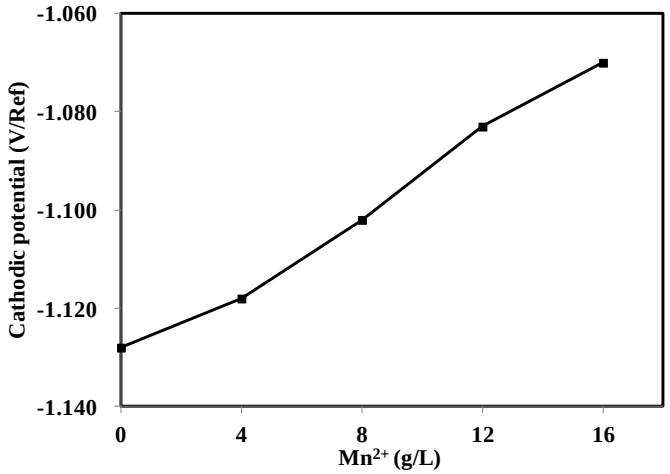

Fig. 4.1 Effect of Mn^{2+} ion concentrations on the cathodic potential employing Pb-0.7%Ag anode on zinc deposit in the electrolyte containing 170 g/L H_2SO_4, 60 g/L Zn^{2+}, at current density of 52.5 mA/cm^2, 40°C and agitation of 60 rpm

Although manganese is beneficial in enhancing the anodic reaction and reducing the lead-base anode corrosion (Ivanov and Stefanov 2002; Tswuoka 1960), its negative effect on the cathodic current efficiency cannot be neglected. The effect of Mn^{2+} concentrations on the CE% was examined for Pb-Ag anodes (Table 4.1). The current efficiency values were decreased by 0.75, 0.81, 0.99, and 2.04% with the addition of 4,8,12, and 16 g/L of Mn^{2+}, respectively. Remarkable decrease in CE% was relatively low at concentrations from 4 to

12 g/L and decreased sharply at the higher concentration of 16 g/L. Increasing the concentration of Mn^{2+} in the electrolyte decreased the CE% by almost 2%. A concentration of 12 g/L was considered for all the following tests, which corresponds to 95.3% CE. The decrease in CE% could be attributed also to the catalytic effect of MnO_4^- ions on the HER, which causes also a decrease in the Zn^{2+} reduction as mentioned by Zhang and Hua (2009).

4.3.1.2 Effect of Pb^{2+} Concentration

The effect of 0, 0.1, 0.15, 0.2, 2 and 2.5 mg/L of Pb^{2+} ions when added to the standard zinc sulfate electrolyte containing 12 g/L of Mn^{2+} on the cathodic potential is shown in Fig. 4.2. During these experiments, Pt was used as anode to study the effect of Pb^{2+} ions alone without the effect of the dissolution of Pb-Ag anode. As shown in Fig. 4.2, the lead addition to the electrolyte increased the cathodic potential. This potential was -1.076 V in absence of lead ions. The observed increase of zinc deposition overpotential (more negative) was sharper for the first low quantities of lead ions up to 0.2 mg/L concentration. This value increased slowly by few millivolts with the addition of Pb^{2+} (-1.083 V), reaching to -1.134 V at the maximum addition of 2.5 mg/L of Pb^{2+} (Table 4.1). This could be due at least partially for the increase of hydrogen overpotential on deposited lead surface.

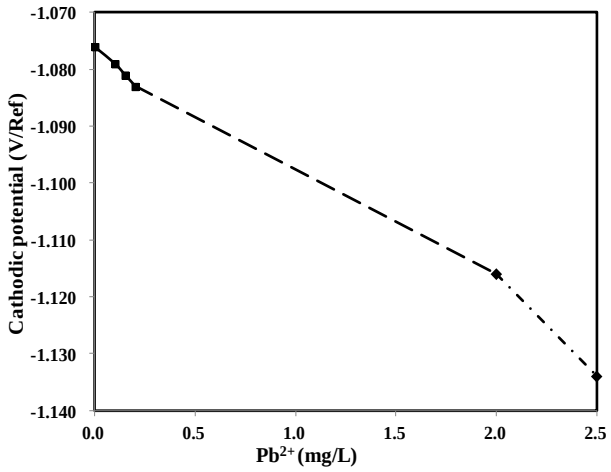

Fig. 4.2 Effect of Pb^{2+} ion concentrations on the cathodic potential of Zn deposit employing Pt anode in the electrolyte containing 170 g/L H_2SO_4, 60 g/L Zn^{2+}, 12 g/L Mn^{2+}, at current density of 52.5 mA/cm^2, 40°C, and agitation of 60 rpm

As shown in Table 4.1, the lead addition increased the CE%. It was found that, during the 2 h of electrodeposition, the current efficiencies increased from 94.2% to 94.7% by 0.2 mg/L Pb^{2+} addition. The maximum addition of 25 g/L of Pb^{2+} increased the CE% up to 95.6%. It should be noted that the effect of long time electrodeposition in the presence of Pb^{2+} is discussed in section 4.3.3.

4.3.1.3 Effect of Zn^{2+} Concentration

Fig. 4.3 shows the evolution of cathodic potential during zinc electrodeposition in an electrolyte containing different concentrations of zinc (56, 60, and 65 g/L of Zn^{2+}). In this series of experiments, Pb-0.7%Ag and Pt were used as anodes, individually. The results showed that the increase of Zn^{2+} ions in the zinc electrolyte for both anodes decreased the overpotential of zinc electrodeposition (Fig. 4.3). However, the overpotentials were slightly higher with Pb-0.7%Ag anode than that with Pt anode. This could be explained by the higher Pb^{2+} ion concentration with Pb-0.7%Ag anode during the initial 2 h of electrolysis.

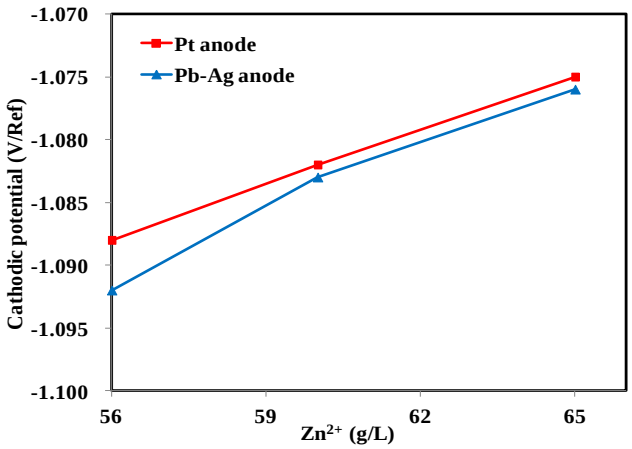

Fig. 4.3 Effect of different zinc contents on cathodic potential during Zn electrowinning employing Pb-0.7%Ag anode (■) or Pt anode (▲) with addition of 0.15 mg Pb^{2+} impurity into zinc electrolyte containing 170 g/L H_2SO_4, Mn^{2+} 12 g/L, at current density of 52.5 mA/cm^2, 40°C, and agitation of 60 rpm

Increasing the Zn^{2+} concentration from 56 to 60 g/L, the CE% was increased by 0.7% (from 94.6 to 95.3%) using Pb-0.7%Ag as anode. However, only a 0.2% increase in CE% was

obtained with a further increase in Zn^{2+} ion up to 65 g/L. The calculated current efficiencies after electrolysis using Pt anode were found to have the same trend. (Table 4.1). This indicates that, at higher concentrations (> 60 g/L Zn^{2+}), the current efficiency is slightly improved by increasing the Zn^{2+} ions in the electrolyte. Increasing the Zn^{2+} concentration renders the Pb^{2+} codeposition more difficult, decreasing the lead effect on current efficiency and cathodic potential. This could be related to the solution viscosity and the availability of active sites on the limited surface. With Pt anode, the CE was lower by ~1% for all zinc concentrations as compared to that with Pb-0.7%Ag anode. It can be noted that Mn effect on the cathodic reaction is stronger with Pt anode due to the cathodic depolarization by MnO_4^-, since part of the added Mn was already consumed as protective layer for the Pb-0.7%Ag anode.

4.3.1.4 Effect of H_2SO_4 Concentration

As shown in Fig. 4.4, the overpotential of zinc deposit was decreased by 17 mV (in case of Pb-0.7%Ag), and 11 mV (in case of Pt anode), with increasing sulfuric acid concentration from 158 to 170 g/L. Increasing the sulfuric acid in the zinc electrolyte accelerated the HER reaction due to the increase of H^+ cations in the double layer. This depolarization was accompanied by a reduction in the current efficiencies (Table 4.1). Considering the lead-base anode during electrolysis, the CE% was decreased from 95.7 to 95.3% by increasing the acid content up to 170 g/L, and the reduction of CE% was more significant in the case of Pt as anode. At such low potential, high evolution of hydrogen gas at the cathode could increase electrolyte agitation, hydrogen ions diffusion and retard relatively the Zn^{2+} reduction process.

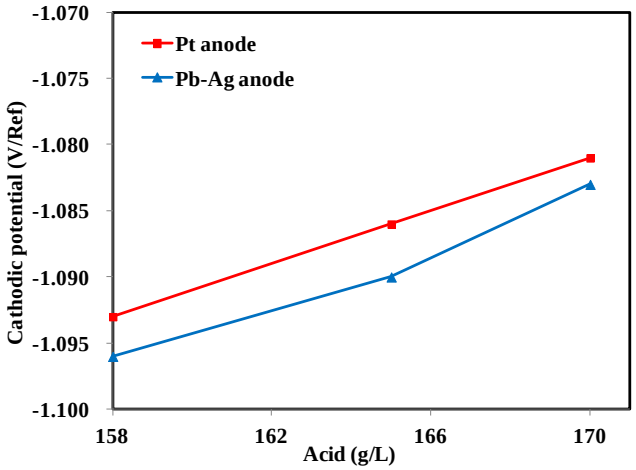

Fig. 4.4 Effect of different sulfuric acid concentrations on cathodic potential during Zn electrowinning employing Pb-0.7%Ag anode (■) or Pt anode (▲) with addition of 0.15 mg Pb^{2+} impurity in zinc electrolyte containing 60 g/L Zn, 12 g/L Mn^{2+}, at current density of 52.5 mA/cm^2, 40°C, and agitation of 60 rpm

4.3.1.5 Effect of Current Density

Fig. 4.5 shows that when the current density increased from 45 to 60 mA/cm^2, the cathodic potential increased from -1.072 to -1.089 mV using Pb-0.7%Ag anode. Comparing the results of the Pb-0.7%Ag and Pt anodes, it was found that the potential of zinc deposit used as Pb-0.7%Ag anode was more negative than that used as Pt anode in the same operating conditions. During zinc electrowinning, Pb^{2+} ions dissolved in zinc electrolyte employing Pb-0.7%Ag anode at higher current densities were more than that with Pt anode, and increased the overpotential of zinc electrodeposition (Table 4.1).

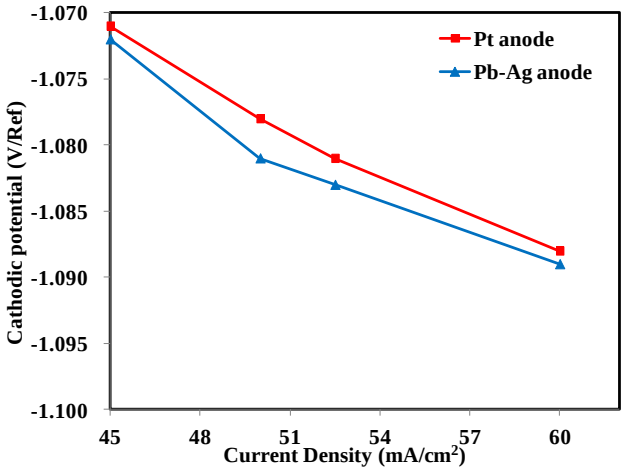

Fig. 4.5 Effect of current density on cathodic potential during Zn electrowinning employing Pb-0.7%Ag anode (■) or Pt anode (▲) with addition of 0.15 mg Pb^{2+} impurity in the electrolyte containig 170 g/L H_2SO_4, 60g/L Zn^{2+}, 12 g/L Mn^{2+}, at 40°C and 60 rpm of agitation

A remarkable influence of the current density on the cathodic CE was observed. For instance, increasing CD from 45 to 60 mA/cm^2 led to an increase in CE% from 94.6% to 95.9% in case of Pb-0.7%Ag anode. A similar trend of increase in current efficiency was also obtained in case of Pt anode. The hydrogen overvoltage increases relatively at high current densities resulting in higher CE, favoring Zn^{2+} reduction.

4.3.1.6 Effect of Electrolyte Agitation Rate

The effect of agitation rates on the cathodic polarization is shown in Fig. 4.6. Increasing electrolyte agitation rate from 60 to 100 rpm, led to an increase in the cathodic potential by 7 mV employing both anodes (Pb-0.7%Ag or Pt anodes). This higher agitation rate increased the overpotential of Zn^{2+} reduction rate and favored the hydrogen parasite reaction. At higher speeds than 100 up to 412 rpm, the cathodic potentials were almost stable. Current efficiency decreased by 0.2, and 0.6% for 100 and 412 rpm as compared to that of 60 rpm (Table 4.1). This could be due to the relative increase of diffusion and reduction rates of hydrogen ions as compared to that of zinc ions. It can be stated that

increasing the agitation speed in this range has negative influence on zinc electrowinning showing more cathodic polarization and lower current efficiency.

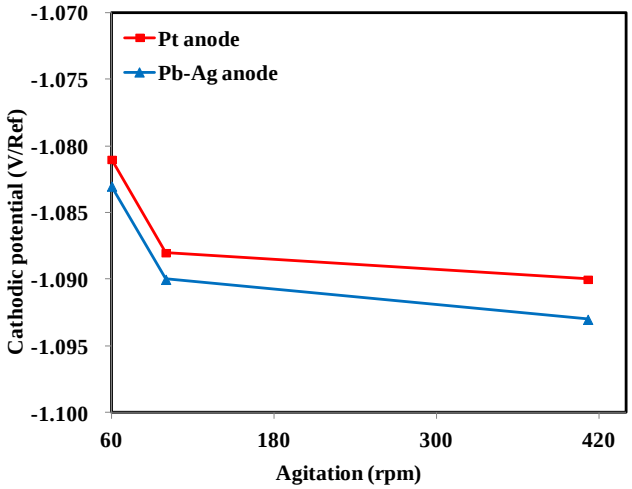

Fig. 4.6 Effect of agitation rate on cathodic potential during Zn electrowinning employing Pb-0.7%Ag anode (■) or Pt anode (▲) and 0.15 mg Pb^{2+} addition as impurity in zinc electrolyte containing 170 g/L H_2SO_4, 60 g/L Zn^{2+}, 12 g/L Mn^{2+}, at current density of 52.5 mA/cm^2 and 40°C

4.3.1.7 Effect of Temperature

Increasing the electrolyte temperature from 35 to 45°C led to a decrease by 22 mV in the overpotential of zinc deposit (Pb-0.7%Ag anode).The increase of temperature has a positive effect for less energy consumption during zinc electrowinning. Also, the cathodic current efficiency increased at higher temperatures (Table 4.1). This could be linked to the increase in diffusion rate of zinc ions in the electrolyte bath due to a decrease in electrolyte viscosity, and the enhancement of the reduction reaction rate of zinc ions at the cathode surface to produce zinc metal ($Zn^{2+} + 2e^- \rightarrow Zn_{(s)}$). Also, the temperature increases the electrolyte conductivity which decreases the cell voltage and the required energy.

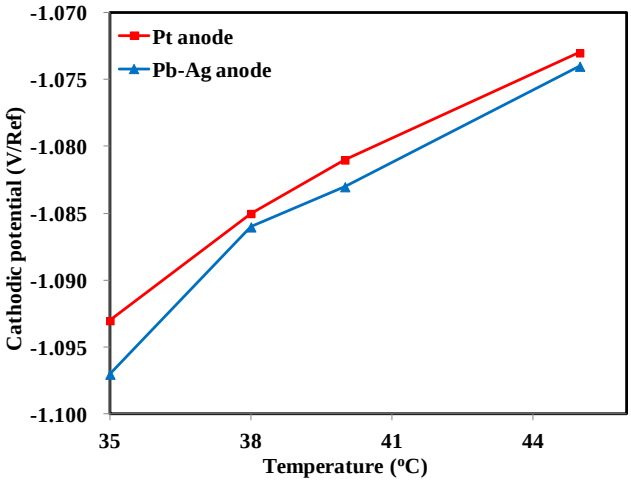

Fig. 4.7 Effect of temperature on cathodic potential during Zn electrowinning employing Pb-0.7%Ag anode (■) or Pt anode (▲) with addition of 0.15 mg Pb^{2+} impurity in zinc electrolyte, containing 170 g/L H_2SO_4, 60 g/L Zn^{2+}, 12 g/L Mn^{2+}, and 0.15 mg Pb^{2+} as impurity, at current density of 52.5 mA/cm^2, and 60 rpm of agitation

The presence of lead ions in the zinc electrolyte at the different temperatures decreased the overpotential of zinc deposit (Fig. 4.7). Both anodes gave the same tendency, however more negative values were observed in case of Pb-0.7%Ag anode. This temperature influence could be a function of several variable factors such as depolarization, diffusion rate and lead ion content. The CE values were increased with increasing temperature regardless of the employed anode. In case of Pb-0.7%Ag anode for example, the CE was found to be 95.1% at 35°C, and increased up to 95.9% at 45°C. This could be due to the hydrogen reduction reaction being less influenced than Zn deposition and also higher temperatures dissolve more lead ions in the solution.

In summary, the effects of Mn^{2+}, Pb^{2+} and different operating parameters on CE% and cathodic potential in zinc electrowinning process are summarized in Table 4.2. The CE% was increased by increasing Pb^{2+} and Zn^{2+} ion concentrations in the electrolyte as well as by increasing the working temperature. The cathodic depolarization was observed by increasing the concentration of Mn^{2+}, Zn^{2+}, acidity and temperature of the electrolyte. The cathodic overpotentials were increased with the increase of lead ion concentrations, and obviously by current density.

Table 4.2 Trend of current efficiency (CE%) and overpotential (η) of increasing different conditions and parameters on the cathodic potential

	Mn^{2+}	**Pb^{2+}**	**Zn^{2+}**	**Acid**	**CD**	**Agitation**	**Temp.**
CE% ↑increase	↓	↑	↑	↓	↑	↓	↑
H ↓increase (more negative)	↑	↓	↑	↑	↓	↓	↑

4.3.2 Deposit Examination

The obtained zinc deposits were examined using SEM and XRD to determine surface morphology and crystallographic orientations, respectively. SEM photomicrographs are shown in Fig. 4.8. The crystallographic orientations and the determined lead contamination by ICP of zinc deposits from zinc electrolyte containing Pb^{2+} and Mn^{2+} ions employing different parameters are given in Table 4.3.

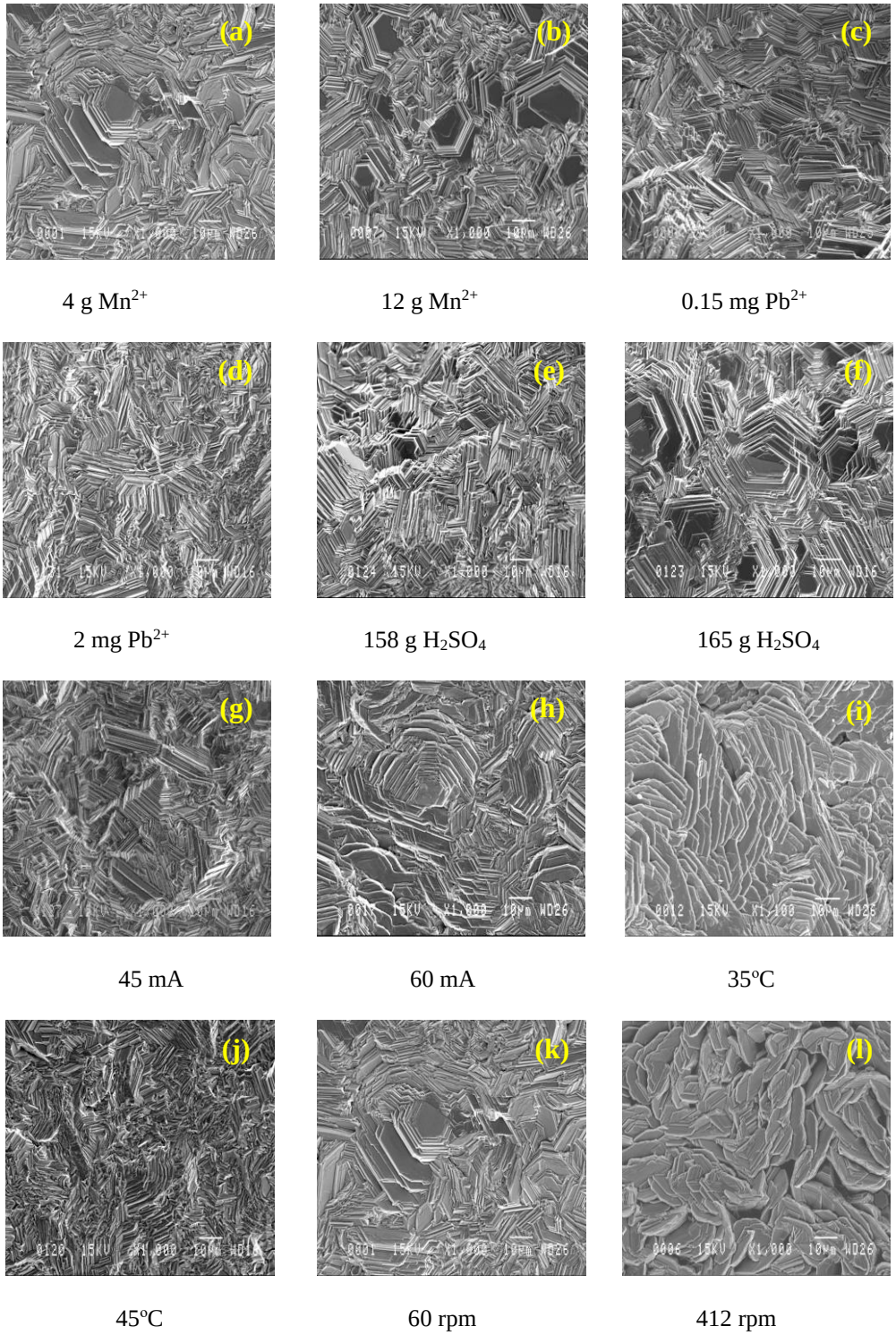

Fig. 4.8 Scanning electron microscopy photomicrographs (1000X) of zinc deposit in presence of Mn^{2+} and Pb^{2+} ions employing different parameters described in Table 4.3 using different anodes (a, b, e, f, i, j for Pb anode and c, d, g, h, k, l for Pt anode)

Table 4.3 Crystallographic orientation and lead content in zinc deposit in presence of Mn^{2+} and Pb^{2+} ions utilizing different working parameters

Parameters		Pb-0.7%Ag anode		Pt anode	
		Crystallographic Orientation（hkl）	Pb cont. (ppm)	Crystallographic Orientation（hkl）	Pb cont. (ppm)
Mn^{2+} (g/L)	0	(101)(102)(103)	5.23	Experiments made with Pt anode had no added manganese	
	4	(101)(102)(103)	2.89		
	8	(101)(102)(103)	1.57		
	12	(101)(103)(102)	1.40		
	16	(101)(103)(102)	1.36		
Pb^{2+} (mg/L)	0	Experiments made with Pb-0.7%Ag anode had no added lead		(101)(102)(103)	-
	0.1			(101)(102)(103)	1.13
	0.15			(101)(102)(103)	1.35
	0.2			(101)(103)(102)	1.46
	2			(103)(101)(102)	8.94
	2.5			(002)(103)(101)	12.70
Zn^{2+} (g/L)	56	(101)(103)(102)	1.67	(101)(102)(103)	1.65
	60	(101)(103)(102)	1.40	(101)(102)(103)	1.35
	65	(103)(101)(102)	1.17	(103)(101)(102)	1.21
H_2SO_4 (g/L)	158	(101)(103)(102)	1.59	(101)(103)(102)	1.50
	165	(101)(102)(103)	1.44	(101)(103)(102)	1.41
	170	(101)(103)(102)	1.40	(101)(102)(103)	1.35
CD (mA/cm^2)	45	(101)(103)(102)	1.29	(101)(102)(103)	1.19
	50	(101)(103)(102)	1.37	(101)(102)(103)	1.29
	52.5	(101)(103)(102)	1.40	(101)(102)(103)	1.35
	60	(101)(102)(103)	1.45	(101)(102)(103)	1.44
Agitation (rpm)	60	(101)(103)(102)	1.40	(101)(102)(103)	1.35
	100	(101)(102)(103)	1.67	(101)(102)(103)	1.64
	412	(101)(103)(102)	1.71	(101)(103)(102)	1.69
Temperature (°C)	35	(002)(103)(101)	1.62	(103)(101)(102)	1.58
	38	(101)(103)(102)	1.46	(101)(102)(103)	1.43
	40	(101)(103)(102)	1.40	(101)(102)(103)	1.35
	45	(101)(103)(102)	1.28	(101)(102)(103)	1.22

These findings have revealed that crystallographic orientation obtained from free-addition standard electrolyte was (101) (102) (103), and the predominate orientation (101) was not affected by the addition of Mn^{2+} ions employing Pb-0.7%Ag anode. Compact smooth deposit with medium grain-size was obtained at higher concentrations of Mn^{2+} (Fig. 4.8b). Lead content in the deposit was decreased from 5.23 (in the absence of Mn^{2+}) to 1.36 ppm by Mn^{2+} addition at 16 g/L. This finding confirms the important beneficial effect of Mn^{2+} addition to form the protective MnO_2 layer on the lead-based anode, leading to less soluble lead in the electrolyte.

The addition of low concentrations (0.1-0.2 mg/L) of Pb^{2+} ions resulted in a similar orientation of the deposit to that of the standard (101) (102) (103) (Fig. 4.8c). Increasing the lead concentration up to 2 mg/L, the deposit became slightly more compact with a complete different orientation (103), as compared to the previous predominate one (Fig. 4.8d). The addition of high concentration of Pb^{2+} (2.5 mg/L), led to the following orientation (002) (103) (101). This indicates that, the high concentration of lead in the electrolyte affects negatively the crystallographic orientation and surface morphology. Addition of soluble lead in the electrolyte, increased generally its contamination in the zinc deposit, and the highest Pb^{2+} ions addition increased lead content up to 12.70 ppm. This codeposition also resulted in a change in morphology.

The increase of zinc ions in the electrolyte has no effect on both morphology and crystallographic orientation but it reduced the contamination of the deposit by lead as the content of lead decreased from 1.67 to 1.17 ppm by addition of 65 g/L as compared to 56 g/L Zn^{2+}, employing lead-base anode (Table 4.3). A similar trend was obtained by employing Pt anode. The studied range of sulfuric acid concentrations (158-170 g/L) did influence the main crystallographic orientation (101), and at high concentrations, the platelet size of deposit was larger than that at low concentrations (Fig. 4.8e-f). As shown in Table 4.3, the lead contamination was reduced by employing both anodes at high acid content; this could be due to the relative H^+ diffusion and the acceleration of the HER.

At low current density (45 mA/cm^2) the morphology of deposit was showing large crystals size although the orientation did not change (Fig. 4.8g). Increasing the current density up to 60 mA/cm^2 improved the grain size (Fig. 4.8h), and was accompanied by an increase in

overpotential, which led to more zinc contamination by lead (Table 4.3). The results showed that, the current density is a critical parameter which influences also the morphology.

Agitation rate did not change the morphology or the orientation of the deposit but resulted in an increase in lead contamination in zinc deposit. At low agitation rate (60 rpm), lead content in the deposit was 1.40 and 1.35 ppm in case of Pb-0.7%Ag and Pt anodes, respectively. The contamination was increased to 1.71 and 1.69 ppm at the highest speed (412 rpm) with both anodes, respectively (Table 4.3).

At low temperature (35°C), the crystallographic orientation was changed to (002) (103) (101) giving random needled deposit (Fig. 4.8i). Increasing the temperature restored the standard orientation of zinc deposit. Lead content in the deposit was decreased as the temperature increased. This shows that temperature is an important factor in grain refining, and the optimal working temperature is 38-40°C.

4.3.3 Long Duration Galvanostatic Tests

4.3.3.1 Cathodic Potential

Electrolysis tests over a period of 72 h were conducted to examine the effect of Pb^{2+} ions and lead-base anode on deposit contamination. The effect of Pb impurity on the cathodic potentials during different electrolysis durations of 1, 2, 4, 24, 48 and 72 h by galvanostatic measurements at 52.5 mA/cm^2 employing Pb-0.7%Ag or Pt anodes was evaluated. The zinc electrolyte was containing 12 g/L Mn^{2+} at 40°C, and two different concentrations of 0.15 and 0.2 mg/L Pb^{2+} ions were added into the zinc electrolyte with Pt anode, while no Pb^{2+} ions were added into the zinc electrolyte when the Pb-0.7%Ag anode was used. Results are shown in Fig. 4.9.

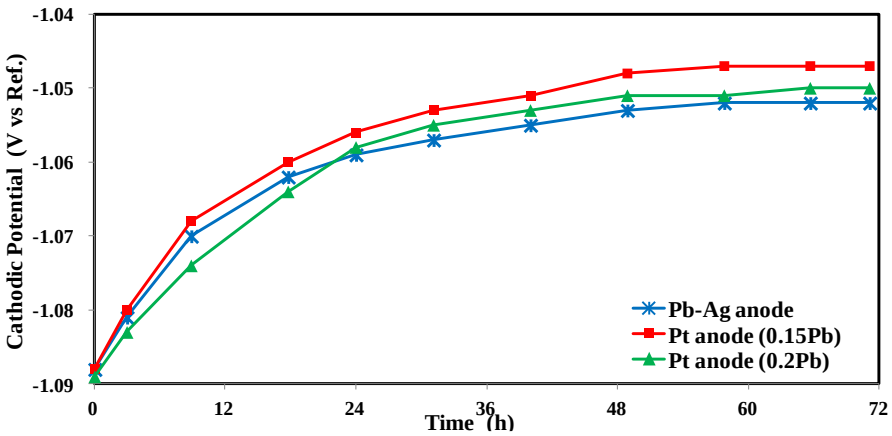

Fig. 4.9 Cathodic polarization curves of zinc deposit at 52.5 mA/cm^2 and 40°C in the zinc electrolyte containing 170 g/L H_2SO_4, 60 g/L Zn^{2+}, 12 g/L Mn^{2+} with Pb-0.7%Ag anode and two different Pb additions for Pt anodes, at different times of electrolysis

It could be observed from Fig. 4.9 that the three curves are close with similar tendency. During the initial 10 h, the potential shifted to less negative values (very possibly because of lead deposition) and then shifts slowly to less negative potentials during 10-24 h. After 24 h, the potential was found to be less negative in case of 0.2 mg/L than that of Pb-0.7%Ag anode, reaching to the plateau till the end of 72 h of deposition. In the zinc electrolyte containing 0.15 mg/L Pb^{2+}, the cathodic potential was -1.047 V, while the polarization was increased to reach -1.050 V when lead ions were increased to 0.2 mg/L. When Pb-0.7%Ag was used as anode, the cathodic potential of zinc deposit without external addition of Pb^{2+} ions; was more negative than the other two curves with Pt, but showing the same tendency. It starts with -1.088 V after first 1 h and reaches -1.052 V after 50 h. It was stable at the end between 50-72 h. This could be attributed to the higher corrosion rate of the lead-base anode during the initial few hours. It can be concluded that, the quantity of soluble lead obtained from the anode corrosion is less than 0.15-0.2 mg/L especially during the first few hours. The nucleation of zinc germs needs higher energy than that of grain size growth (Milazzo 1969). The zinc reduction becomes relatively easier with time as the first layer of zinc is formed and zinc is deposited on zinc rather than on the aluminum substrate.

4.3.3.2 Lead Content in Deposit and Electrolyte

The Pb content in zinc deposit and in the zinc electrolyte was analyzed using ICP. The results are shown in Table 4.4 and Fig. 4.10.

Table 4.4 Lead content in the zinc deposit and electrolyte after different time of 1, 2, 4, 24, 48 and 72 h electrolysis in the standard zinc electrolyte containing 170 g/L H_2SO_4, 60 g/L Zn^{2+}, 12 g/L Mn^{2+}, and various lead ion concentrations using Pb-Ag or Pt anode at 52.5 mA/cm^2, 40°C, and agitation of 60 rpm

Time (h)	Lead content (ppm)					
	Pb-Ag anode		Pt anode (0.15 mg/L Pb^{2+})		Pt anode (0.2 mg/L Pb^{2+})	
	Electrolyte	Deposit	Electrolyte	Deposit	Electrolyte	Deposit
1	0.92	1.38	0.88	1.34	0.96	1.45
2	0.74	1.40	0.85	1.35	0.95	1.46
4	0.66	1.44	0.83	1.38	0.93	1.48
24	0.69	1.66	0.71	1.47	0.88	1.57
48	0.63	1.73	0.46	1.65	0.64	1.70
72	0.74	1.98	0.17	1.90	0.25	1.94

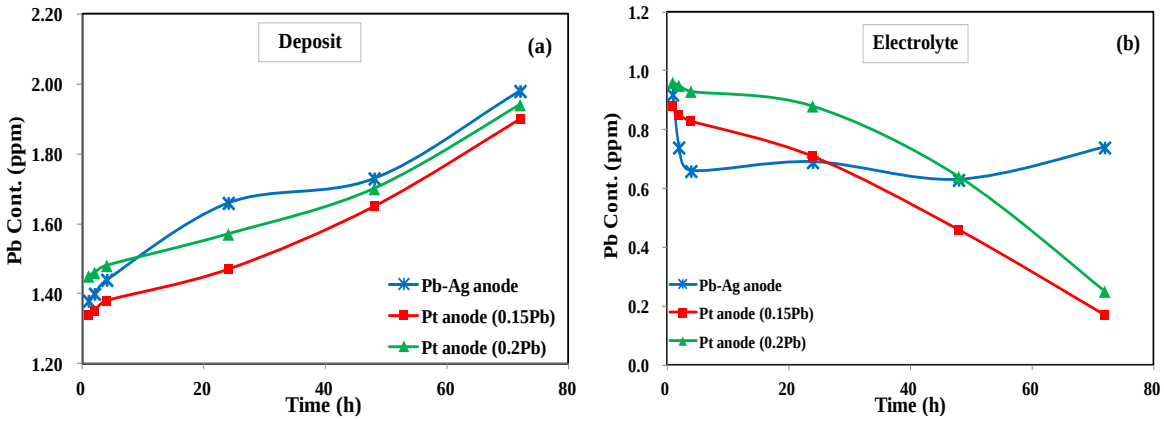

Fig. 4.10 Pb contamination in the (a) zinc deposit and (b) zinc electrolyte containing 170 g/L H_2SO_4, 60 g/L Zn^{2+}, 12 g/L Mn^{2+}, at 52.5 mA/cm^2, 40°C and agitation of 60 rpm with Pb-0.7%Ag anode and Pt anode at different Pb additions (0.15 and 0.2 mg/L) during different time periods of 1, 2, 4, 24, 48 and 72 h electrolysis

Fig. 4.10a shows that when platinum was used as anode, the 0.2 mg/L of Pb^{2+}addition resulted in more Pb content in zinc deposit than that of 0.15 mg/L, and lead contamination

was slightly increased as function of time. Employing Pb-0.7%Ag anode from 1 to 72 h showed a big increase of contamination (1.38-1.98 ppm) (Table 4.4).

At the end of 2 h of electrowinning, the Pb content in zinc deposit employing Pb-0.7%Ag anode was more than that of Pt anode with addition of 0.15 mg/L Pb^{2+} and lower than that of Pt anode with addition of 0.2 mg/L Pb^{2+}. However, at the end of 72 hours of electrowinning, the Pb content in zinc deposit using Pb-0.7%Ag anode (1.98 ppm) was almost the same as that with Pt anodes (1.90 and 1.94 ppm for addition of 0.15 to 0.2 mg/L of Pb^{2+}, respectively). This could confirm that, the lead contamination coming from the lead anode is almost between 0.15-0.2 mg/L.

Fig. 4.10b shows the evolution of the Pb content in the electrolyte as function of time for Pb-0.7%Ag anode and for two different quantities of added lead ions with the Pt anode. This could provide better understanding about the remaining non deposited Pb^{2+} in the electrolyte.

During the first hour, the electrolyte with Pb-0.7%Ag anode was having more lead than that after 2 h, because the relative protection of the anode by the MnO_2 layer was not complete. A steady value of the lead content in the electrolyte was observed (around 0.7 ppm) after 8h up to 72 h, showing an equilibrium between the lead dissolution from the anode covered by MnO_2 layer and the Pb^{2+} deposition rate. In case of external addition of lead employing Pt anode, the remaining lead in the examined two electrolytes was decreased to 26-29% during the last 48 h. This could be due to the electrodeposition potential of lead was becoming less negative, favoring lead deposition and leading to a very sensible decrease of lead ion in the electrolyte.

4.3.3.3 Current Efficiency

The calculated current efficiency values during 72 h of electrodeposition are given in Table 4.5. Results showed that, the CE% was reduced with the increase of electrodeposition time. In the case of Pb-0.7%Ag anode, the determined CE after 2 h was 95.3%, and then decreased to 92.8% after 24 h then to 88.5% after 72 h. This could be partially explained by the lower lead quantity in the electrolyte from around 0.92 to an average of 0.70 ppm and

the effect of such impurity on the incubation time and current efficiency in zinc electrowinning (Fukubayashi 1972).

The same trend was obtained employing platinum anode by adding soluble lead ions into the electrolyte at the beginning. The starting CE was 94.4-94.5% by adding 0.15-0.2 mg/L Pb^{2+} ions, respectively. After 72 h the CE was dropped to 87.2-88.5%. This sharp drop in CE values with long time of galvanostatic polarization could be explained by minor effect of deposited lead since soluble lead was highly decreased. Non-adherent deposit and a re-dissolution of zinc deposit into the electrolyte could be also considered.

Table 4.5 Current efficiency values after different times of 2, 4, 24, 48 and 72 h electrolysis

Time	Current Efficiency (%)		
(h)	Pb-0.7%Ag anode	Pt anode (0.15 mg/L Pb^{2+})	Pt anode (0.2 mg/L Pb^{2+})
2	95.3	94.5	94.4
4	95.1	94.3	94.1
24	92.8	92.5	92.4
48	91.4	91.1	90.7
72	89.5	88.5	87.2

4.3.4 Electrochemical Measurements

Electrochemical measurements based on potentiodynamic polarization, cyclic voltammetry, and electrochemical impedance spectroscopy have been conducted on the zinc deposition under atmospheric conditions in order to study the effect of different temperatures (35, 38, 40, 45°C), concentrations of sulfuric acid and zinc sulfate with 0.15 mg/L Pb^{2+} ions.

4.3.4.1 Potentiodynamic Polarization

Important information about the kinetic parameters such as cathodic Tafel slope and overpotential of zinc reduction can be obtained using potentiodynamic polarization. During polarization from -1.35 V to -1.05 V at scan rate of 5 mV/s, the theoretical cathodic overpotential is calculated as follows:

$$E_{e,Zn} = -0.763 + (RT/2F)\, ln[\, a_{Zn^{2+}} / a_{Zn}] \qquad (4.1)$$

$$E_{e,H_2} = 0.0 + (RT/F)\ln[\, a_{H^+} / (a_{H_2})^{0.5}\,] \quad (4.2)$$

$$\eta_{Zn} = E_m - (E_{e,Zn} + E_{e,H_2}) \quad (4.3)$$

where, E_e is the equilibrium potential, R the gas constant, T the working temperature in K, F the Faraday's constant (equal to 96500 C/mol), and E_m the measured potential at specific current density (52.5 mA/cm^2) (Barton and Scott 1992).

The cathodic Tafel slope was determined by extrapolating two selected points on the cathodic curve of log I-E, first point was far by ~50-100 mV from the corrosion potential and the other point was far by one decade of current density (Kelly et al. 2002). Results are shown in Table 4.6.

Fig. 4.11 shows the effect of different concentrations of zinc ions on the cathodic behavior. It was found that can increase in zinc ion concentrations from 56 g/L to 65 g/L in the presence of manganese alone, decreased the cathodic overpotential from 117 mV to 107 mV, respectively. The same trend of decrease was obtained also by combining manganese with 0.15 mg/L of Pb^{2+} ions. For all cases, Tafel slope values were increased slightly by increasing the zinc concentration. However, values of cathodic Tafel slope were between 114 and 122 mV/decade. This indicates that there was no change in the mechanism of hydrogen (Fletcher 2009) and zinc reduction reactions.

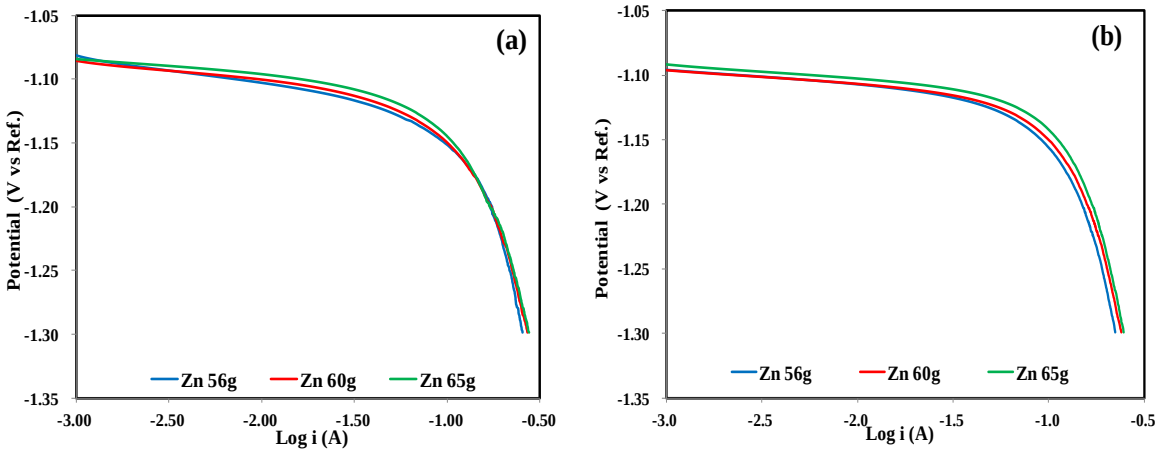

Fig. 4.11 Effect of zinc ion on cathodic polarization during zinc electrodeposition on aluminum cathode in zinc electrolyte containing 170 g/L H_2SO_4, 12 g/L Mn^{2+} and 0.15 mg/L Pb^{2+} (a) 12 g/L Mn^{2+} only, (b) 12 g/L Mn^{2+} and 0.15 mg/L Pb^{2+} at 40°C with 60 rpm of agitation

The effect of sulfuric acid concentration on zinc reduction is shown in Fig. 4.12. It can be observed that, increasing the concentration of acid decreased significantly the cathodic overpotential in presence and absence of lead. In absence of lead, η value decreased from 136 mV to 113 mV, by increasing acid concentration from 158 g/L to 170 g/L, respectively. This decrease in overpotential was much more pronounced in presence of lead, it is decreased from 153 mV to 114 mV at the same acid concentrations. It can be concluded that, by increasing the acid content in the electrolyte results in higher H^+ ions in the solution, which increased hydrogen evolution and reduced zinc reduction. Also, addition of lead (0.15 mg/L) to the zinc electrolyte showed higher overpotential due to the co–deposition of lead with zinc. Value of b_c was decreased as well by increasing acid concentration but still stayed in the range of 115 to 123 mV/decade (Table 4.6).

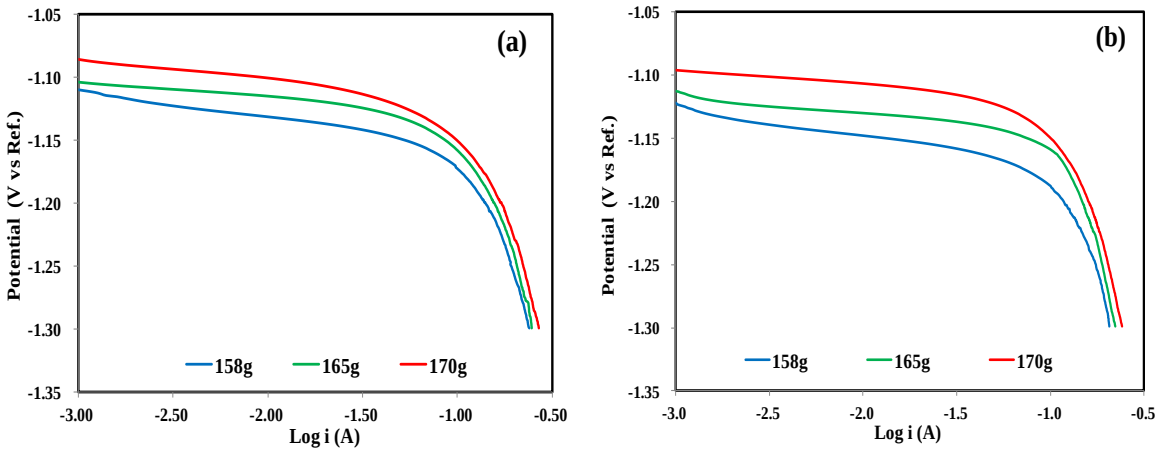

Fig. 4.12 Effect of sulfuric acid on cathodic polarization during zinc electrodeposition on aluminum cathode in zinc electrolyte containing 170 g/L H_2SO_4, 60 g/L Zn^{2+}, and (a) 12 g/L Mn^{2+} only, (b) 12 g/L Mn^{2+} and 0.15 mg/L Pb^{2+}, at 40°C and 60 rpm of agitation

It was found that increasing of temperature resulted in a decrease of the overpotential. This could be due to the decrease in viscosity and high movement of ions in electrolyte at high temperature. This results in more cations moving towards the cathode, obtaining more electrons and decreasing cathodic potential. The increase in the agitation rate from 60 to 412 rpm increased the overpotential from 113 to 120 mV, respectively, which confirms the galvanostatic results. It is significant that this parameter increases the hydrogen diffusion more effectively in the double layer (Table 4.6). However, none of the mentioned

parameters changed the mechanism of reduction according to the obtained values of cathodic Tafel slopes.

Table 4.6 The cathodic overpotential and Tafel slope value at different working parameters with Pt anode

Parameters		12 g/L Mn^{2+}		12 g/L Mn^{2+} and 0.15 g/L Pb^{2+}	
		$-\eta_{(52.5)}$ (mV/SHE)	*Tafel Slope* ($-b_c$) (mV/decade)	$-\eta_{(52.5)}$ (mV/SHE)	*Tafel Slope* ($-b_c$) (mV/decade)
Zn^{2+} (g/L)	56	117	119	116	122
	60	113	115	114	119
	65	107	114	108	117
H_2SO_4 (g/L)	158	136	123	153	123
	165	120	117	130	122
	170	113	115	114	119
Agitation (rpm)	60	113	115	114	119
	100	118	122	116	123
	412	120	126	118	128
Temperature (°C)	35	124	118	121	123
	38	120	117	114	123
	40	113	115	114	119
	45	109	117	108	117

4.3.4.2 Cyclic Voltammetry Study

The cyclic voltammetry was carried out by scanning from the potential -1.30 to -0.70 V at 10 mV/s. It was found that this high scan rate is enough to determine the oxidation - reduction peaks. The voltammograms were initiated at point (A) (Fig. 4.13-4.14) at potential of -1.30 V, scanned in the positive direction, and then reversed at the potential -0.70 V in the negative direction, crossed-over at point (B). No significant current was observed from point (C) until the potential reached the point (B), corresponding to the reduction of Zn^{2+} ions. Nucleation overpotential (NOP) is the difference between the crossover potential (B) (the start of the dissolution), and the point at which the Zn begins to

deposit (D). Fig. 4.13 shows the effect of sulfuric acid concentrations on cyclic voltammogram of the aluminum electrode in the zinc electrolyte containing 60 g/L Zn^{2+}, 12g/L Mn^{2+} and 0.15 mg/L Pb^{2+}. NOP values were 50 mV, 54 mV, and 58 mV for 170, 165, and 158 g/L H_2SO_4, respectively. It was found that increasing sulfuric acid concentrations decreased the NOP of zinc deposit on aluminum electrode.

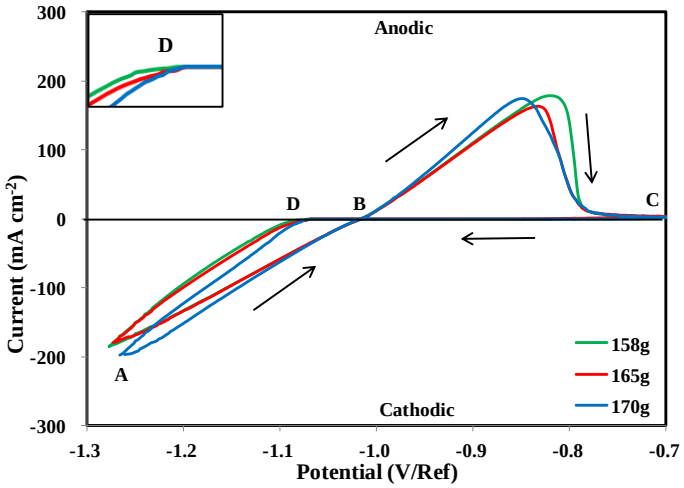

Fig. 4.13 Effect of different contents of sulfuric acid (158, 165 and 170 g/L) on cyclic current-potential curve of the aluminum electrode in the zinc electrolyte containing 60 g/L Zn^{2+}, 12 g/L Mn^{2+}, and 0.15 mg/L Pb^{2+}, at 40°C, without agitation and scan rate of 10 mV/s.

Fig. 4.14 shows the effect of different temperatures on cyclic voltammogram of the aluminum electrode in the zinc electrolyte containing 170 g/L H_2SO_4 and 60 g/L Zn^{2+}. The nucleation overpotentials of zinc deposit on aluminum electrode from the curves are as follows: 56 mV, 50 mV and 42 mV at 35, 40, and 45°C, respectively. It was found that increasing the electrolyte temperature decreased the nucleation overpotential of zinc deposit on aluminum electrode.

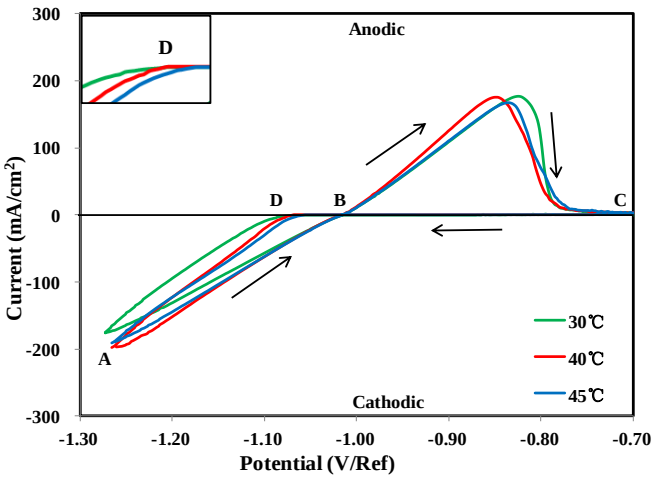

Fig. 4.14 Effect of different temperatures (35, 40, and 45°C) on cyclic current vs potential curve of the aluminum electrode in the zinc electrolyte containing 170 g/L H_2SO_4, 60 g/L Zn^{2+}, 12 g/L Mn^{2+}, and 0.15 mg/L Pb^{2+}, without agitation at a scan rate of 10 mV/s

4.3.4.3 Electrochemical Impedance Spectroscopy

The impedance plots obtained at low potentials along the polarization curves (Fig. 4.15) give mainly a high-frequency capacitive loop in the studied frequency domain. This corresponds to the charge transfer resistance R_{ct}, of zinc deposit in parallel with double layer capacitance C_{dl}.

Fig. 4.15 shows the effect of sulfuric acid concentrations, temperatures, and lead ions on Nyquist plots of zinc deposit during zinc electrodeposition on aluminum cathode and zinc cathodes in zinc electrolyte containing 60 g/L Zn^{2+} and 12 g/L Mn^{2+}, at agitation of 60 rpm.

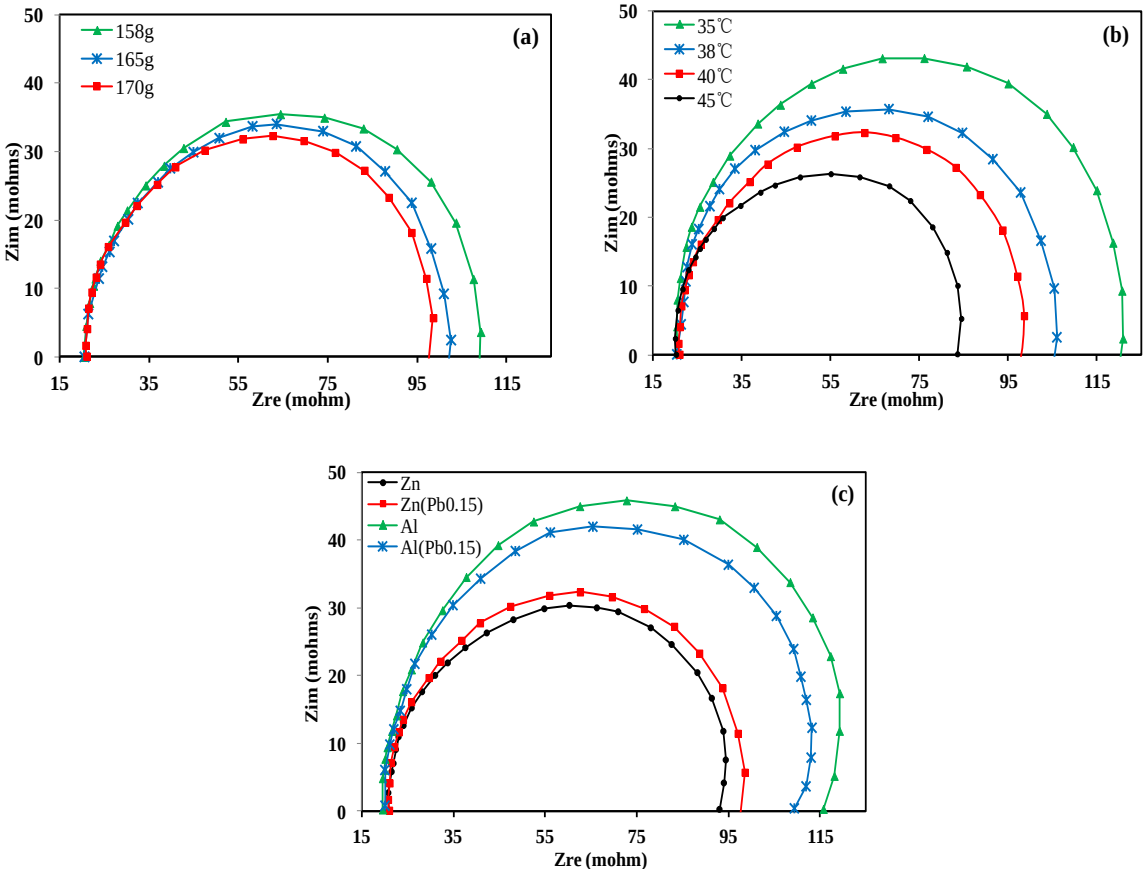

Fig. 4.15 Effect of concentrations of (a) sulfuric acid, (b) temperatures, and (c) lead content on Nyquist plots of polarization resistances of zinc deposit during zinc electrodeposition on aluminum cathode and zinc cathodes in zinc electrolyte containing 60 g/L Zn^{2+}, 12 g/L Mn^{2+}, at 40°C and agitation of 60 rpm

The equivalent circuit is presented in Fig. 4.16. R_S corresponds to the electrolyte resistance between the electrode surface and the salt bridge tip, R_{ct} to the charge transfer resistance of the zinc deposit in zinc electrolyte, and C_{dl} the double layer capacitance for the zinc deposit.

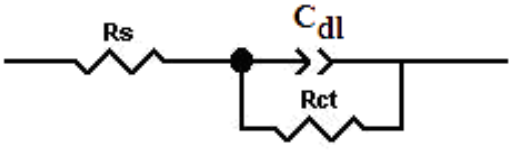

Fig. 4.16 Equivalent circuit proposed for fitting the experimental data of electrochemical impedance measurements for zinc deposit reaction on aluminum substrate

The results have showed that, the solution resistance did not change and was always around 20 mΩ cm^2. The zinc deposit in the electrolyte containing 158 g/L H_2SO_4 had the highest charge transfer resistance (108.2 mΩ cm^2), followed by that of 165 g/L (95.6 mΩ cm^2), and 170 g/L (93.4 mΩ cm^2). Temperature decreased as well the resistance of charge transfer and C_{dl}. R_{ct} is decreased from 121.7 to 82.3 mΩ cm^2 by increasing the temperature from 35 to 45°C (Table 4.7). It indicates that the reduction reactions are easier at higher temperatures, and confirms the results obtained from potentiodynamic polarization. High C_{dl} indicates more electrons were adsorbed on the surface of metal, meaning that low temperature results in an increase of overpotential during zinc deposit.

Table 4.7 Comparison of the parameters for the equivalent circuit of the zinc deposit reaction on aluminum cathodes during zinc electrodeposition

Parameter		R_{ct} (mΩ cm^2)	C_{dl} (mF/cm^2)
H_2SO_4 (g/L)	158	108.2	24.3
	165	95.6	26.4
	170	93.4	94.1
Temperature (°C)	35	121.7	103.8
	38	105.8	98.6
	40	93.4	94.1
	45	82.3	85.3

The values of charge transfer resistance (R_{ct}) and capacitance double layer (C_{dl}) for zinc deposition on zinc and aluminum cathodes in presence of Pb^{2+} are shown in Table 4.8. It was found that zinc reduction on zinc electrode was easier than on Al electrode. R_{ct} was found to be 93.4 mΩ cm^2 in case of Zn deposition on Zn, while this value was increased to 109.4 mΩ cm^2 for Zn deposition on Al. Also, C_{dl} was increased from 94.1 (Zn on Zn) to 99.7 mF/cm^2 (Zn on Al anode). The addition of Pb^{2+} ions increased the R_{ct}, which means that the zinc reduction is more difficult in presence of lead ions. This is confirmed by C_{dl} values as it was 86.7 mF/cm^2 for zinc deposition on zinc substrate then increased to 90.6 mF/cm^2 for zinc deposition on Al substrate.

Table 4.8 Comparison of the parameters for the equivalent circuit of the zinc deposit reaction on aluminum and zinc substrate in zinc electrolyte with and without 0.15 mg Pb^{2+} additive measured by electrochemical impedance

Parameter	Zn	Zn (0.15 mg/L Pb^{2+})	Al	Al (0.15 mg/L Pb^{2+})
R_{ct} ($m\Omega\ cm^2$)	93.4	98.6	109.4	115.7
C_{dl} (mF/cm^2)	94.1	86.7	99.7	90.6

4.4 Conclusions

An investigation was conducted to evaluate the effect of electrolyte composition and operating conditions of electrolysis on the overall performance of zinc deposition. The following conclusions can be derived from this study:

1. It has been revealed that lead contamination from the Pb-0.7wt.%Ag anode is very close to 0.15-0.2 mg/L Pb^{2+}. After 2 h of galvanostatic polarization employing Pt anode with addition of 0.1 up to 2.5 mg/L of Pb^{2+} to the zinc electrolyte, led to an increase of the cathodic potential by 55 mV and current efficiency by 1.2%. Electrolysis duration up to 72 h, using both anodes, the cathodic potential decreased by ~35mV, and a decrease in CE value by ~6.8% was observed.

2. Addition of Mn^{2+} in different concentrations (4-16 g/L) to the electrolyte employing Pb-Ag anode, decreased the CE by 0.7-2%, and shifted the cathodic potential to less negative values by 10 to 56 mV. Also, a decrease of the lead content in zinc deposit by 2.3 up to 3.8 ppm was observed. The concentration of 12 g/L of Mn^{2+} in the electrolyte could be considered as an optimum quantity since it gives CE of 95.3%, with relative low overpotential (45 mV), and reduced the lead contamination in the zinc deposit by 3.8 ppm. The catalytic effect of manganese addition could be due to the formed MnO_4^- ions which accelerates the HER and decrease the rate of Zn^{2+} reduction.

3. Increasing Zn^{2+} concentration from 56 to 65 g/L in the electrolyte increased the CE by ~0.85% after 2 h of electrolysis. The cathodic potential was decreased by 13 mV for Pt and 18 mV for Pb-Ag. The increase of acid content from 158 to 170 g/L had a negative

effect on the CE due to high hydrogen evolution which hinders the reduction of Zn^{2+} ions.

4. Changing the current density from 45 to 60 mA/cm^2 resulted in an increase in cathodic potential and an increase in current efficiency. Electrolyte agitation from 60 to 412 rpm showed less current efficiency and more negative overpotentials, due to higher hydrogen mobility and relatively slow reduction of zinc. There is an optimum value at 100 rpm, above which cathodic potential was almost stable and current efficiency decreased by only 0.4%.

5. The effect of increasing electrolyte temperature from 35 to 45°C showed a decrease in the cathodic potential. The current efficiency was slightly increased by ~0.3% with changing temperature from 35 to 40°C, and increased sensibly by 0.8% from 40 to 45°C. Generally, the influence of temperature is complex to explain especially for close changes. However, this could be due to the relatively more important effect on overpotential values and Zn^{2+} diffusion than that in hydrogen reaction.

6. Electrochemical impedance spectroscopy technique confirmed the obtained results from potentiodynamic and cyclic voltammetry, showing that the zinc reduction on zinc electrode is easier than of that on aluminum electrode. R_{ct} was found to be 93.4 mΩ cm^2 in case of Zn on Zn, while this value was increased to 109.4 mΩ cm^2 for Zn on Al. C_{dl} was increased from 94.1 to 99.7 mF/cm^2. The addition of Pb^{2+} ions increased the R_{ct}, indicating that zinc reduction requires more overpotential in presence of lead ions.

Acknowledgments

Canadian Electrolytic Zinc (CEZinc), Hydro-Québec and Natural Sciences and Engineering Research Council of Canada (NSERC) are gratefully acknowledged for their financial support. The authors would like to express their sincere thanks and appreciation to Mr. Nabil Sorour and Mr. Ahmet Deniz Bas for their valuable advice and guidance. Also thanks to Mr. André Ferland for SEM analysis, Mr. Jean Frenette for XRD analysis, Mrs. Vicky Dodier and Mr. Alain Brousseau for ICP analysis.

CHAPTER 5

THE EFFECT OF LEAD IMPURITY IN PRESENCE OF MANGANESE ADDITION ON ZINC ELECTROWINNING

The Effect of Lead Impurity in Presence of Manganese Addition on Zinc Electrowinning

*C. Su[1], N. Sorour[1], W. Zhang[1], E. Ghali[1], and G. Houlachi[2]

[1]*Department of Mining, Metallurgical and Materials Engineering, Laval University, Québec, Canada, G1V 0A6*

[2]*Hydro-Québec research centre (LTE), Shawinigan, QC, Canada, G9N 7N5*

* Corresponding author. Tel.: +1 418-656 8657 Fax: +1 418-656 5343.
E-mail address: chaoran.su.1@ulaval.ca (C. Su)

This paper was presented in the XXVIII International Mineral Processing Congress (IMPC 2016), Québec City, Canada (September 11-15) and published in the proceedings, paper #952, ISBN: 978-1-926872-29-2.

Résumé

Le procédé d'extraction électrolytique du zinc est sensible à la présence d'impuretés métalliques telles que les ions de plomb qui pourraient affecter de façon importante et négative la consommation d'énergie et la morphologie de la surface du dépôt de zinc. On a étudié l'effet de différentes concentrations d'ions de manganèse et de traces d'ions de plomb jusqu'à 2,5 mg/L ajoutés à l'électrolyte pendant l'électrolyse en utilisant des techniques de polarisation électrochimique telles que la galvanostatique, la voltammétrie cyclique et la potentiodynamique. La microscopie électronique à balayage (MEB) et la diffraction des rayons-X (DRX) ont été appliquées pour examiner la morphologie de la surface et l'orientation cristallographique du dépôt, respectivement. La spectrométrie d'émission atomique plasma-micro-ondes a été utilisée pour déterminer la teneur en plomb du dépôt et de l'électrolyte après l'électrodéposition. On a montré que des ions de plomb ajoutés à l'électrolyte de sulfate de zinc conduisaient à une augmentation de la surtension cathodique et des rendements de courant lors du dépôt de zinc. Cependant, l'addition de Mn^{2+} dans l'électrolyte a entraîné la diminution du potentiel cathodique et du rendement de courant. On peut constater, par exemple, que la polarisation galvanostatique à 52,5 mA/cm^2 et 40°C en présence de plomb jusqu'à 0,1-0,2 mg/L et de manganèse jusqu'à 8-12 g/L dans l'électrolyte pourrait être considérée avantageusement pour fixer les paramètres lors de la pratique des opérations du procédé d'extraction électrolytique du zinc.

Abstract

Zinc electrowinning process is sensitive to the presence of metallic impurities such as lead ions that could substantially and negatively affect the power consumption and surface morphology of the zinc deposit. Effects of various concentrations of manganese ions and traces of lead ions up to 2.5 mg/L added to the electrolyte during electrowinning have been investigated by electrochemical polarization techniques such as galvanostatic, cyclic voltammetry, and potentiodynamic. Scanning electron microscopy (SEM) and X-ray diffraction (XRD) were applied to examine the surface morphology and crystallographic orientation, respectively. Microwave plasma-atomic emission spectrometry has been used to determine the lead content in the deposit and in the electrolyte after electrodeposition. It was found that lead ions added to the zinc electrolyte led to the increase of cathodic overpotential and current efficiencies of zinc deposit. However, addition of Mn^{2+} into the zinc electrolyte resulted in the decrease of cathodic potential and current efficiency. It can be stated, for example, that galvanostatic polarization at 40°C and 52.5 mA/cm^2 in presence of lead up to 0.1-0.2 mg/L and manganese up to 8-12 g/L in the electrolyte could be considered advantageously as practical working parameters for electrowinning process of zinc**.**

Keywords

Zinc electrowinning, Electrochemical techniques, Lead impurity, Current efficiency, Cathodic potential, Surface morphology.

5.1 Introduction

Approximately 85% of the global production of zinc metal is produced by electrolytic process (Sinclair 2005). The main goal of the zinc plant is to obtain pure zinc deposits with high current efficiencies. Smooth and pure deposits with high current efficiency (CE) are always obtained from pure electrolytes (Alfantazi and Dreisinger 2001). The presence of metallic impurities in the zinc sulfate electrolyte is a major problem for the zinc electrowinning industry, since decreases in current efficiency, changes in deposit morphology and cathodic polarization are observed for electrolytes containing small concentrations of impurities (Ault and Frazer 1988; Muresan et al. 1996). It is reported that low level concentrations as parts per million of these impurities influences negatively the zinc electrodeposition (Beshore et al. 1987).

Lead is one of the major metallic impurities, which has a detrimental effect on the zinc electrodeposition (Ault and Frazer 1988). As far as lead-based anodes are still used in this process, the possibility of varying degrees of Pb contamination of the zinc deposits exists; either because of improperly conditioned anodes or because the anodes have been deteriorated over a period of time (Mackinnon and Brannen 1979). Pb^{2+} ions are usually co-reduced with Zn^{2+} ions leading to a decrease in the purity of the produced zinc metal. Mackinnon and Brannen (1979) found also that, an increase in overpotential and vertical deposit orientations were obtained for zinc deposits contaminated by lead up to 0.07wt.%. For lead concentrations higher that 0.07%, heavily pitted deposits with a basal orientation were obtained.

Due to the costly purification steps for the zinc electrolytes, many plants are optimizing the working parameters such as the current density, temperature, Zn^{2+} ions concentration, pH, and agitation in order to obtain compact zinc deposits with high current efficiencies (Mackinnon et al. 1987). However, developing alternative methods to reduce the negative effect of metallic impurities are always subject of many studies and researches such as (Tripathy et al. 1998 and Zhang and Hua 2009). Searching for appropriate organic or inorganic additives was always the objective of many studies. Additives showed their beneficial effects on producing fine-grained, smooth, and compact deposit with high current efficiency (Tripathy et al, 1998).

It was found that maintaining 1.5 to 3.0 mg/L of Mn^{2+} in the electrolyte is sufficient to minimize the lead anode corrosion and to reduce the contamination of the cathodic zinc by lead (Ivanov and Stefanov 2002). The lead anode is protected from corrosion by MnO_2 and PbO_2 layers, since the well adherent oxide film of MnO_2 increases the thickness and oxide layer PbO_2-MnO_2 which protects the lead anode from corrosion. The presence of Mn^{2+} ions affects slightly the anodic potential since the potential decreases as a result of depolarization effect during the oxidation of Mn^{2+} on the anode (Ivanov et al. 2000). The behavior of manganese during zinc electrodeposition by using chemical analysis and absorption spectroscopy demonstrated that Mn^{2+} ions are anodically oxidized to MnO_4^- ions. The latter immediately reacted with Mn^{2+} ions and produce Mn^{3+} ions then MnO_2 which can absorb deleterious ions. It was also found that the amount of MnO_2 formed depends on the anode material (Tswuoka 1960).

Low concentrations of $MnSO_4$ did not impact significantly on the cathodic process in zinc electrowinning, whereas they played a significant role in the anodic process. This was intimately involved in the formation of oxide layers on the Pb-Ag anodes and thus helped to minimize anode corrosion and hence the Pb content of the zinc deposit. With high concentrations of $Mn^{2+} > 10$ g/L, a slight decrease in current efficiency may occur because of the reduction of the higher valent manganese species at the cathode. Similar results are also observed by (Zhang and Hua 2009, MacKinnon 1994, MacKinnon and Brannen 1991, and Vakhidov and Kiryakov 1959). MnO_2 demonstrated good catalytic activity for the OER in both acidic and alkaline solutions. Since manganese usually exists in the zinc sulfate electrolyte, its dissolution in the electrolyte does not affect the electrowinning process (Mohammadi and Alfantazi 2015).

Although the effect of low level of Mn^{2+} and Pb^{2+} separately on zinc electrowinning has been investigated by many researchers, however, the influence of high level of Mn^{2+} and Pb^{2+} together were rarely reported. The aim of this work is to study the effect of different concentrations of Mn^{2+} ions of 8, 12, 16 g/L with traces of Pb^{2+} ions of 0.1, 0.2, and 2.5 mg/L on zinc electrodeposition and lead contamination in the deposited zinc. Also, scanning electron microscopy (SEM) and X-ray diffraction (XRD) were applied to examine the surface morphology and crystallographic orientation, respectively. Microwave plasma-

atomic emission spectroscopy was used to determine the lead content in the deposit and in the electrolyte after electrodeposition.

5.2 Experimental

5.2.1 Reagents and Electrolysis

The zinc sulfate electrolytes used in this study were prepared from $ZnSO_4 \cdot 7H_2O$, and pure H_2SO_4 (Conc. 98%). The foreign cations of Mn^{2+} and Pb^{2+} were added under the form of $MnSO_4 \cdot 2H_2O$, and Pb $(C_2H_3O_2)_2$, respectively. The blank electrolytic solution was always prepared from 170 g/L H_2SO_4 and 60 g/L Zn^{2+}. The standard zinc electrolyte was based on electrolytic solution with 12 g/L Mn^{2+}. The analyzed prepared electrolyte contains Pb concentration of 0.8 ppm. Reagents were supplied from Lab mat and VWR Canada.

Small-scale galvanostatic electrolysis was performed in 1000 ml solution in double-glazed beaker. The solution was heated by flowing thermostated water in order to maintain a constant working temperature. One plate of pure Al and one plate of Pb-0.7wt.%Ag were used as cathode, and anode respectively. During the examination of the effect of Pb^{2+} ions in the electrolyte, a plate of Pt was also used as anode. All plates were casted in polyester resin in order to obtain an exposed surface area of 1 cm^2. Ag, $AgCl/KCl_{(sat)}$ (0.199 V/SHE) was used as reference electrode. Electrodes were mounted in three-cell electrode with inter distance of 2 cm. Before electrolysis, both cathode and anode were manually polished by several grits SiC papers then washed with distilled water and ethanol, and dried before the immersion in the electrolyte. The three-cell electrode was connected to a potentiostat Gamry PC4-270–Gamry USA.

5.2.2 Deposit Examination

Morphology of the surfaces of deposits was examined by scanning electron microscopy (SEM) using JOEL JSM-840a. The crystal orientation of the zinc deposit was determined using X-ray diffractometer model Siemens-D5000. Lead concentration in the deposit has been measured by using Microwave plasma-atomic emission spectrometry model 4200 MP-AES–Agilent Technologies.

5.2.3 Electrochemical Measurements

Electrochemical studies were based on the analysis of cyclic voltammetric measurements and potentiodynamic polarization tests without agitation in atmospheric conditions by using potentiostat Gamry reference 3000. A pure Al sample of 1 cm^2 was used as working electrode, and the Pt sample of 1 cm^2 was employed as counter electrode. Ag, AgCl/KCl $_{(sat)}$ was always used as the reference electrode.

Cyclic voltammetry experiments were carried out from initial potential of -1.3 V to final potential of -0.7 V at scan rate 10 mV/s. The potential was scanned from -1.05 to -1.30 V for the cathodic potentiodynamic polarization with a constant scan rate 5 mV/s.

5.3 Results and Discussion

5.3.1 Galavanostatic Measurements

In galvanostatic study, a constant current was applied between the working electrode and the counter electrode. The potential of working electrode was recorded as function of time. In addition, galvanostatic measurements were performed to characterize the cathodic behavior of the zinc deposition in the standard zinc electrolyte of 170 g/L H_2SO_4, 60 g/L Zn^{2+}, and 12 g/L Mn^{2+} with and without various concentrations of Pb^{2+} impurity such as 0.1, 0.2 and 2.5 mg/L, at current density of 52.5 mA/cm^2, 40°C, and agitation of 60 rpm. Also, after 2 h electrolysis the deposits have been dried and weighed and current efficiency (CE) has been measured according to Faraday's law as follows:

$$CE\% = (W.F.n/I.t.M) \times 100\% \quad (5.1)$$

where W is the weight of deposit (g), F the Faraday's constant, n the number of electrons, I the total cell current (A), t the time of electrodeposition, and M the atomic weight of metal (Scott, Pitblado & Barton, 1987). Current efficiency values obtained are listed in Table 5.1.

The effect of Mn^{2+} on the cathodic potential versus the reference electrode has been shown in Fig. 5.1. In fact, the relation between Mn^{2+} addition at different concentrations (0, 8, 12, and 16 g/L) in the electrolyte containing 170 g/L H_2SO_4, 60 g/L Zn^{2+}, and the cathodic

current potential illustrates that by increasing the Mn^{2+} ions concentration, the potential value is decreasing. For zero addition, the measured potential was about -1.095 V/Ref, while this potential was shifted to less negative values gradually by increasing the Mn^{2+} concentration reaching -1.084 to -1.078 V/Ref at concentrations of 8-12 g/L, respectively. By increasing the concentration up to 16 g/L Mn^{2+}, the cathodic potential was dropped to -1.070 V. This depolarization effect could be corresponding to the effect of MnO_4^- ions formation at high concentration of Mn^{2+}, which catalyzes the hydrogen evolution reaction (HER) and reduces its overpotential (Zhang and Hua, 2009). The current efficiency values, using different concentrations of Mn^{2+} ions, are listed in Table 5.1, indicate that CE% is reduced with increasing the Mn^{2+} concentration. CE% is dropped from 96.3% to 95.5% with addition of 8 g/L Mn^{2+}, and then further drop by 0.2% was observed at 12 g/L Mn^{2+}. At 16 g/L Mn^{2+}, the current efficiency is reduced to 94.3% which could be explained due to the hydrogen evolution reaction which affects the reduction of Zn^{2+} ions.

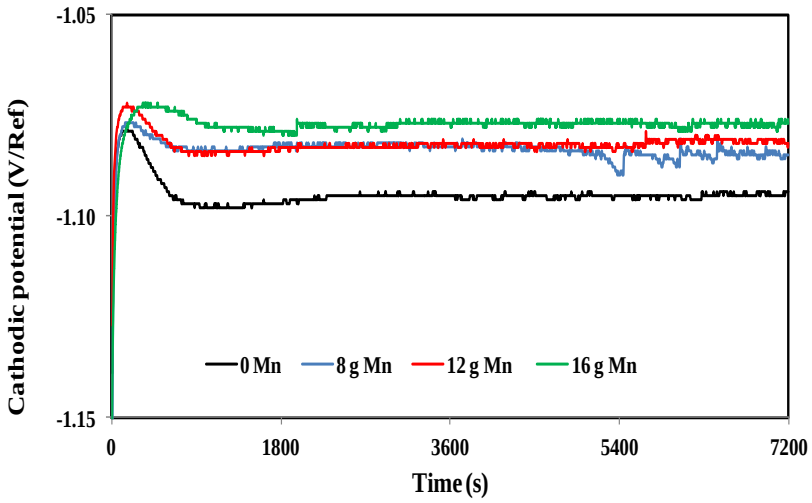

Fig. 5.1 Cathodic potential for 2 h zinc deposition on Al cathode in zinc electrolyte containing 170 g/L H_2SO_4, 60 g/L Zn^{2+}, and 0, 0.8, 12, and 16 g/L Mn^{2+} at a current density of 52.5 mA/cm^2, 40°C, with agitation of 60 rpm

The effect of Pb^{2+} on the cathodic potential versus the reference electrode is reported in Fig. 5.2. The relation between Pb^{2+} addition at different concentrations (0.1, 0.2, 2.5 mg/L) to the electrolyte containing 170 g/L H_2SO_4, 60 g/L Zn^{2+}, and 12 g/L Mn^{2+} and the cathodic

current potential shows that by increasing the Pb^{2+} ion concentration, the potential is increasing. Addition of Pb^{2+} also increased the CE%, reaching 95.6% at a high concentration of 2.5 mg/L Pb^{2+} as shown in Table 5.1. The same trend of results was also reported previously by (Ault and Frazer 1988; Mackinnon et al. 1979). The reason of that is due to Pb ion addition into zinc electrolyte which increases hydrogen overpotential, leading then to higher zinc current efficiency.

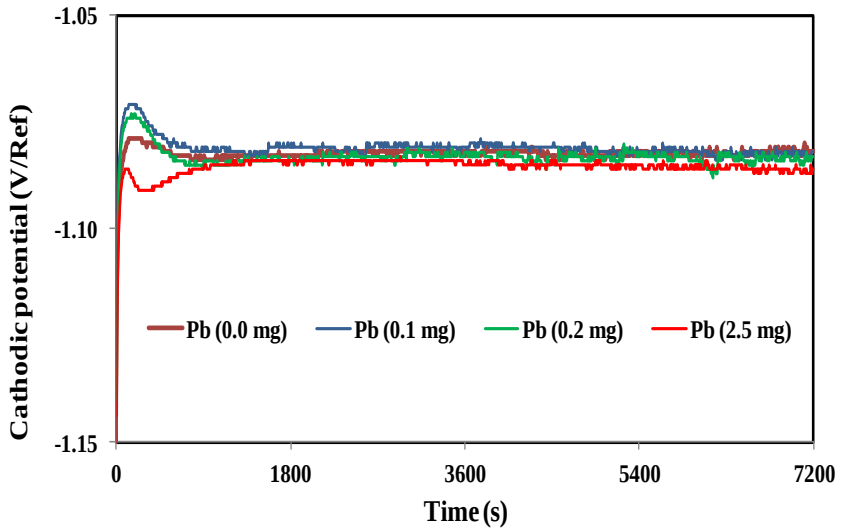

Fig. 5.2 Cathodic potential for 2 h zinc deposition on aluminum cathode in zinc electrolyte containing 170 g/L H_2SO_4, 60 g/L Zn^{2+}, 12 g/L Mn^{2+} and 0, 0.1, 0.2, or 2.5 g/L Pb^{2+}, at a current density of 52.5 mA/cm^2, 40°C, with agitation of 60 rpm

Table 5.1 shows the results of cathodic potentials and current efficiencies of zinc deposit from Fig. 5.1 and 5.2. Mn^{2+} was added to the blank electrolyte containing 170 g/L H_2SO_4, 60 g/L Zn^{2+}, while Pb^{2+} was added to the standard electrolyte containing 170 g/L H_2SO_4, 60 g/L Zn^{2+}, and 12 g/L Mn^{2+}. It is interesting to find that the type of anode has effect on the current efficiencies with the same standard electrolyte. The current efficiency (94.2%) of zinc deposit with Pt anode was lower than that (95.3%) with Pb-Ag alloy anode, very possibly because of lead traces.

Table 5.1 Effect of different parameters on the cathodic potential and current efficiency during the zinc electrodeposition in electrolyte containing 170 g/L H_2SO_4, 60 g/L Zn^{2+}, for 2 h at 52.5 mA/cm^2, 40°C, and agitation of 60 rpm

Parameter		Cathodic Potential (V/Ref)	CE (%)
Blank	0	-1.095	96.3
Mn^{2+} (g/L)	8	-1.084	95.5
	12	-1.078	95.3
	16	-1.070	94.3
Pb^{2+} (mg/L)* (12 g/L Mn^{2+})	0.0	-1.079	94.2
	0.1	-1.081	94.4
	0.2	-1.083	94.7
	2.5	-1.087	95.6

* Electrodeposition by using Pt anode

5.3.2 Deposit Examination

The zinc deposits have been examined by scanning electron microscope (SEM) (Fig. 5.3), and crystal orientation has been determined by X-ray diffraction (XRD) (Table 5.2). Also lead content in the deposits has determined by microwave plasma-atomic emission spectroscopy and listed in Table 5.2. The 1000X micrographs of zinc deposit obtained from blank electrolyte (Fig. 5.3) shows a medium grain size deposit with typical crystallographic orientation of (101) (102) (103) (002). The zinc deposit obtained from the electrolyte containing 8 g/L of Mn^{2+} ions is characterized by larger platelet size as the orientation (002) is inhibited and the crystallographic orientation is changed to (101) (100) (103) (102). Increasing the concentration of Mn^{2+} ions to 12-16 g/L, the zinc deposit restored the standard orientation (101) (103) (102) (002) with compact grain-sized deposit.

By adding Pb^{2+} ions with concentrations 0.1-0.2 mg/L, the deposit was found to have larger platelet size with orientation (101) (103) (102) (002) as the orientation (103) became the second predominate. By increasing the lead concentration up to 2.5 mg/L the deposit was neither compact nor smooth and orientation is completely changed to orientation (103) as the predominate one which indicates that the high concentration of lead in the electrolyte affects negatively the surface morphology and crystallographic orientation.

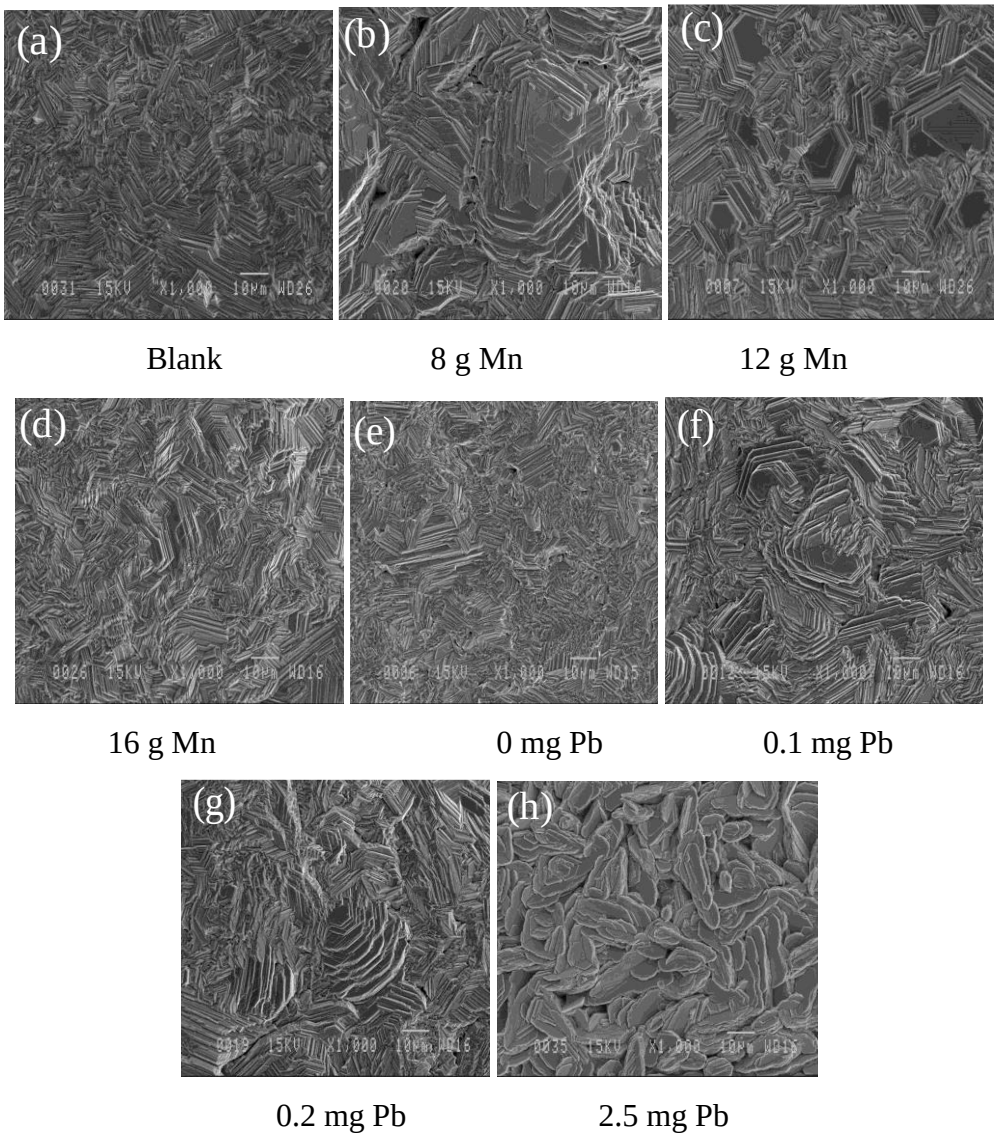

Fig. 5.3 Scanning electron micrographs (1000X) of zinc deposits after 2 h zinc electrolysis in the standard zinc electrolyte containing 170 g/L H_2SO_4, 60 g/L Zn^{2+}, 12 g/L Mn^{2+} and various concentration of lead ions, at 52.5 mA/cm^2, 40°C, and agitation of 60 rpm

Table 5.2 shows the results of lead contents (ppm) in the zinc electrolyte and zinc deposit after 2 h electrolysis. It was found that there is 23 ppm in the zinc deposit from the blank solution. Addition of lead ion into the blank solution increased the Pb contamination in the zinc electrolyte and zinc deposit after 2 h electrolysis. It can be observed that the lead content in zinc deposit reached to 12.7 ppm when 2.5 mg/L Pb was added to the zinc electrolyte. This means that higher lead ions in the zinc electrolyte caused higher lead contamination in the zinc deposit.

Table 5.2 Crystallographic orientation and Pb content in the Zn deposit after 2 h zinc electrolysis in the standard zinc electrolyte containing 170 g/L H_2SO_4, 60 g/L Zn^{2+}, 12 g/L Mn^{2+} with various lead ion concentrations, at 52.5 mA/cm^2, 40°C, and agitation rate of 60 rpm

	Parameter	Crystallographic Orientation (*hkl*)	Lead Content (ppm) Deposit
Blank	0	(101) (102) (103) (002)	23.8
Mn^{2+} (g/L)	8	(101) (100) (103) (102)	15.1
	12	(101) (103) (102) (002)	10.0
	16	(101) (103) (102) (002)	13.6
Pb^{2+} (g/L)* (12 g/L Mn^{2+})	0.0	(101) (102) (103) (002)	-
	0.1	(101) (103) (102) (002)	1.1
	0.2	(101) (103) (102) (002)	1.3
	2.5	(103) (102) (101) (002)	12.7

* Electrodeposition by using Pt anode

5.3.3 Potentiodynamic Polarization for Zinc Deposit

In potentiodynamic polarization tests the zinc deposit on aluminum cathode was polarized in the standard zinc electrolyte (170 g/L H_2SO_4, 60 g/L Zn^{2+}, and 12 g/L Mn^{2+}) with and without Pb^{2+} impurity, at T = 40°C, and under atmospheric conditions from -1.05 V to a final potential of -1.30 V, at a scanning rate of 5 mV/s. The cathodic polarization curves show the effect of different concentrations of Mn^{2+} and Pb^{2+} ions on the cathodic behavior of the zinc deposition (Fig. 5.4). Kinetic parameters presented in the cathodic Tafel slope and cathodic overpotential at 52.5 mA/cm^2 from potentiodynamic measurements are given in Table 5.3. By increasing the quantity of Mn^{2+} ions, a depolarization is observed and Tafel slope values are also decreased from 118 mV/decade at zero Mn^{2+} to 114 mV/decade at 8 g/L Mn^{2+} ions. Further decrease is caused by further addition of Mn^{2+} reaching 108 mV/decade at 16 g/L Mn^{2+} ions. It also can be stated that the potential becoming more negative as the current densities on the Zn surface in the four baths increased. The current for Zn deposit in the zinc electrolyte increased with Mn^{2+} addition at the same potentials. The difference in current density became smaller with increasing negative potentials, due to

diffusion overpotential for the employed agitation rate, which was limiting the current density at high cathodic potentials in the presence of Mn^{2+} (limiting current plateau).

In addition, the addition of Pb^{2+} ions to the zinc electrolyte is found to increase the Tafel slope value from 110 mV/decade to 122 mV/decade by increasing the concentration from 0 to 0.1 mg/L Pb^{2+}, respectively. Then this value is increased up to 128 mV/decade at high concentration of 2.5 mg/L Pb^{2+}. Overpotential values confirm that, small traces of Pb^{2+} ions are shifting the cathodic polarization to more negative values. Moreover, the current for the Zn deposit in zinc electrolyte decreased with Pb^{2+} addition at the same potentials.

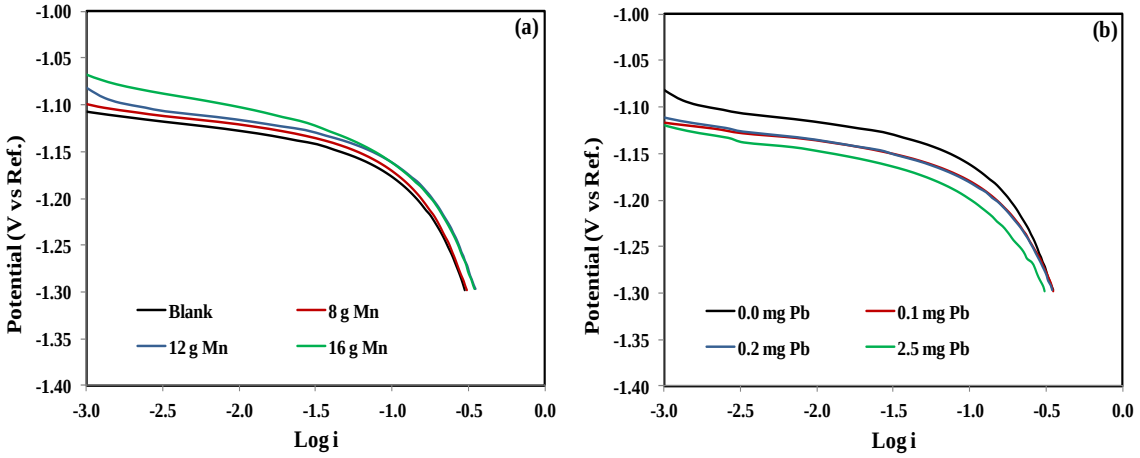

Fig. 5.4 Cathodic polarization during zinc electrodeposition on aluminum cathode with different concentrations of (a) Mn^{2+} ions, and (b) Pb^{2+} ions with 12 g/L Mn^{2+}, in the standard zinc electrolyte under atmospheric conditions

5.3.4 Voltammetric Characteristics of the Zinc Electrodeposition on Aluminum Cathode

Cyclic voltammetry can be considered to be an ideal “in situ” measuring technique, since it can allow investigating the cathodic deposit sensitively in non-agitated solutions. Cyclic voltammetry studies of the zinc electrodeposition on aluminum cathode were carried out from an initial potential of -1.3 V to final potential of -0.7 V at a scanning rate of 10 mV/s and 40°C. The typical CV curves for the zinc deposit on cathode in the standard zinc electrolyte of 170 g/L H_2SO_4, 60 g/L Zn^{2+}, and 12 g/L Mn^{2+} with and without Pb^{2+} impurity are shown in Fig. 5.5.

The voltammogram was initiated at point (A) at a potential of -1.30 V, scanned in the positive direction, and then reversed at -0.70 V in the negative direction, cross-over at point (B), the start of the dissolution and the point at which the Zn begins to deposit (D). It was found that Mn^{2+} ion additions into the zinc electrolyte shifted the cathodic curves to more positive values leading to a decrease in NOP values. NOP obtained from blank electrolyte was 73 mV which gradually decreased to 63-67 mV by adding 8-16 g/L Mn^{2+}. Low NOP could indicate weak polarization, which is possibly due to the depolarization effect of MnO_4^- ions on the reduction rate of H^+ ions and consequently coarse-grain zinc deposit was obtained. Also, it was observed that adding Mn^{2+} into the zinc electrolyte leads to an increase in anodic current from 0.17 to 0.23 A/cm^2.

Actually, it was observed that addition of Pb^{2+} ions into the zinc electrolyte shifted the cathodic curves to more negative values leading to an increase in NOP values. NOP obtained from blank electrolyte was 73 mV which gradually increased to 79-83 mV by adding 0.1-2.5 g/L Pb^{2+}. However, addition of Pb^{2+} into the zinc electrolyte leads to decrease in anodic current from 0.24 to 0.18 A/cm^2. The cathodic overpotential is also found to increase by increasing the Pb^{2+} concentration. The cathodic overpotential reaching 375 mV, could be the result of Pb^{2+} ions effect on decreasing the hydrogen evolution rate.

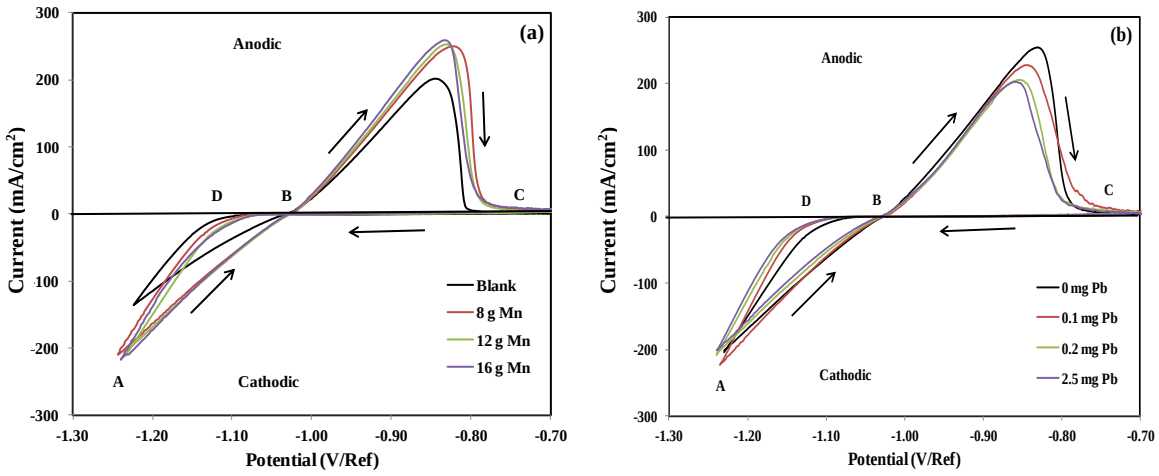

Fig. 5.5 Cyclic voltammograms during zinc electrodeposition on aluminum cathode with different concentrations of (a) Mn^{2+} ions, and (b) Pb^{2+} ions with 12 g/L Mn^{2+} in the standard zinc electrolyte under atmospheric conditions

Table 5.3 Effect of different concentrations of Mn^{2+} and Pb^{2+} ions on Tafel slopes, cathodic overpotential at 52.5 mA/cm^2 and NOP at 40°C under atmospheric conditions

Parameter	Concentration	*Tafel Slope ($-b_c$)* (mV/decade)	$-\eta_{(52.5)}$ (mV)	*NOP* (mV)
Blank	0	118	354	78
Mn^{2+} (g/L)	8	114	345	54
	12	110	341	49
	16	108	336	47
Pb^{2+}(g/L) (12 g/L Mn^{2+})	0	110	341	49
	0.1	122	362	60
	0.2	122	364	62
	2.5	128	375	65

5.4 Conclusions

Effect of various concentrations of lead and manganese ions added to the zinc electrolyte containing 170 g/L H_2SO_4 and 60 g/L Zn^{2+} during zinc electrowinning has been studied by electrochemical measurements. Certain conclusions can be summarized as follows:

I. From galvanostatic polarization at 52.5 mA/cm^2 and 40°C:

1. Lead ions added to the zinc electrolyte containing 12 g/L Mn^{+2} ions led to the increase of cathodic potential and current efficiencies of zinc deposit;
2. Addition of Mn^{2+} without Pb^{2+} ions into the zinc electrolyte resulted in the decrease of cathodic potential and current efficiency of zinc deposit;
3. Addition of Pb^{2+} up to 2.5 mg/L into the zinc electrolyte containing 12 g/L Mn^{2+} ions has negative effect on the surface morphology and crystallographic orientation; while increasing the concentrations of Mn^{2+} ions to 12 or 16 g/L, the zinc deposit restored the standard orientation with compact grain-sized deposit;

II. From potentiodynamic:

4. Addition of Pb^{2+} from 0 to 2.5 mg/L into the zinc electrolyte containing 12 g/L Mn^{2+} increased the overpotential by 34 mV, and Tafel slope by 18 mV/decade; while Mn^{2+} added from 0 to 16 g/L to the zinc electrolyte without Pb^{2+} decreased overpotential by 9 mV and Tafel slope by 10 mV/decade;

III. From cyclic voltammetry:

5. Addition of Pb^{2+} from 0 to 2.5 mg/L into the zinc electrolyte containing 12 g/L Mn^{2+} ions increased the nucleation overpotential by 16 mV, and decreased anodic peak current density by 62 mA/cm^2, while Mn^{2+} added to the zinc electrolyte without Pb^{2+} from 8 to 16 g/L decreased nucleation overpotential by 31 mV and increased anodic peak current density by 75 mA/cm^2.

Acknowledgments

Zinc Électrolytique du Canada (CEZinc), Hydro-Québec and Natural Sciences and Engineering Research Council of Canada (NSERC) are gratefully acknowledged for their financial support. The authors would like to express their sincere thanks and appreciation to Mr. André Ferland for SEM analysis, Mr. Jean Frenette for XRD analysis and Mrs. Vicky Dodier for Microwave plasma analysis.

CHAPTER 6

INVESTIGATION OF THE ZINC DEPOSIT CONTAMINATION BY LEAD DURING ELECTROWINNING EMPLOYING ELECTROCHEMICAAL NOISE MEASUREMENTS

Investigation of the Zinc Deposit Contamination by Lead during Electrowinning Employing Electrochemical Noise Measurements

*F. Safizadeh[1], C. Su[1], E. Ghali[1], and G. Houlachi[2]

[1]*Department of Mining, Metallurgical and Materials Engineering, Laval University, Québec, Canada, G1V 0A6*

[2]*Hydro-Québec research centre (LTE), Shawinigan, QC, Canada, G9N 7N5*

This paper was presented in the XXVIII International Mineral Processing Congress (IMPC 2016), Québec city, Canada (September 11-15) and published in the proceedings, paper #953, ISBN: 978-1-926872-29-2.

Résumé

L'influence des ions plomb sur le procédé d'extraction électrolytique de zinc a été étudiée au moyen de mesures du bruit électrochimique (ENM) et de voltammétrie cyclique en conjonction avec la microscopie électronique à balayage (MEB) et la diffraction des rayons-X (DRX). Toutes les expériences électrochimiques ont été effectuées dans un électrolyte d'acide sulfurique contenant différentes concentrations d'ions de plomb comme impuretés. Le plomb a été ajouté en six niveaux de traces entre 0,05 et 0,8 mg/L dans le bain. La teneur en plomb des dépôts de zinc dépendait des concentrations de plomb introduites dans la solution. La surtension associée à l'électrodéposition de zinc a décalé à des valeurs plus élevées avec l'augmentation de la concentration de plomb dans la solution. Une corrélation appropriée a été trouvée entre les différentes concentrations de plomb dans l'électrolyte et la morphologie du dépôt de zinc par ENM. Les résultats ont montré que l'augmentation des concentrations d'ions de plomb est généralement accompagnée de la diminution de l'inclinaison "Skew" et de l'augmentation des valeurs de Kurtosis qui pourraient être liées à la morphologie de dépôt de zinc. Effectivement, la morphologie passe de plaquettes hexagonales bien définies à de grandes plaquettes hexagonales en couches, et finalement à une structure cristalline raffinée non symétrique, respectivement.

Abstract

The influence of lead ions on zinc electrowinning process was investigated by means of electrochemical noise measurements (ENM) and cyclic voltammetry (CV) in conjunction with scanning electron microscopy (SEM) and X-ray diffraction (XRD). All electrochemical experiments were performed in sulfuric acid electrolyte containing different lead ion concentrations as impurity. Lead was added at six trace levels between 0.05-0.8 mg/L in the bath. The lead content of the zinc deposits was dependent on the introduced lead concentrations in the solution. The overpotential associated with zinc electrodeposition was shifted to higher values with the increase of lead concentration in the solution. An appropriate correlation was found between the different concentrations of lead in the electrolyte and the morphology of zinc deposit by ENM. The results showed that the increase of lead ion concentrations is generally accompanied with the decrease of skew and increase of kurtosis values that could be related to the morphology of zinc deposit. Effectively, the morphology changes from well-defined hexagonal platelets to large hexagonal and layered platelets, and finally to non-symmetric refined crystalline structure, respectively.

Keywords

Zinc electrowinning, Electrodeposition, Electrochemical noise measurements, Morphology, Lead impurity, Cyclic voltammetry

6.1 Introduction

In commercial zinc electrowining, zinc oxide is leached from the roasted calcine with an aqueous acid sulfate electrolyte. Then the zinc-rich solution is purified and transferred into an electrolytic cell. During electrolysis, zinc is deposited on an aluminum cathode where lead-silver or pure lead is served as anode. Electrodeposition of zinc could be influenced by several parameters such as bath acidity, temperature, current density, the nature and concentration of impurities as well as additives in the electrolyte.

Metallic impurities play a complex role during zinc electrowining and they can adversely influence the cathodic current efficiency (CE), energy consumption, deposit quality and the cathodic polarization behavior (Sarangi et al. 2009). Some impurities such as Ge, Sb and Ni were already known for their deleterious effect on current efficiency during zinc electrowining (Ivanov 2004; Ault and Frazer 1988; Maja and Spinelli 1971). Maja and Spinelli (1971) presented the decreasing effect of impurities on CE in the following order: Ge>Sb>Ni>Co>Bi>Cu>As>Sn. The presence of trace lead impurity in tankhouse is inevitable since zinc ores and anodes contain lead. Lead has been reported as an impurity that can show small positive (Ault and Frazer 1988; Frazer 1988; Ivanov 2004) or negative (MacKinnon et al. 1979) effect on current efficiency during zinc electrowining depending on the electrolysis conditions, solution purity of added lead and method of the CE measurements (Frazer 1988). The beneficial effect of lead on CE, *i.e.* the increase in current efficiency of zinc deposition could be attributed to the fact that the overpotential of the hydrogen evolution on lead is higher than that of zinc (Kuhn et al. 1972). In fact, when Pb is adsorbed on zinc, it generates lessened activation of hydrogen evolution with increasing cathodic polarization and enhances the formation of H_{ad} on the zinc deposit (Ichino et al. 1995). Frazer (1988) mentioned that the most of lead's beneficial effects must occur at ≤2 mg/L Pb. He indicated also that the level of lead [$PbCl_2$ solution] ≤5 mg/L shows only a small (≤1%) beneficial effect on CE.

Several studies on zinc electrolysis have shown a definite correlation between morphology with type and concentrations of impurities (Mackinnon et al. 1979; Mackinnon and Brannen 1977; Lamping and O'Keefe 1976). Mackinnon and Brannen (1977) showed that the zinc morphology and crystalline orientation are extremely sensitive to lead

concentrations as low as 1 mg/L. Mackinnon et al. (1979) examined the effect of Pb contamination under chemical form of lead acetate (0, 1, 3 and 9 mg/L), lead sulfate (3 and 9 mg/L) and lead oxide (3 and 9 mg/L) on the morphology and orientation of zinc deposits obtained from acid sulfate electrolytes. They reported that the morphology and orientations on zinc deposits are dependent on the lead content present on deposit. Furthermore, they found that the lead amount present in the zinc deposits was affected by the chemical form of the lead existing in the electrolyte, electrolysis temperature and current density.

Our previous works showed that the electrochemical noise measurements (ENM) could provide important information about morphology of the copper and zinc deposits (Safizadeh et al. 2010a, 2010b, 2012; Lafront et al. 2009). The term "electrochemical noise" refers to the spontaneous fluctuations of potential and current as a function of time. ENM technique was shown as a sensitive tool to monitor the evolution of the deposition process during electrodeposition.

The object of the present work was the investigation of the contamination effect of lead on zinc deposits during electrolysis. Furthermore, the utility of the electrochemical noise (EN) technique for monitoring the zinc deposit morphology during electrodeposition process was also examined. In this study, the EN technique was employed in the presence of trace concentrations of Pb (0.05-0.8 mg/L), in acidic sulfate electrolytes. The cyclic voltammetry was used to obtain more complementary information about the influence of cathodic activation overpotential on morphology of the zinc deposits.

6.2 Experimental Conditions

The standard electrolyte (STD) contained 170 g/L H_2SO_4 and 60 g/L Zn^{2+}. Lead was added to the electrolyte in several concentrations (0.05, 0.1, 0.15, 0.2, 0.4, 0.8 mg/L) as requested by CEZinc Company, in chemical form of lead acetate ($Pb(CH_3COO)_2$). The electrolyte was heated and maintained at 40 ºC using flowing thermostated water in a double-wall cell. Three electrodes including Pt as auxiliary, Al as working and silver chloride (Ag, $AgCl/KCl_{sat}$) as reference electrodes were mounted in a set-up using a Teflon holder to perform electrochemical tests. Both cathode and anode had a square surface of 1 cm^2.

Before each electrochemical experiment, the surface of the working electrode mounted in resin was manually polished with 240 and 600 SiC papers. The electrode was then rinsed successively with distilled water and ethanol, and dried.

Galvanostatic tests were conducted at least three times applying the current density 525 A/m^2 during 2 h. The stirring rate was fixed at 60 rpm.

The current efficiency was calculated according to the following equation:

$$CE(\%) = \frac{WFn}{ItM} \times 100\% \tag{6.1}$$

where W presents deposit weight (g), F the Faraday number, n the electron number, M the molecular weight, I the total cell current (A), and t the deposition time (s).

A GAMRY® PC4 750/ESA400 software and analyzer v. 2.35 was employed to conduct EN experiments and data treatment. ENM records containing 1024 data points were collected at a scan rate of f_s =10 Hz. EN data were analyzed in time domain using the two statistical parameters of skewness (S) and kurtosis (K). Skew and kurtosis are dimensionless measurements indicating the shape and symmetry of the data distribution around the mean value of the data, respectively (Cottis and Turgoose 1999). A positive value of skewness indicates a distribution tail in the positive direction and vice versa. A positive kurtosis implies a more spiky distribution while negative kurtosis implies a flatter distribution. When the distribution of the data is symmetric around the mean, skewness and kurtosis are equal to zero (Cottis 2001). These parameters could be calculated as follows:

$$S = \frac{1}{n-1}\sum_{i=1}^{n}\left(\frac{x_i - \bar{x}}{\sqrt{x_i^2}}\right)^3 \tag{6.2}$$

$$K = \frac{1}{n-1}\sum_{i=1}^{n}\left(\frac{x_i - \bar{x}}{\sqrt{x_i^2}}\right)^4 - 3 \quad , \tag{6.3}$$

Where x_i is the value of i^{th} data, $\bar{x}$ the sample mean of data and n the number of data points in the block. The average of skewness and kurtosis were calculated over each bracket of 1000 s of zinc deposition over a total of 7200 seconds.

Data from at least two sets of cyclic voltammetry (CV) experiments were collected in the presence of different concentration of lead in the electrolyte. The electrodes Pt and Al played the role of auxiliary and working electrode during CV tests. Silver chloride (Ag, AgCl/sat) was used as reference electrode. All cyclic voltammograms were carried out over a wide range of potential (-1.3 to -0.7 V) at 40°C in atmospheric conditions without agitation using a potential sweep rate 10 mV/s. The voltammograms were initiated at a potential of -1.30 V, scanned in the positive direction, and then reversed at -0.70 V in the negative direction. These measurements were conducted using a potentiostat (Gamry Reference 3000-GAMRY USA).

The surface characterization was performed using scanning electron microscopy (SEM) using JEOL JSM-840a. A Siemens D5000 diffractometer using monochrome CuK_{α} radiation at 40 kV and 30 mA was used for X-ray diffraction characterization with different angles varied up to 80º at 0.02º per 1.2 s. Deposited lead content during zinc electrowining was determined using an Optima 8300 ICP-OES spectrometer.

6.3 Results and Discussion

6.3.1 Characterization of the Lead Effect on Zinc Deposits

Electrowining tests were carried out for standard electrolyte (STD) and the solutions containing different lead concentrations over 2 h. The results of the current efficiency calculations and the lead content in zinc deposits can be found in Table 6.1. The current efficiency was calculated for different experimental conditions according to Equation 6.1. The results are also illustrated graphically in Fig. 6.1.

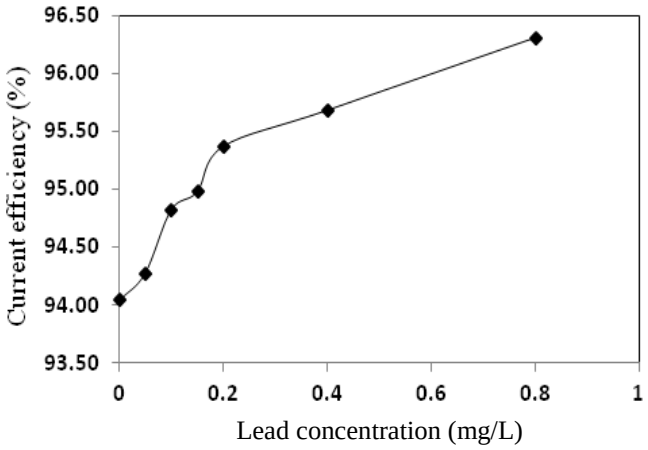

Fig. 6.1 Current efficiency curves for a 2 h of zinc electrodeposition on Zn cathodes as a function of initial concentration of lead in electrolyte containing 170 g/L H_2SO_4 and 60 g/L Zn^{2+}, at 52.5 mA/cm^2, 40°C, and stirring rate of 60 rpm

Fig. 6.1 showed a general increase of the current efficiency with addition of lead concentration. The improvement of the CE in the presence of lead in the electrolyte was already reported by many researchers (Ault and Frazer 1988; Frazer 1988; Mackinnon et al. 1979). The increase of the current efficiency alongside the increase of lead amount in the electrolytic bath could be explained as follows (Ault & Frazer 1988; Frazer 1988; Mackinnon et al. 1979; Ichino et al. 1995): the Pb ions could be easily adsorbed on the cathode and thereby strongly inhibit all the reactions taking place on these sites on the electrode surface. In fact, the adsorbed lead on the zinc electrode generates lessened activation for hydrogen evolution reaction (HER) and zinc deposition with increasing cathodic polarization. Accordingly, deposition of Pb leads to a decrease of the accessible sites for HER on the electrode surface. Therefore, the current density consumed by HER is decreased leading to an increase in CE for zinc deposition. According to the results presented in Table 6.1, the current efficiency value of 94.04% was obtained for the electrolyte without lead (STD). By adding of 0.2 mg/L Pb^{2+} in the bath, the current efficiency was increased sharply by 1.33%. Then, the CE was found to increase gradually from 95.37 to 96.31% for the lead ion concentrations from 0.2 to 0.8 mg/L, respectively. Thus, it seems that the presence of very low concentrations of lead impurity (0.05-0.2 mg/L) in the electrolyte affects strongly the current efficiency than higher concentrations (0.2-0.8

mg/L). Since lead could inhibit also the zinc deposition reaction, a slower increase of current efficiency in the presence of higher concentrations of lead can be considered reasonable.

The lead contents in zinc deposits are also shown in Table 6.1. It is be observed that with an increase in lead concentration in the electrolyte, the lead content of deposited or adsorbed lead also increases. These results confirmed that the lead content of the zinc deposits is dependent on lead concentration added to the electrolyte (Mackinnon et al. 1979). This can be explained better with the results of CE where higher concentrations of introduced lead in the electrolyte lead to more deposited lead on zinc and consequently the CE% is significantly promoted.

The SEM micrographs of STD and the deposits containing different lead contents are shown in Fig. 6.2. These deposits were also examined by XRD to determine crystallographic orientations of zinc. The results of morphology as well as preferred orientations are summarized in Table 6.1.

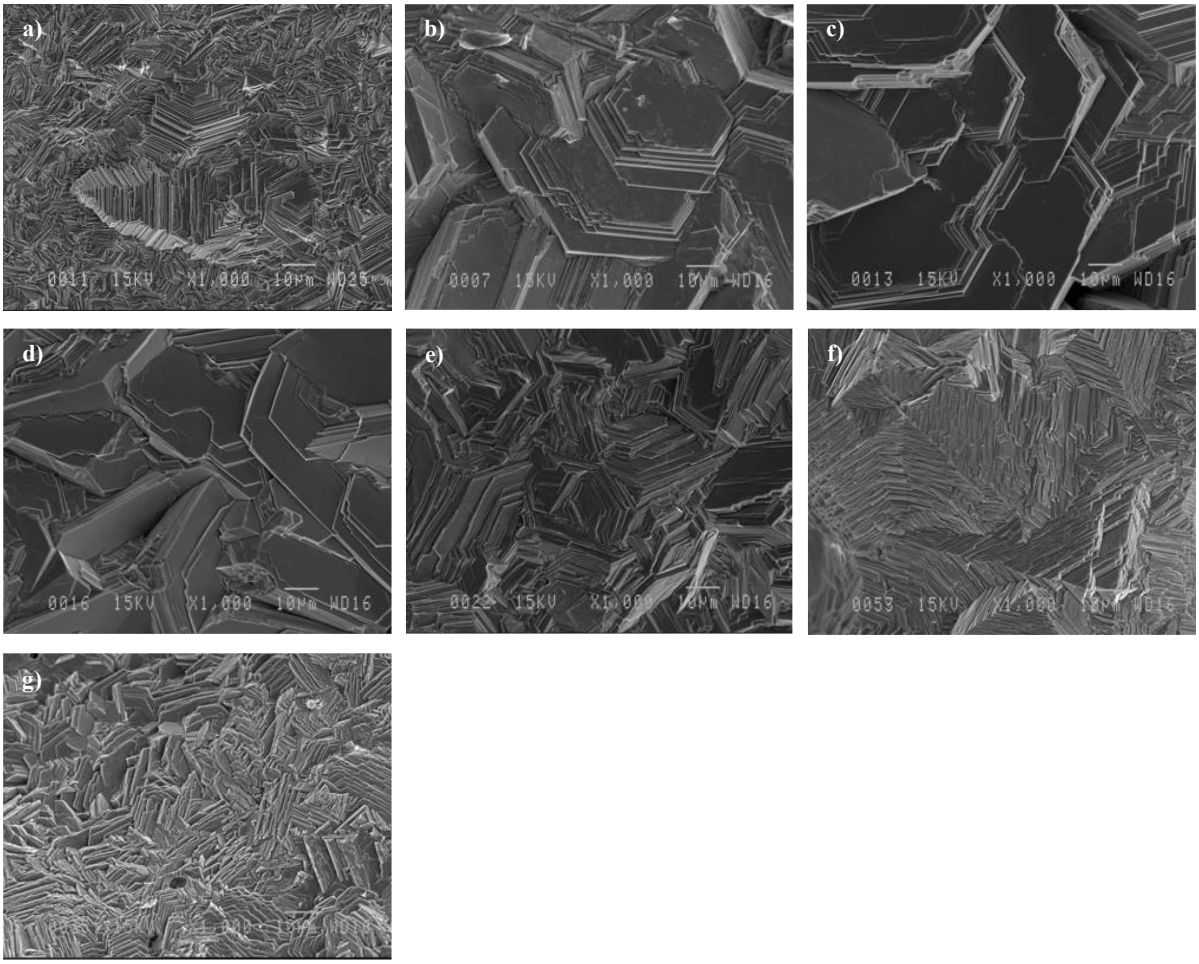

Fig. 6.2 SEM images of different zinc cathodes electrowon at 52.5 mA/cm^2 and 40°C after 2 h in electrolyte containing 170 g/L H_2SO_4 and 60 g/L Zn^{2+} and (a) 0, (b) 0.05, (c) 0.1, (d) 0.15, (e) 0.2, (f) 0.4 and (g) 0.8 mg/L Pb, under 60 rpm agitation

According to SEM micrographs, the standard electrolyte resulted in a zinc deposit consisting of well-defined hexagonal platelets aligned at low angles to the Al cathode and oriented randomly with varying size as reported by (Mackinnon et al. 1987). The preferred orientation for STD was predominately (101) (102) (103). The addition of 0.05, 0.1 and 0.15 mg/L of lead in the electrolyte conducted to increase the size of medium individual zinc platelets giving an orientation of (103) (102) (101). With increasing the lead content in the bath to more than 0.2 to 0.8 mg/L, large grains appeared more layered and they have tendency to form more refined grains with preferred orientation (002) (101) (103). In the

presence of 0.8 mg/L lead in the electrolyte, the grains started to lose the symmetrical structure and became more refined giving rise to a more compact deposit. In summary, with addition and increase of lead ions concentrations in the electrolyte, the morphology changes from well-defined hexagonal platelets to large hexagonal, layered platelets and finally non-symmetric refined crystalline structure, respectively. Porosities (depression or pits) were observed on the zinc electrodeposits due to adherent hydrogen bubbles (25X, not shown).

Table 6.1 The current efficiency, morphology, crystallography and lead content measured in zinc cathodes as a function of lead concentration in the electrolyte 170 g/L H_2SO_4 and 60 g/L Zn^{2+} at 52.5 mA/cm^2, 40°C and 60 rpm agitation

Lead added to electrolyte (mg/L)	CE (%)	Morphology	Crystallographic orientation	Cathode lead (ppm)
0	94.04	Well-defined hexagonal platelets	(101)(102)(103)	-
0.05	94.27	Large hexagonal platelets	(103)(102)(101)	0.5
0.1	94.82	Large hexagonal platelets	(103)(102)(101)	0.9
0.15	94.98	Large hexagonal platelets	(103)(102)(101)	1.3
0.2	95.37	Layered platelets	(002)(101)(103)	2.4
0.4	95.68	Layered platelets	(002)(101)(103)	5
0.8	96.31	Non-symmetric refined	(002)(101)(103)	16

6.3.2 Cyclic Voltammetry

Cyclic voltammetry is a popular technique used during the evaluation of zinc electrodeposition process in the presence of metallic impurities in the electrolyte. This technique involves measuring the relative increases or decreases in nucleation overpotential (NOP) for zinc deposition on aluminum cathodes as caused by specified addition of certain metallic impurities or additives to similar zinc electrolytes (Kerby et al. 1977).

All voltammograms in the presence of different experimented concentrations of lead in the electrolytes are presented in Fig. 6.3, and nucleation overpotential (NOP) values are listed in Table 6.2. The voltammograms were initiated at point (A) and scanned in the positive direction, and then reversed at the point (C) in the negative direction. At point (C), the current becomes anodic corresponding to the dissolution of the deposited zinc previously formed, then followed by a current loop as the direction of sweeping is reversed. This

reversed scanning results in a decrease in current that subsequently reaches zero at the crossover potential at point (B), the cathodic current increases sharply once zinc electro-reduction begins at point (D). NOP is the difference between the crossover potential (B) and the point at which the Zn^{2+} ions begin to be reduced and deposited on the cathode (D) (Mackinnon et al. 1990a, 1990b).

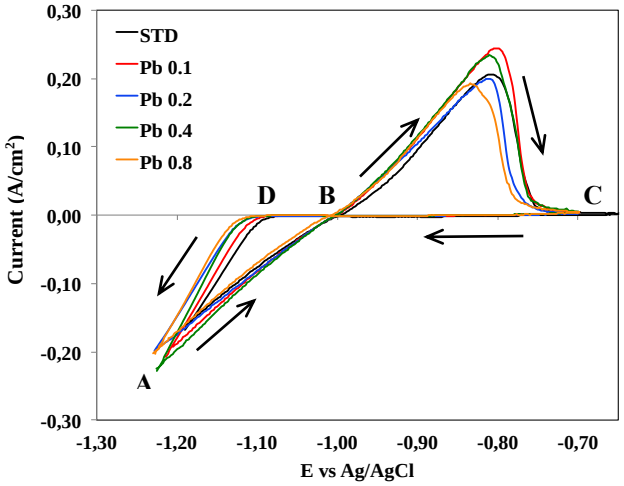

Fig. 6.3 Voltammograms for acidic sulfate electrolytes containing different values of lead during zinc electrodeposition on aluminum substrate at 40°C in electrolyte containing 170 g/L H_2SO_4 and 60 g/L Zn^{2+} and 0, 0.05, 0.1, 0.15, 0.2, 0.4 and 0.8 mg/L Pb, without agitation

Table 6.2 Overpotential (NOP) values determined from the voltammograms, obtained in acidic sulfate electrolytes containing different values of lead during zinc electrodeposition on aluminum substrate

Lead concentration in the electrolyte (mg/L)	Nucleation overpotenial (NOP) (mV)
0	89
0.1	95
0.2	98
0.4	109
0.8	114

According to the CV results, NOP value for STD electrolyte was equal to 89 mV. It was found that, by increasing the concentration of Pb^{2+} ions in the solution up to 0.8 mg/L, the

NOP value increases up to 114 mV (*i.e.* an increase of 25 mV as compared to STD). It could be seen that with increase of lead concentrations in solution, the NOP variations become more important at higher concentrations. This could be the reason of grain refinement of the zinc deposits (Table 6.1). The grain-refining effect of lead was already reported by Ault and Frazer (1988). As it was mentioned by Mackinnon and co-workers, the higher cathodic overpotential could be the origin of current efficiency increase and the change of the deposit orientation (MacKinnon et al. 1983).

6.3.3 Electrochemical Noise Measurements and Morphology

The results of electrochemical noise analyses are illustrated in Figs 6.4 and 6.5. For the standard electrolyte, the average of potential skewness increased gradually with the time of electrodeposition in the positive direction (a tail in the positive direction). In the same way, the kurtosis values for STD were changed quasi-linearly in the positive direction during the time evolution. This form of skew and kurtosis evolution has been already correlated with the typical morphology of the zinc deposit for the standard electrolyte (Lafront et al. 2009). Disregarding some non-linear variations appearing during the first 3000 s for some of the electrolytes, an appropriate trend for skew and kurtosis values could be observed in the presence of various lead concentrations. Fig. 6.4 shows that the addition of lead in electrolyte shifted the values of potential skew from positive to negative. Moreover, the increase of lead amount resulted in a gradual decrease in potential skew values with the evolution of time. In the case of kurtosis, the positive values were increased progressively with the increase of lead quantity in the bath. Negative values of skew evolution are indicating that the symmetry was skewed left or the potential domain fluctuation had a tendency to deviate left from the mean oscillations (Safizadeh et al. 2010a). The average of kurtosis potential showed a tendency to take away far from the normal distribution of data ($K \rightarrow 0$) at increasing lead concentration in the electrolyte. In fact, the distribution of the data became less symmetric and more peaked with the increase of Pb^{2+} ions concentrations in the bath. Regarding morphology results by SEM, it could be seen that the increase of lead ions concentrations from 0.05 to 0.8 mg/L accompanied with the gradual decrease of skew and increase of kurtosis values, morphology of zinc deposits changed from well-defined hexagonal platelets to large hexagonal, pyramidal layered and finally non-symmetric refined crystalline structure, respectively.

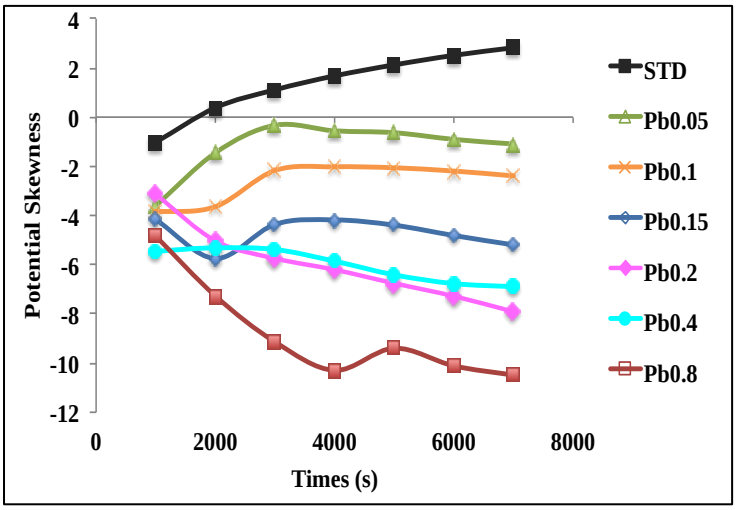

Fig. 6.4 Average of skewness of potential during zinc deposition in the presence of lead as impurity at 52.5 mA/cm^2 and 40°C after 2 h in electrolyte containing 170 g/L H_2SO_4 and 60 g/L Zn^{2+} and 0, 0.05, 0.1, 0.15, 0.2, 0.4 and 0.8 mg/L Pb, under 60 rpm agitation

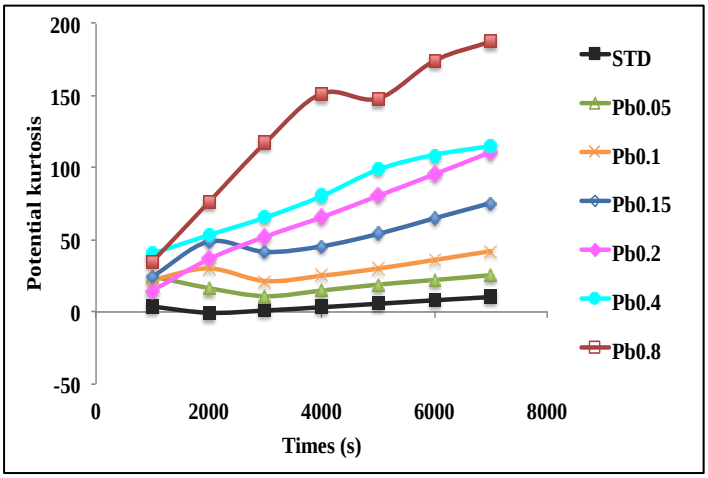

Fig. 6.5 Average of kurtosis of potential during zinc deposition in the presence of lead as impurity at 52.5 mA/cm^2 and 40°C after 2 h in electrolyte containing 170 g/L H_2SO_4 and 60 g/L Zn^{2+} and 0, 0.05, 0.1, 0.15, 0.2, 0.4 and 0.8 mg/L Pb, under 60 rpm agitation

6.4 Conclusions

The influence of several lead concentrations (0.05-0.8 mg/L) on zinc electrowining was investigated by electrochemical techniques such as electrochemical noise measurements (ENM) and cyclic voltammetry (CV) in conjunction with different characterization techniques. The ENM presented complementary information to CV technique. The following conclusions could be drawn from this study:

1. By addition of lead in the electrolytic bath up to 0.2 mg/L Pb^{2+}, the current efficiency was increased sharply by 1.33%. Afterwards, the current efficiency was increased gradually from 95.37 to 96.31% for the lead ion concentrations increasing from 0.2 to 0.8 mg/L, respectively.

2. The content of deposited lead on zinc cathode was increased from 0.5 to 16 ppm with the increase of lead ion concentration from 0.05 up to 0.8 mg/L in the solution.

3. The crystallographic orientation results showed a change of crystalline orientation in the presence of the different lead concentrations in the following order: (101) (102) (103) for STD (without lead) $\rightarrow$ (103) (102) (101) for 0.05, 0.1 and 0.15 mg/L $\rightarrow$ (002) (101) (103) for 0.2 to 0.8 mg/L.

4. By increasing the concentration of Pb^{2+} ions in the solution up to 0.8 mg/L, the nucleation overpotential (NOP) values after CV studies gradually increased up to 25 mV as compared to STD. The increase in cathodic overpotential could be the reason of grain refinement observed by morphology studies.

5. According to ENM results, the addition of lead in the electrolyte shifted the values of potential skew from positive to negative while in the case of kurtosis, the values stayed positive and was increased progressively with the increase of lead concentrations in bath.

The correlation between the results of ENM and morphology revealed that with an increase in lead ion concentrations (0.05-0.8 mg/L) in the electrolyte conducting to the decrease of skew and increase of kurtosis values, morphology of zinc deposits changes from well-

defined hexagonal platelets to large hexagonal, layered platelets and finally non-symmetric refined crystalline structure, respectively.

Acknowledgments

Zinc Électrolytique du Canada (CEZinc), Hydro-Québec and Natural Sciences and Engineering Research Council of Canada (NSERC) are gratefully acknowledged for their financial support.

CHAPTER 7

CONCLUSIONS AND OUTLOOK

7.1 General Conclusions

The effect of different concentrations of Mn^{2+} and Pb^{2+} added to the acidic zinc sulfate electrolyte during zinc electrowinning process has been studied. Working parameters such as zinc ions concentration, sulfuric acid concentration, current density, magnetic agitation and temperature were investigated in presence of Mn^{2+} and Pb^{2+}. Traditional electrochemical measurements and recent electrochemical test methods such as electrochemical noise measurements and electrochemical impedance spectroscopy have been considered to examine the cathodic behavior of zinc deposit in the zinc electrolyte with Pt and Pb-0.7wt.%Ag anode, respectively. Scanning electron microscopy (SEM) and X-ray diffraction (XRD) have been employed to characterize the deposit surfaces in order to provide useful and complementary data and explanations. According to the research work during this project, the following conclusions can be drawn:

I. Pb^{2+} and Mn^{2+} Effect

1. a) Electrochemical polarization studies revealed that after 2 h of galvanostatic polarization with 12 g/L Mn^{2+} using Pt anodes, adding Pb^{2+} from 0.1 up to 2.5 mg/L to the zinc electrolyte, led to an increase of the cathodic potential by 55 mV and current efficiency by 1.2%. It was proved that lead contamination from the Pb-0.7%Ag anode is very close to 0.15-0.20 mg/L.

   b) The cathodic potential was decreased by ~45 mV (less negative) for the longest period of electrolysis (72 h) for the two anodes (Pt and Pb-0.7%Ag) with added 12 g/L Mn^{2+} and 0.15-0.20 mg/L Pb^{2+}, while the CE was also decreased after 72 h by an average of ~6.6% as compared to that of 2 h. These two observations could be due to lower Pb^{2+}.

   c) According to ENM results, the addition of lead in the electrolyte in absence of manganese shifted the values of skew potential from positive to negative while in the case of kurtosis, the values stayed positive and was increased progressively with the increase of lead concentrations in the bath. Also, an increase in lead ion concentration (0.05-0.8 mg/L) in the electrolyte with Pt anode conducted to a decrease in skew and

increase in kurtosis values. A correlation between skew/kurtosis values and morphology of zinc deposit has been established.

d) According to the results of electrochemical impedance spectroscopy, the addition of Pb^{2+} ions to the zinc electrolyte increased the charge transfer resistance (R_{ct}) and decreased the double capacitance (C_{dl}) which proves that zinc reduction requires high potential in presence of lead ions.

2. Employing Pb-0.7%Ag anode after 2 h of galvanostatic polarization, with addition of Mn^{2+} in different quantities to the electrolyte between 4 and 16 g/L: decreased the CE by almost 0.7-2%, shifted the cathodic potential to less negative potentials by 10 to 56 mV, and decreased the lead content in the deposit by 2.3 to 3.8 ppm. 12 g/L Mn^{2+} in the electrolyte could be considered as an optimum concentration since it gives 95.3% CE, 45 mV shift and decreased lead by 3.8 ppm.

3. Potentiodynamic polarization studies showed that addition of Pb^{2+} from 0 to 2.5 mg/L into zinc electrolyte containing 12 g/L manganese ions increased the overpotential by 34 mV, and Tafel slope by 18 mV/decade; while 0 to 16 g/L Mn^{2+} added to the lead free zinc electrolyte decreased overpotential by 9 mV and Tafel slope by 10 mV/decade.

4. a) Increasing the concentration of Pb^{2+} ions in the solution up to 0.8 mg/L, the nucleation overpotential (NOP) values after cyclic voltammetric studies gradually increased up to 25 mV as compared to the standard electrolyte.

   b) Cyclic voltammetry studies showed that addition of Pb^{2+} from 0 to 2.5 mg/L into the zinc electrolyte containing 12 g/L manganese ion increased the nucleation overpotential by 16 mV, and decreased anodic peak current density by 62 mA/cm^2; while Mn^{2+} added from 8 to 16 g/L to the zinc electrolyte without lead decreased nucleation overpotential by 31 mV and increased anodic peak current density by 75 mA/cm^2. This decrease in NOP values indicates that surface morphology is affected by high manganese addition.

5. The zinc deposit examined by SEM and XRD showed that the addition of low concentrations (0.1-0.2 mg/L) of Pb^{2+} ions resulted in a similar orientation of the deposit as that of the standard orientation. Increasing the lead concentration up to 2

mg/L, the deposit was neither compact nor smooth and orientation was completely changed as the predominate one, morphology of zinc deposits changes from well-defined hexagonal platelets to large hexagonal, layered platelets and finally non-symmetric refined crystalline structure, respectively.

6. The results of SEM and XRD showed that crystallographic orientation obtained from free-addition standard electrolyte was (101) (102) (103), and the predominate orientation (101) was not affected by the addition of Mn^{2+} ions employing Pb-0.7%Ag anode.

II. Other Parameters

7. Increasing Zn^{2+} concentration (by 16%) in the electrolyte increased the CE by ~0.85 %. The cathodic overpotential was decreased by 13 mV for Pt and 18 mV for Pb-0.7%Ag. The increase of zinc ions in the electrolyte has no effect on both morphology and crystallographic orientation but it reduces the contamination of the deposit, as lead content decreased from 1.67 to 1.17 ppm by addition of 65 g/L Zn^{2+}, employing Pb-0.7%Ag anode.

8. The increase of acid content (H^+) by 7% had a negative effect on the CE due to a lower reduction rate of Zn (0.4% only with Pb-Ag anode because of significant lead dissolution instead of 1.1% with Pt). The cathodic overpotential was decreased by ~12 mV for both anodes.

9. Increase of current density from 45 to 60 mA/cm^2 resulted in the increase of cathodic potential and the decrease of current efficiency. Agitation rate from 60 to 412 rpm showed in less efficiency and more negative overpotential. There is an optimum value of 100 rpm, above which cathodic potential was almost stable and current efficiency decreased by 0.4%.

10. Increase of temperature from 35 to 45°C decreased cathodic potential. The current efficiency was slightly increased from 35 to 40°C and increased sensibly (~0.8%) from 40 to 45°C. Electrochemical impedance spectroscopy showed that an increase in

concentration of sulfuric acid and temperature of zinc electrolyte decreased the charge transfer resistance which facilities the hydrogen evolution reaction.

11. Electrochemical impedance spectroscopy showed that the charge transfer resistance in case of Zn deposition on Zn was lower than that for Zn deposition on Al. Also, the double layer capacitance (C_{dl}) was increased from 94.1 (Zn on Zn) to 99.7 mF/cm^2 (Zn on Al).

7.2 Outlook

Based on the obtained results in this research study, the following perspectives and future work could be considered:

1. Electrochemical impedance spectroscopy (EIS) study for different parameters such as agitation, Zn^{2+} concentration, Pb^{2+} concentration with and without Mn^{2+} addition for Zn deposition on Zn and Zn deposition on Al.

2. Examine the effect of different sulfuric acid concentrations (<158 g/L) from manganese additions between 12-16 g/L Mn^{2+} such as: 155 g/L H_2SO_4 +13 g/L Mn^{2+}, 150 g/L H_2SO_4 +14 g/L Mn^{2+} and 145 g/L H_2SO_4 +15 g/L Mn^{2+}.

3. Study the effect of different electrolyte agitation rates between 60 to 100 rpm, since it showed a sharp decrease in cathodic overpotential. It is also recommended to consider lower agitation rates than 60 rpm for the laboratory scale.

Bibliography

Aballe, A., M. Bethencourt, F. J. Botana, and M. Marcos. "Using wavelets transform in the analysis of electrochemical noise data." *Electrochimica Acta* 44, no. 26 (1999): 4805-4816.

Aballe, A., and F. Huet. "Noise resistance applied to corrosion measurements: VI. partition of the current fluctuations between the electrodes." *Journal of the Electrochemical Society* 149, no. 3 (2002): 89-96.

Aballe, A., M. Bethencourt, F. J. Botana, M. Marcos, and R. M. Osuna. "Electrochemical noise applied to the study of the inhibition effect of $CeCl_3$ on the corrosion behaviour of Al-Mg alloy AA5083 in seawater." *Electrochimica Acta* 47, no. 9 (2002): 1415-1422.

Alfantazi, A. M., and D. B. Dreisinger. "The role of zinc and sulfuric acid concentrations on zinc electrowinning fromindustrial sulfate based electrolyte". *Journal of Applied Electrochemistry* 3, (2001): 641–646.

Ault, A. R., and E. J. Frazer. "Effects of certain impurities on zinc electrowinning in high-purity synthetic solutions." *Journal of Applied Electrochemistry* 18, no. 4 (1988): 583-589.

Baboian, R., and S. W. Dean. *Corrosion Testing and Evaluation*, ASTM, 1991. pp 268-275.

Bai, L., D. Y. Qu, B. E. Conway, Y. H. Zhou, G. Chowdhury, and W. A. Adams. "Rechargeability of a chemically modified MnO_2/Zn battery system at practically favorable power levels." *Journal of the Electrochemical Society* 140, no. 4 (1993): 884-889.

Bard, A. J., L. R. Faulkner, J. Leddy, and C. G. Zoski. *Electrochemical Methods: Fundamentals and Applications*. Vol. 2. New York: Wiley, 1980. pp 1-19.

Barsoukov, E., and J. R. Macdonald, eds. *Impedance Spectroscopy: Theory, Experiment, and Applications*. John Wiley & Sons, 2005. pp 1-6.

Barton, G. W., and A. C. Scott. "A validated mathematical model for a zinc electrowinning cell." *Journal of Applied Electrochemistry* 22, no. 2 (1992): 104-115.

Beavers, J., J. A. Beavers, N. G. Thompson, and D. C. Silverman. "Corrosion engineering applications of electrochemical techniques: Laboratory testing." *Paper* 348 (1993).

Bertocci, U., C. Gabrielli, F. Huet, and M. Keddam. "Noise resistance applied to corrosion measurements I. theoretical analysis." *Journal of the Electrochemical Society* 144, no. 1 (1997): 31-37.

Beshore, A. C., B. J. Flori, Go Schade, and T. J. O'Keefe. "Nucleation and growth of zinc electrodeposited from acidic zinc solutions." *Journal of applied electrochemistry* 17, no. 4 (1987): 765-772.

Bratt, G. C. "A view of zinc electrowinning theory." *Proceedings of the AusI.M.M. Conference, Tasmania. Australasian Institute of Mining and Metallurgy, Melbourne, Australia*, (1977): 277-290.

Bozhkov, C., I. Ivanov, and S. J. Rashkov. "The relationship between the growth rate of hydrogen bubbles and the duration of the 'induction period' in the electrowinning of zinc from sulphate electrolytes." *Journal of Applied Electrochemistry* 20, no. 3 (1990a): 447-453.

Bozhkov, C., M. Petrova and S. J. Rashkov. "The effect of nickel on the mechanism of the initial stages of zinc electrowinning from sulphate electrolytes. Part II. Investigations on aluminium cathodes alloyed with iron impurities." *Journal of applied electrochemistry* 20, no. 1 (1990b): 17-22.

Ciavatta, L., and M. Grimaldi. "The potential of the couple Mn (III)-Mn (II) in aqueous 3M $HClO_4$." *Journal of Inorganic and Nuclear Chemistry* 31, no. 10 (1969): 3071-3082.

Cole, E. R. *Electrode reactions in zinc electrolysis*. 1970. pp 1-19.

Compton, R.G., and C.E. Banks. *Understanding Voltammetry.* World Scientific, 2011. pp 73-94.

Corrosion Terms Tagged with 'Corrosion 101', Corrosion Pedia. https://www.corrosionpedia.com/dictionary/tags/corrosion-101, (accessed on 14-01-2017)

Cottis, R. A. "Interpretation of electrochemical noise data." *Corrosion* 57, no. 3 (2001): 265-285.

Cottis R., and S. Turgoose. *Electrochemical Impedance and Noise*, NACE International, 1440 South Creek Drive, Houston, 1999. TX 77084, US 611.

Dawson, J. L., K. Hladky, and D. Eden. "Electrochemical Noise--Some New Developments in Corrosion Monitoring." *UK Corrosion'83-Proceedings of the Conference*, (1983): 99-108.

Eden, D. A., M. Hoffman, and B. S. Skerry. "Application of electrochemical noise measurements to coated systems." *ACS Publications,* 1986. pp 36-47.

Fletcher, S. "Tafel slopes from first principles." *Journal of Solid State Electrochemistry* 13, no. 4 (2009): 537-549.

Fosnacht, D. R., and T. J. O'keefe. "Evaluation of zinc sulphate electrolytes containing certain impurities and additives by cyclic voltammetry." *Journal of Applied Electrochemistry* 10, no. 4 (1980): 495-504.

Frazer, E. J. "The Effect of Trace Lead on the Coulombic Efficiency of Zinc Electrowinning in High-Purity Synthetic Solutions." *Journal of the Electrochemical Society* 135, no. 10 (1988): 2465-2471.

Gouveia-Caridade, C., M. Isabel, S. Pereira, and C. M. Brett. "Electrochemical noise and impedance study of aluminium in weakly acid chloride solution." *Electrochimica Acta* 49, no. 5 (2004): 785-793.

Greene, N. D. "Predicting behavior of corrosion resistant alloys by potentiostatic polarization methods." *Corrosion* 18, no. 4 (1962): 136t-142t.

Greisiger, H., and T. Schauer. "On the interpretation of the electrochemical noise data for coatings." *Progress in organic Coatings* 39, no. 1 (2000): 31-36.

Han, J. S., and T. J. O'Keefe. "Electrochemical evaluation of the adherence of zinc to aluminum cathodes." *Surface and Coatings Technology* 53, no. 3 (1992): 231-238.

Heineman, W. R., and P. T. Kissinger. "Cyclic voltammetry." *Journal of Chemical Education* 60, no.9 (1983): 702-706.

Heinze, J. "Cyclic voltammetry-"electrochemical spectroscopy". New analytical methods (25)." *Angewandte Chemie International Edition in English* 23, no. 11 (1984): 831-847.

Hosny, A. Y., Thomas J. O'Keefe, James W. Johnson, and W. J. James. "Correlation between mass transfer and operating parameters in zinc electrowinning." *Journal of Applied Electrochemistry* 21, no. 9 (1991): 785-792.

Hosny, A. Y. "Electrowinning of zinc from electrolytes containing anti-acid mist surfactant." *Hydrometallurgy* 32, no. 2 (1993): 261-269.

Ichino, R., C. C., and R. Wiart. "Influence of Ge^{4+} and Pb^{2+} ions on the kinetics of zinc electrodeposition in acidic sulphate electrolyte." *Journal of Applied Electrochemistry* 25, no. 6 (1995): 556-564.

Isaac, J. W., and K. R. Hebert. "Electrochemical current noise on aluminum microelectrodes." *Journal of the Electrochemical Society* 146, no. 2 (1999): 502-509.

Ivanov, I., Y. Stefanov, Z. Noncheva, M. Petrova, Ts Dobrev, L. Mirkova, R. Vermeersch, and J-P. Demaerel. "Insoluble anodes used in hydrometallurgy: Part I. Corrosion resistance of lead and lead alloy anodes." *Hydrometallurgy* 57, no. 2 (2000): 109-124.

Ivanov, I., and Y. Stefanov. "Electroextraction of zinc from sulphate electrolytes containing antimony ions and hydroxyethylated-butyne-2-diol-1, 4: Part 3. The influence of manganese ions and a divided cell." *Hydrometallurgy* 64, no. 3 (2002): 181-186.

Ivanov, I. "Increased current efficiency of zinc electrowinning in the presence of metal impurities by addition of organic inhibitors." *Hydrometallurgy* 72, no. 1 (2004): 73-78.

Iverson, W. P. *Transient voltage changes produced in corroding metals and alloys.* Fort Detrick Frederick MD, 1968. pp115, 617.

Iverson, W. P., G. J. Olsen, and L. F. Heverly. *The Role of Phosphorus and Hydrogen Sulfide in the Anaerobic Corrosion of Iron and the Possible Detection of This Corrosion by an Electrochemical Noise Technique*. National Association of Corrosion Engineers, 1985. pp 154.

Jaimes, R., M. Miranda-Hernández, Luis Lartundo-Rojas, and I. González. "Characterization of anodic deposits formed on Pb-Ag electrodes during electrolysis in mimic zinc electrowinning solutions with different concentrations of Mn (II)." *Hydrometallurgy* 156 (2015): 53-62.

Jones, D. A. *Principles and Prevention of Corrosion, second ed*., Prentice-Hall, 1996. pp 119.

Kelly, R. G., J. R. Scully, D. Shoesmith, and R. G. Buchheit. *Electrochemical techniques in corrosion science and engineering*. CRC Press, New York 2002. pp 53.

Kerby, R. C., H. E. Jackson, T. J. O'keefe, and Y. Wang. "Evaluation of organic additives for use in zinc electrowinning." *Metallurgical Transactions B* 8, no. 3 (1977): 661-668.

Kiryakov, G. Z., F. K. Baynietova, and R. S. Vakhidov. "Role of manganese in the electrolytic deposition of zinc." *Tr. Inst. Khim. Akad. Nauk. S.S.R.* 3 (1958): 72-81

Kopistko, O. A., and S. E. Batyrbekova. "On the theory of the galvanostatic relaxation technique as applied to redox electrodes with two consecutive charge-transfer steps." *Journal of Electroanalytical Chemistry* 336, no. 1-2 (1992): 223-244.

Krauses, C. J., R. C. Kerby, R. D. H. Williams and D. Ybena. "Anodes for electrowinning proceeding processes." *Metall. Soc. AIME,* (1984): 37.

Kuhn, A. T., C. J. Mortimer, G. C. Bond, and J. Lindley. "A critical analysis of correlations between the rate of the electrochemical hydrogen evolution reaction and physical properties of the elements." *Journal of Electroanalytical Chemistry and Interfacial Electrochemistry* 34, no. 1 (1972): 1-14.

Lafront, A. M., W. Zhang, E. Ghali, and G. Houlachi. "Effect of gelatin and antimony on zinc electrowinning by electrochemical noise measurements." *Canadian Metallurgical Quarterly* 48, no. 4 (2009): 337-345.

Lamping, B. A., and T. J. O'Keefe. "Evaluation of zinc sulfate electrolytes by cyclic voltammetry and electron microscopy." *Metallurgical Transactions B* 7, no. 4 (1976): 551-558.

Lasia, A. "Electrochemical impedance spectroscopy and its applications." In *Modern aspects of electrochemistry*. Springer US, 2002. pp. 143-248.

Lee, M. G., and J. Jorné. "On the kinetic mechanism of zinc electrodeposition in the region of negative polarization resistance." *Journal of the Electrochemical Society* 139, no. 10 (1992): 2841-2844.

Lowe, A. M., H. Eren, and S. I. Bailey. "Electrochemical noise analysis: detection of electrode asymmetry." *Corrosion science* 45, no. 5 (2003): 941-955.

Lu, J., H. Guo, D. Dreisinger, and B. Downing. "Effects of Current Density and Nickel as an Impurity on Zinc Electrowinning." *Journal of Metallurgical Engineering* 2, no. 3 (2013): 79-87.

Macdonald, Digby, ed. *Transient techniques in electrochemistry*. Springer Science & Business Media, 2012. pp 2-24.

MacKinnon, D. J., and J. M. Brannen. "Zinc deposit structures obtained from high purity synthetic and industrial acid sulphate electrolytes with and without antimony and glue additions." *Journal of Applied Electrochemistry* 7, no. 5 (1977): 451-459.

Mackinnon, D. J., J. M. Brannen, and R. C. Kerby. "The effect of lead on zinc deposit structures obtained from high purity synthetic and industrial acid sulphate electrolytes." *Journal of Applied Electrochemistry* 9, no. 1 (1979): 55-70.

MacKinnon, D. J., J. M. Brannen, and R. M. Morrison. "Zinc electrowinning from aqueous chloride electrolytes." *Journal of Applied Electrochemistry* 13, no. 1 (1983): 39-53.

Mackinnon, D. J., R. M. Morrison, and J. M. Brannen. "The effects of nickel and cobalt and their interaction with antimony on zinc electrowinning from industrial acid sulphate electrolyte." *Journal of Applied Electrochemistry* 16, no. 1 (1986): 53-61.

Mackinnon, D. J., J. M. Brannen, and P. L. Fenn. "Characterization of impurity effects in zinc electrowinning from industrial acid sulphate electrolyte." *Journal of Applied Electrochemistry* 17, no. 6 (1987): 1129-1143.

Mackinnon, D. J., R. M. Morrison, J. E. Mouland, and P. E. Warren. "The effects of saponin, antimony and glue on zinc electrowinning from Kidd Creek electrolyte." *Journal of Applied Electrochemistry* 20, no. 6 (1990 a): 955-963.

MacKinnon, D. J., R. M. Morrison, J. E. Mouland, and P. E. Warren. "The effects of antimony and glue on zinc electrowinning from Kidd Creek electrolyte." *Journal of Applied Electrochemistry* 20, no. 5 (1990 b): 728-736.

MacKinnon, D. J., and J. M. Brannen. "Effect of manganese, magnesium, sodium and potassium sulphates on zinc electrowinning from synthetic acid sulphate electrolytes." *Hydrometallurgy* 27, no. 1 (1991): 99-111.

MacKinnon, D. J. "The effects of foaming agents, and their interaction with antimony, manganese and magnesium, on zinc electrowinning from synthetic acid sulphate electrolyte." *Hydrometallurgy* 35, no. 1 (1994): 11-26.

Mahon, M., S. Peng, and A. Alfantazi. "Application and optimisation studies of a zinc electrowinning process simulation." *The Canadian Journal of Chemical Engineering* 92, no. 4 (2014): 633-642.

Maja, M., and P. Spinelli. "Detection of metallic impurities in acid zinc plating baths." *Journal of the Electrochemical Society* 118, (1971):1538-1540.

Maja, M., N. Penazzi, R. Fratesi, and G. Roventi. "Zinc Electrocrystallization from Impurity-Containing Sulfate Baths." *Journal of the Electrochemical Society* 129, no. 12 (1982): 2695-2700.

Mansfeld, F., and S. Gilman. "The effect of lead ions on the dissolution and deposition characteristics of a zinc single crystal in 6 N KOH." *Journal of the Electrochemical Society* 117, no. 5 (1970): 588-592.

Mansfeld, F., and C. C. Lee. "The Frequency Dependence of the Noise Resistance for Polymer-Coated Metals." *Journal of the Electrochemical Society* 144, no. 6 (1997): 2068-2071.

Mansfeld, F., Z. Sun, C. H. Hsu, and A. Nagiub. "Concerning trend removal in electrochemical noise measurements." *Corrosion Science* 43, no. 2 (2001): 341-352.

McColm, T. D., and J. W. Evans. "A modified Hull cell and its application to the electrodeposition of zinc." *Journal of Applied Electrochemistry* 31, no. 4 (2001): 411-419.

Milazzo, G. *Électrochimie, Tome 1: Bases Théoriques. Applications Analytiques Électrochimie des Colloïdes,* Dunod, Paris. 1969. pp 150-151.

Mohammadi, Maysam, and Akram Alfantazi. "The performance of Pb–MnO_2 and Pb–Ag anodes in 2 Mn (II)-containing sulphuric acid electrolyte solutions." *Hydrometallurgy* 153, (2015): 134-144.

Mohammadi, M., F. Mohammadi, G. Houlachi, and A. Alfantazi. "The role of electrolyte hydrodynamic properties on the performance of lead-based anodes in electrometallurgical processes." *Journal of the Electrochemical Society* 160, no. 3 (2013): E27-E33.

Mohanty, U. S., B. C. Tripathy, P. Singh, and S. C. Das. "Effect of pyridine and its derivatives on the electrodeposition of nickel from aqueous sulfate solutions. Part II: Polarization behaviour." *Journal of Applied Electrochemistry* 31, no. 9 (2001): 969-972.

Morrison, R. M., D. J. MacKinnon, D. A. Uceda, P. E. Warren, and J. E. Mouland." The effect of some trace metal impurities on the electrowinning of zinc from Kidd Creek electrolyte." *Hydrometallurgy* 29, no. 1-3 (1992): 413-430.

Mureşan, L., G. Maurin, L. Oniciu, and D. Gaga. "Influence of metallic impurities on zinc electrowinning from sulphate electrolyte." *Hydrometallurgy* 43, no. 1-3 (1996): 345-354.

Newnham, R. H. "Corrosion rates of lead based anodes for zinc electrowinning at high current densities." *Journal of Applied Electrochemistry* 22, no. 2 (1992): 116-124.

Oppenheim, A. V., and A. S. Willsky. *Signals and Systems*. Prentice-Hall, 1983. pp 26-90.

Park, S. M., and J. S. Yoo. "Electrochemical impedance spectroscopy for better electrochemical measurements." *American Chem. Soc.* 1(2003): 455-461.

Petrova, M., Y. Stefanov, Z. Noncheva, Ts Dobrev, and St Rashkov. "Electrochemical behaviour of lead alloys as anodes in zinc electrowinning." *British Corrosion Journal* 34, no. 3 (1999): 198-200.

Plonski, I. H. "Concentration Polarization and Mass Transfer Influence on the Kinetics of Two Stepwise-Proceeding Electrode Reactions under Galvanostatic Conditions." *Journal of the Electrochemical Society* 116, no. 12 (1969): 1688-1691.

Porter, F. C. *Zinc Handbook: Properties, Processing, and Use in Design*. CRC Press, 1991. pp 1-6.

Pourbaix, M. *Lectures on Electrochemical Corrosion*, Plenum Press, New York, 1973. pp 252.

Prengaman, R. D. "The Metallurgy of Lead Alloys for Electrowinning Anodes, Proceedings of the sessions sponsored by The electrolytic Processes Committee of the Metallurgical Society of AIME." *The Metallurgical Society of AIME*, (1984):49-55.

Randle, T. H., and A. T. Kuhn. "The Lead Dioxide Anode. II. The Kinetics and Participation of the Lead Dioxide Electrode in Electrochemical Oxidation Reactions in Sulfuric Acid." *Australian Journal of Chemistry* 42, no. 9 (1989): 1527-1545.

Revie, R. W., and H. H. Uhlig. *Uhlig's Corrosion Handbook*. Vol. 51. John Wiley & Sons, 2011. pp 1227-1238.

Safizadeh, F., A-M. Lafront, E. Ghali, and G. Houlachi. "Monitoring the influence of gelatin and thiourea on copper electrodeposition employing electrochemical noise technique." *Canadian Metallurgical Quarterly* 49, no. 1 (2010 a): 21-28.

Safizadeh, F., A-M. Lafront, E. Ghali, and G. Houlachi. "Monitoring the quality of copper deposition by statistical and frequency analyses of electrochemical noise." *Hydrometallurgy* 100, no. 3 (2010 b): 87-94.

Safizadeh, F., A-M. Lafront, E. Ghali, and G. Houlachi. "An investigation of the influence of selenium on copper deposition during electrorefining using electrochemical noise analysis." *Hydrometallurgy* 111 (2012): 29-34.

Safizadeh F., C. Su, E. Ghali and G. Houlachi "The Effect of Lead Content and Some Operating Parameters on Zinc Contamination during Electrowinning." (submit to *Hydrometallurgy* and under review), 2016.

Sarangi, C. K., B. C. Tripathy, I. N. Bhattacharya, T. Subbaiah, S. C. Das, and B. K. Mishra. "Electrowinning of zinc from sulphate solutions in the presence of perfluoroglutaric acid." *Minerals Engineering* 22, no. 14 (2009): 1266-1269.

Scott, A. C., R. M. Pitblado, and G. W. Barton. "A mathematical model of a zinc electrowinning cell." In *Proceedings of the Twentieth International Symposium on the Application of Computers and Mathematics in the Mineral Industries, Metallurgy* 2, (1987):51-62.

Scott, A. C., R. M. Pitblado, G. W. Barton, and A. R. Ault. "Experimental determination of the factors affecting zinc electrowinning efficiency." *Journal of Applied Electrochemistry* 18, no. 1 (1988): 120-127.

Scully, J. R., and D. C. Silverman. *Electrochemical Impedance: Analysis and Interpretation*. No. 1188. ASTM International, 1993. pp 24-86.

Sinclair, R. J. "The extractive metallurgy of zinc." *Victoria: Australasian Institute of Mining and Metallurgy*, (2005): 3-54.

Smulko, J., K. Darowicki, and A. Zieliński. "Detection of random transients caused by pitting corrosion." *Electrochimica Acta* 47, no. 8 (2002): 1297-1303.

Smulko, J., and K. Darowicki. "Nonlinearity of electrochemical noise caused by pitting corrosion." *Journal of Electroanalytical Chemistry* 545 (2003): 59-63.

Soofastaei, E., and S. A. Mirenayat. "Psyche in Eco-Apocalypse: A Reading of Ballard's The Drowned World." *International Letters of Social and Humanistic Sciences* (2015):17-21.

Sorour, N., W. Zhang, G. Gabra, E. Ghali, and G. Houlachi. "Electrochemical studies of ionic liquid additives during the zinc electrowinning process." *Hydrometallurgy* 157, (2015): 261-269.

Stefanov, Y., and I. Ivanov. "The influence of nickel ions and triethylbenzylammonium chloride on the electrowinning of zinc from sulphate electrolytes containing manganese ions." *Hydrometallurgy* 64, no. 3 (2002): 193-203.

Stelter, M., H. Bombach, and P. Saltykov. "Corrosion behavior of lead-alloy anodes in metal winning." *SISAPMM* 6, no. 1 (2006.): 451-461.

Stender, V. V. and A. G. Pecherskaya "Influence of impurities in the electrodeposition of zinc from sulfate solutions." *Zhurnal. Prikladnoi. Khimii. Sankt-Peterburg, Russian Federation* 23, no. 9 (1950): 920-935.

Tan, Y., S. Bailey, and B. Kinsella. "Studying the formation process of chromate conversion coatings on aluminium using continuous electrochemical noise resistance measurements." *Corrosion Science* 44, no. 6 (2002): 1277-1286.

Thompson N. G. and J. H. Payer. *DC Electrochemical Test Methods.* NACE international, 1998. pp 13-45.

Tikkanen, M. H. and O. Hyvarinen. "On the Anodic Behaviour of Pb-Ag Alloys in Sulfuric Acid Solutions." *Proc. Int. Congr. Metai. Corros.*, 4th (1972): 669-675.

Tozawa K., Y. Umetsu and S. Qing-quan, I. G. Mathew (Ed.) "World Zinc'93, Proceedings of the international symposium on 'zinc'." *Hobart Tasmania*, (1993): 267

Tripathy, B. C., S. C. Das, G. T. Hefter, and P. Singh. "Zinc electrowinning from acidic sulphate solutions Part II: Effects of triethylbenzylammonium chloride." *Journal of Applied Electrochemistry* 28, no. 9 (1998): 915-920.

Tripathy, B. C., S. C. Das, P. Singh, and G. T. Hefter. "Zinc electrowinning from acidic sulphate solutions. Part III: Effects of quaternary ammonium bromides." *Journal of Applied Electrochemistry* 29, no. 10 (1999): 1229-1235.

Tripathy, B. C., S. C. Das, and V. N. Misra. "Effect of antimony (III) on the electrocrystallisation of zinc from sulphate solutions containing SLS." *Hydrometallurgy* 69, no. 1 (2003): 81-88.

Tswuoka, T. "Behaviour of manganese in the electrodeposition of zinc." *Nippon Kogyo. Kaishi* 76, (1960):311-318

Tuaweri, T. J., E. M. Adigio, and P. P. Jombo. "A Study of Process Parameters for Zinc Electrodeposition from a Sulphate Bath." *International Journal of Engineering Science Invention Volume* 2, no. 8 (2013): 17-24.

Umetsu, Y., H. Nozoka and K. Tozawa. "Anodic Behaviour of Pb-Ag Alloys in Sulfuric Acid Solution, Proceedings of the International Symposium on Extract." *Metall. Zinc* (1985):265-279.

Vakhidov, R. S., and G. Z. Kiryakov. "Role of manganese during the electrodeposition of zinc." *Izv Vissh Ucheb Zaved Khim Technol* 2 (1959): 238-243.

Walter, G. W. "A review of impedance plot methods used for corrosion performance analysis of painted metals." *Corrosion Science* 26, no. 9 (1986): 681-703.

Wark, I. W. "The electrodeposition of zinc from acidified zinc sulphate solution." *Journal of Applied Electrochemistry* 9, no. 6 (1979): 721-730.

Welsh, J. Y. "Role of manganic ion in production of electrolytic manganese dioxide." *In Electrochemical Technology* 5, no. 11-1 (1967, January): 504.

West, J. M. "Applications of potentiostats in corrosion studies." *British Corrosion Journal* 5, no. 2 (1970): 65-71.

Wiart, R., C. Cachet, and C. Bozhkov. "On the nature of the ‘induction period’during the electrowinning of zinc from nickel containing sulphate electrolytes." *Journal of Applied Electrochemistry* 20, no. 3 (1990): 381-389.

Wood, R. J. K., J. A. Wharton, A. J. Speyer, and K. S. Tan. "Investigation of erosion–corrosion processes using electrochemical noise measurements." *Tribology International* 35, no. 10 (2002): 631-641.

Xiao, H., and F. Mansfeld. "Evaluation of coating degradation with electrochemical impedance spectroscopy and electrochemical noise analysis." *Journal of the Electrochemical Society* 141, no. 9 (1994): 2332-2337.

Yang, H., and A. J. Bard. "The application of fast scan cyclic voltammetry. Mechanistic study of the initial stage of electropolymerization of aniline in aqueous solutions." *Journal of Electroanalytical Chemistry* 339, no. 1-2 (1992): 423-449.

Yokogawa. *Application Note: Measurement of pH of Leachate in Zinc Hydrometallurgy and Air Jet Cleaning to Prevent Scaling.* 2016 https://web-material3.yokogawa.com/AN10B01G20-09E_Rev2_pH_of_Leachate_in_Zinc_Hydrometallurgy.pdf (accessed on 01-02-2017)

Yu, P., and T. J. O'Keefe. "Evaluation of lead anode reactions in acid sulfate electrolytes. I. Lead alloys with cobalt additives." *Journal of the Electrochemical Society* 146, no. 4 (1999): 1361-1369.

Yu, P., and T. J. O'Keefe. "Evaluation of lead anode reactions in acid sulfate electrolytes II. Manganese reactions." *Journal of the Electrochemical Society* 149, no. 5 (2002): 558-569.

Zhang, H., and S. Park. "Electrochemical oxidation of manganese (II) in HClO4 solutions." *Journal of the Electrochemical Society* 141, no. 9 (1994): 2422-2429.

Zhang, Q., Y. Hua, T. Dong, and D. Zhou. "Effects of temperature and current density on zinc electrodeposition from acidic sulfate electrolyte with [BMIM] HSO_4 as additive." *Journal of Applied Electrochemistry* 39, no. 8 (2009): 1207-1216.

Zhang, Q., and Y. Hua. "Effect of Mn^{2+} ions on the electrodeposition of zinc from acidic sulphate solutions." *Hydrometallurgy* 99, no. 3 (2009): 249-254.

Zhang, W. *Performance of Lead Anodes Used for Zinc Electrowinning and Their Effects on Energy Consumption and Cathode Impurities*. Doctoral dissertation, Université Laval, 2010. pp 34-52.

Zhang, W., C. Q. Tu, Y. F. Chen, W. Y. Li, and G. Houlachi. "Effect of MnO_4^- and silver content on electrochemical behaviour of Pb–Ag alloy anodes during potential decay periods." *Journal of Materials Engineering and Performance* 22, no. 6 (2013): 1672–1679.

Zhang, W., Y. F. Chen, and G. Houlachi. "Influence of silver content and $MnSO_4$ addition on performance of different lead–silver alloys during polarisation and decay periods." *Canadian Metallurgical Quarterly* 52, no. 1 (2013): 60-68.